stretch for the *tmhd* compounds, **71-74** and **79-82** is *ca.* 5-10 cm<sup>-1</sup> lower than that of *dbm* analogues consistent with the strong electron donating effect of the *t*-butyl groups. The imine stretches of coordinated bridging ligands which are expected to be between 1600 and 1630 cm<sup>-1</sup> are not observed as they masked by the strong C=O stretch of the  $\beta$ -diketonate ligand.

#### **Experimental**

#### Synthesis of [(dbm)<sub>2</sub>Ni(μ-1,3-bpmba)Ni(dbm)<sub>2</sub>] 67

To a stirred light green suspension of  $[Ni(dbm)_2(H_2O)_2]$  (0.1082 g , 0.2 mmol ) in  $CH_2CI_2$  (10 cm<sup>3</sup>) was added 1,3-bpmba (0.0286 g, 0.1 mmol) to give a light yellow brown solution. The light yellow brown solution was stirred overnight. The mixture was filter through filter paper to give a light yellow brown solution and then the solution was evaporated on to rotary evaporator and remove volume to small amount. The residue was washed diethyl ether to give a light yellow brown precipitate, yield 0.0394 g (31 %).

#### Synthesis of [(dbm)<sub>2</sub>Ni(μ-1,4-bpmba)Ni(dbm)<sub>2</sub>] 68

To a stirred light green suspension of  $[Ni(dbm)_2(H_2O)_2]$  (0.2167 g , 0.4 mmol ) in  $CH_2CI_2$  (10 cm<sup>3</sup>) was added 1,4-bpmba (0.0570 g, 0.2 mmol) to give a light yellow brown solution. The yellow brown solution was stirred overnight. The solution was filter through celite to give a light yellow brown solution and then the solution was evaporated on to rotary evaporator and remove volume to small amount. n-Hexane (10 cm<sup>3</sup>) was added a red crystals precipitated, yield 0.2300 g (89%).

#### Synthesis of [(dbm)<sub>2</sub>Ni(μ-1,5-bpmna)Ni(dbm)<sub>2</sub>] 69

To a stirred light green suspension of  $[Ni(dbm)_2(H_2O)_2]$  (0.1085 g, 0.2 mmol) in  $CH_2CI_2$  (10 cm<sup>3</sup>) was added 1,5-bpmna (0.0339 g, 0.1 mmol). The solution was then stirred at room temperature. After four hours, the brown solution was filtered and left to evaporate slowly at room temperature to give red- brown crystals, yield 0.1017 g (75%).

#### Synthesis of [(dbm)<sub>2</sub>Ni(μ-bpmhd)Ni(dbm)<sub>2</sub>] 70

To a stirred lime green solution of  $[Ni(dbm)_2(H_2O)_2]$  (0.1509 g, 0.2 mmol) in THF (10 cm<sup>3</sup>), bpmhd (0.0213 g, 0.1 mmol) was added. The red-brown solution was stirred for 2 hours then the solvent was removed to small volume. n-Hexane (5 cm<sup>3</sup>) was added to induce precipitation. The yellow brown micro crystals was filtered and washed with n-hexane (2 x 5 cm<sup>3</sup>) yields 0.0555 g (45%).

#### Synthesis of $[(tmhd)_2Ni(\mu-1,3-bpmba)Ni(tmhd)_2]$ 71

To a stirred green suspension of  $[Ni(tmhd)_2(H_2O)_2]$  (0.0461 g, 0.1 mmol) in THF (5 cm<sup>3</sup>) was added 1,3-bpmba (0.0143 g, 0.05 mmol) to give a light yellow brown solution. The light yellow brown solution was stirred overnight. The mixture was filtrated through celite to give a light yellow

brown solution and then the solution was evaporated on to rotary evaporator and remove volume to small amount. The residue was washed diethyl ether to give light yellow orange precipitates, yield 0.0273 g (48%).

#### Synthesis of [(tmhd)<sub>2</sub>Ni(μ-1,4-bpmba)Ni(tmhd)<sub>2</sub>] 72

To a stirred purple solution of  $[Ni(tmhd)_2(H_2O)_2]$  (0.0461 g, 0.1 mmol) in  $CH_2CI_2$  (15 cm<sup>3</sup>) was added 1,4-bpmba (0.0567 g, 0.2 mmol) to give a deep orange solution. The solution was stirred overnight. The mixture was filtrated through celite to give a deep orange solution and then the solution was evaporated on to rotary evaporator and remove volume to small amount. The residue was washed diethyl ether to give red precipitates, yield 0.1250 g (55 %).

#### Synthesis of $[(tmhd)_2Ni(\mu-1,5-bpmna)Ni(tmhd)_2]$ 73

To a stirred purple solution of  $[Ni(tmhd)_2(H_2O)_2]$  (0.0923 g, 0.2 mmol) in  $CH_2CI_2$  (10 cm<sup>3</sup>) was added 1,5-bpmna (0.0338 g, 0.1 mmol). After stirring for 24 hours, the dark brown solution was filtered through filtered paper. The solution was then evaporated slowly at room temperature to low volume. Then hexane was added on top of the solution and the solution was left to crystallize to give red-brown crystals yield 0.0611 g (51%).

#### Synthesis of [(tmhd)<sub>2</sub>Ni(μ-bpmhd)Ni(tmhd)<sub>2</sub>] 74

To a stirred green solution of  $[Ni(tmhd)_2(H_2O)_2]$  (0.0922 g, 0.2 mmol) in THF (10 cm<sup>3</sup>), bpmhd (0.0228 g, 0.1 mmol) was added. The red-orange solution was stirred for 2 hours then the solvent was removed to small volume. n-Hexane (5 cm<sup>3</sup>) was added to induce precipitation but no precipitation occurred. The solvent was removed to dryness. The salmon pink solid was filtered and dried in air yields 0.0306 g (22%).

#### Synthesis of $[(dbm)_2Co(\mu-1,3-bpmba)Co(dbm)_2]$ 75

To a stirred light orange yellow suspension of  $[Co(dbm)_2(H_2O)_2]$  (0.0542 g, 0.1 mmol) in  $CH_2Cl_2$  (5 cm<sup>3</sup>) was added 1,3-bpmba (0.0143 g, 0.05 mmol) to give a dark red suspension. The dark red suspension was stirred overnight. The mixture was filter through filter paper to give a light red brown solution and then the solution was evaporated on to rotary evaporator and remove volume to small amount. The residue was washed diethyl ether to give a light brown precipitate, yield 0.0206 g (32%)

#### Synthesis of [(dbm)<sub>2</sub>Co( $\mu$ -1,4-bpmba)Co(dbm)<sub>2</sub>] 76

To a stirred yellow orange suspension of  $[Co(dbm)_2(H_2O)_2]$  (0.0541 g, 0.1 mmol) in  $CH_2CI_2$  (5 cm<sup>3</sup>) was added 1,4-bpmba (0.0143 g, 0.05 mmol) to give a red orange suspension. The red orange suspension was stirred overnight. The mixture was filter through filter paper to give a dark red brown solution and then the solution was left to slowly evaporate at room temperature. Then hexane was added on top of the solution to give red crystals, yield 0.0378 g (58%).

Synthesis of  $[(dbm)_2Co(\mu-1,5-bpmna)Co(dbm)_2]$  77To a stirred purple solution of  $[Co(dbm)_2(H_2O)_2]$  (0.1083 g, 0.2 mmol) in THF (7 cm<sup>3</sup>) was added 1,5-bpmna (0.0340 g, 0.1 mmol). After 4 hours, the red-brown solution was filtered through celite and left to evaporate slowly at room temperature to give red-brown crystals, yield 0.0744 g (74%).

#### Synthesis of [(dbm)<sub>2</sub>Co(μ-bpmhd)Co(dbm)<sub>2</sub>] 78

To a stirred bright orange solution of  $[Co(dbm)_2(H_2O)_2]$  (0.1086 g, 0.2 mmol) in THF (10 cm<sup>3</sup>), bpmhd (0.0219 g, 0.1 mmol) was added. The red-brown solution was stirred for 2 hours then the solvent was removed to small volume. n-Hexane (5 cm<sup>3</sup>) was added to induce precipitation. The brown micro crystals was filtered and washed with n-hexane (2 x 5 cm<sup>3</sup>) yields 0.044 g (36%).

#### Synthesis of $[(tmhd)_2Co(\mu-1,3-bpmba)Co(tmhd)_2]$ 79

To a stirred light purple solution of  $[Co(tmhd)_2(H_2O)_2]$  (0.0462 g , 0.1 mmol) in THF (5 cm<sup>3</sup>) was added 1,3-bpmba (0.0143 g, 0.05 mmol) to give a dark purple brown solution. The dark purple brown solution was stirred 4 hrs. The mixture was filtrated through celite to give a light purple brown solution and then the solution was evaporated on to rotary evaporator and remove volume to small amount. The residue was washed diethyl ether to give a dark brown precipitate, yield 0.0362 g (64%).

Synthesis of  $[(tmhd)_2Co(\mu-1,4-bpmba)Co(tmhd)_2]$  80To a stirred light purple solution of  $[Co(tmhd)_2(H_2O)_2]$  (0.0462 g, 0.1 mmol) in THF (4 cm<sup>3</sup>) was added 1,4-bpmba (0.0143 g, 0.05 mmol) to give a dark red brown solution. The dark red brown solution was stirred 3 hours. The mixture was filtrated through celite to give a dark purple brown solution and then the solvent was removed on to rotary evaporator to small amount. Then diethyl ether (10 cm<sup>3</sup>) was added to give a dark brown precipitate, yield 0.0448 g (79%).

#### Synthesis of [(tmhd)<sub>2</sub>Co(μ-1,5-bpmna)Co(tmhd)<sub>2</sub>] 81

To a stirred purple solution of  $[Co(tmhd)_2(H_2O)_2]$  (0.0924 g, 0.2 mmol) in THF (7 cm<sup>3</sup>) was added 1,5-bpmna (0.0339 g, 0.1 mmol). After 4 hours, the brown solution was filtered through celite and left to evaporate slowly at room temperature to give a red-brown crystals, yield 0.0765 g (76%).

#### Synthesis of [(tmhd)<sub>2</sub>Co(μ-bpmhd)Co(tmhd)<sub>2</sub>] 82

To a stirred red solution of  $[Co(tmhd)_2(H_2O)_2]$  (0.065 g, 0.14 mmol) in THF (5 cm<sup>3</sup>), bpmhd (0.0158 g, 0.075 mmol) was added. The deep purple solution was stirred for 2 hours then the solvent was removed to small volume. n-Hexane (5 cm<sup>3</sup>) was added to induce precipitation but no precipitation occurred. The solvent was removed to dryness. The purple brown solid was filtered and dried in air yields 0.0635 g (80%).

#### X-ray structural studies of [( $\theta$ -diketonate)<sub>2</sub>M( $\mu$ -L)M( $\theta$ -diketonate)<sub>2</sub>] complexes

The suitable crystals of  $[(dbm)_2Co(\mu-1,4-bpmba)Co(dbm)_2]$  76 was grown by allowing n-hexane to diffuse slowly into a concentrated solution of the complex in  $CH_2CI_2$  at room temperature. Complex 76 assumes slightly distorted octahedral coordination geometries (Figure 18). The  $\beta$ -diketonate ligands exhibit a cis arrangement enforced by the bridging ligand, 1,4-bpmba. The Co-O bond lengths are slightly longer to that of  $[Co(dbm)_2(ppa^{OMe})]$  36 and  $[Co(dbm)_2(ppa^{Cl})]$  38. Interestingly, the Co-O4 bond length is considerably longer than the others. The cobalt bond to the pyridine of the bridging ligand of complexes 76 is considerably shorter than the bond to the imine nitrogen differing by ca. 0.1 Å.

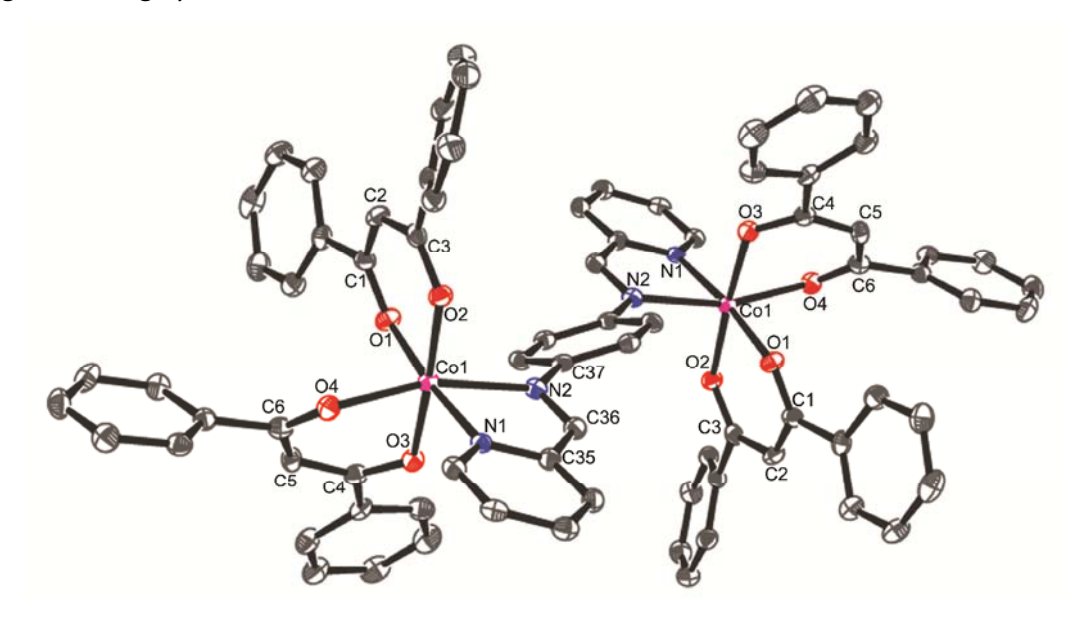


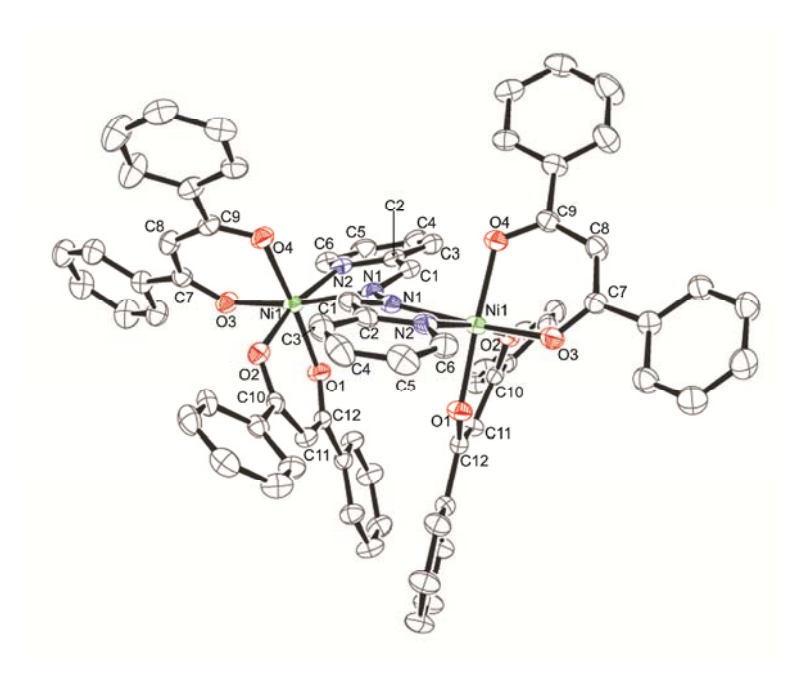
Figure 18 ORTEP diagram of  $[(dbm)_2Co(\mu-1,4-bpmba)Co(dbm)_2]$  76. The thermal ellipsoids are drawn to 50% probability level. Hydrogen atoms are omitted for clarity.

**Table 17** Bond lengths and bond angles of  $[(dbm)_2Co(\mu-1,4-bpmba)Co(dbm)_2]$  **76**.

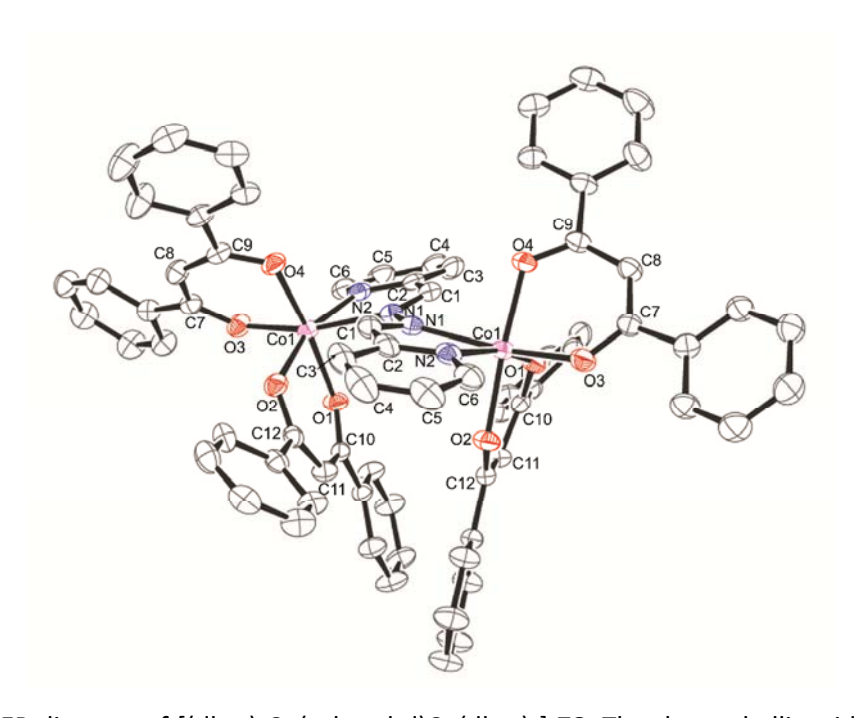
	(Å)		(°)
Co(1)-O(1)	2.045(2)	O(1)-Co(1)-O(2)	87.22(9)
Co(1)-O(2)	2.047(2)	O(1)-Co(1)-O(3)	87.23(9)
Co(1)-O(3)	2.052(2)	O(2)-Co(1)-O(3)	174.45(9)
Co(1)-O(4)	2.095(2)	O(1)-Co(1)-O(4)	91.61(9)
Co(1)-N(1)	2.115(3)	O(2)-Co(1)-O(4)	94.69(9)
Co(1)-N(2)	2.232(2)	O(3)-Co(1)-O(4)	85.37(8)
N(1)-C(31)	1.339(3)	O(1)-Co(1)-N(1)	173.63(9)
N(1)-C(35)	1.357(4)	O(2)-Co(1)-N(1)	88.25(9)
N(2)-C(36)	1.278(4)	O(3)-Co(1)-N(1)	97.29(9)
N(2)-C(37)	1.434(3)	O(4)-Co(1)-N(1)	93.23(9)

O(1)-C(1)	1.267(4)	O(1)-Co(1)-N(2)	99.94(9)
O(2)-C(3)	1.274(4)	O(2)-Co(1)-N(2)	97.87(9)
O(3)-C(4)	1.279(4)	O(3)-Co(1)-N(2)	83.19(9)
O(4)-C(6)	1.272(4)	O(4)-Co(1)-N(2)	163.29(9)
		N(1)-Co(1)-N(2)	76.25(9)

The suitable crystals of  $[(dbm)_2M(\mu-bpmhd)M(dbm)_2]$  (M= Ni **70** and Co **78**) were grown by allowing *iso*-propanol to diffuse slowly into a concentrated solution of the complex in  $CH_2CI_2$  at room temperature. Both structures assume slightly distorted octahedral coordination geometries (Figures 19 and 20). The  $\beta$ -diketonate ligands exhibit a *cis* arrangement enforced by the bridging ligand, bpmhd. The M-O bond in **78** lengths are slightly longer to that of **70** but similar to that of  $[(dbm)_2Co(\mu-1,4-bpmba)Co(dbm)_2]$  **76**. The metal bond to the pyridine of the bridging ligand of complexes **70** and **78** is considerably shorter than the bond to the imine nitrogen differing by *ca*. 0.1 Å.



**Figure 19** ORTEP diagram of  $[(dbm)_2Ni(\mu-bpmhd)Ni(dbm)_2]$  **70**. The thermal ellipsoids are drawn to 50% probability level. Hydrogen atoms are omitted for clarity.



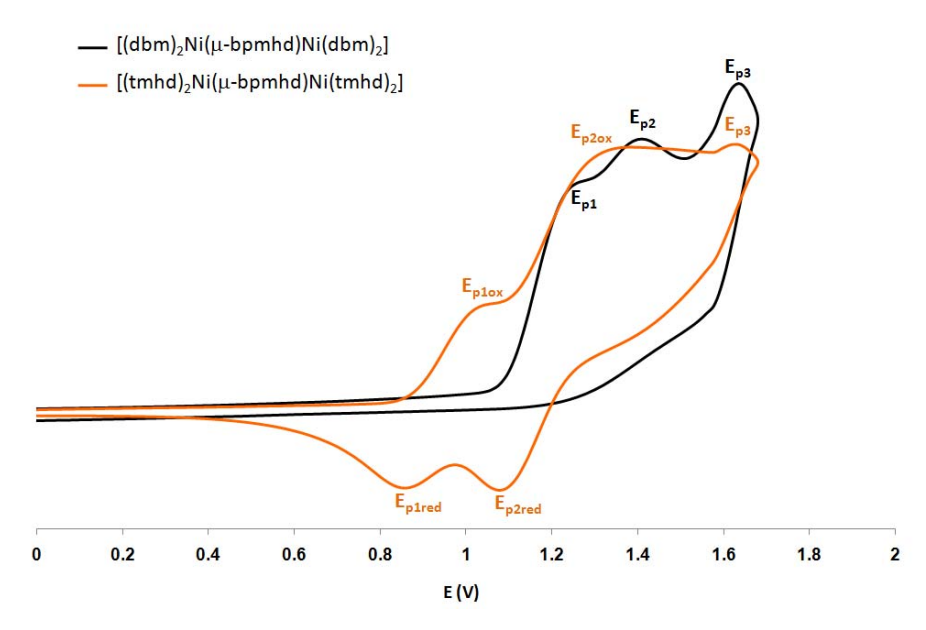
**Figure 20** ORTEP diagram of  $[(dbm)_2Co(\mu-bpmhd)Co(dbm)_2]$  **78**. The thermal ellipsoids are drawn to 50% probability level. Hydrogen atoms are omitted for clarity.

Table 18 Selected bond lengths (Å) and angles (°) of 70 and 78

	70	78		70	78
M(1)-O(1)	2.0093(18)	2.0421(13)	O(1)-M(1)-O(2)	88.98(8)	86.12(5)
M(1)-O(2)	1.9949(19)	2.0278(14)	O(1)-M(1)-O(3)	89.84(8)	92.12(6)
M(1)-O(3)	1.996(2)	2.0164(14)	O(1)-M(1)-O(4)	175.21(8)	172.53(6)
M(1)-O(4)	2.0105(18)	2.0261(13)	O(2)-M(1)-O(3)	96.15(8)	98.62(6)
M(1)-N(1)	2.159(2)	2.2122(16)	O(2)-M(1)-O(4)	86.32(8)	86.50(6)
M(1)-N(2)	2.081(2)	2.1173(17)	O(3)-M(1)-O(4)	89.78(8)	87.81(5)
N(1)-C(1)	1.287(4)	1.283(3)	O(1)-M(1)-N(1)	94.18(8)	94.86(6)
N(1)-N(1)'	1.407(5)	1.404(3)	O(2)-M(1)-N(1)	95.06(8)	94.95(6)
N(2)-C(2)	1.347(4)	1.349(3)	O(3)-M(1)-N(1)	168.15(8)	165.12(6)
N(2)-C(6)	1.339(4)	1.333(3)	O(4)-M(1)-N(1)	87.13(8)	86.96(6)
O(1)-C(12)	1.264(3)	1.258(2)	O(1)-M(1)-N(2)	82.87(8)	81.83(6)
O(2)-C(10)	1.269(3)	1.265(2)	O(2)-M(1)-N(2)	167.99(8)	163.68(6)
O(3)-C(7)	1.272(3)	1.271(2)	O(3)-M(1)-N(2)	92.63(9)	92.82(6)
O(4)-C(9)	1.273(3)	1.272(2)	O(4)-M(1)-N(2)	101.92(8)	105.63(6)

#### Electron transfer studies of [( $\theta$ -diketonate)<sub>2</sub>M( $\mu$ -L)M( $\theta$ -diketonate)<sub>2</sub>] complexes

Electrochemical studies of the dimer complexes 67-82 were conducted in  $CH_2CI_2$  between  $\pm 1.8$  V *versus* the Ag-AgCl electrode at room temperature using a three-electrode configuration. All of the Ni dimer complexes show two irreversible oxidation peaks with exception of [(tmhd)<sub>2</sub>Ni( $\mu$ -bpmhd)Ni(tmhd)<sub>2</sub>] 74 that shows two reversible and one irreversible process (Figure 21, Table 19).



**Figure 21** Cyclic voltammograms of  $[(dbm)_2Ni(\mu-bpmhd)Ni(dbm)_2]$  **70** and  $[(tmhd)_2Ni(\mu-bpmhd)Ni(tmhd)_2]$  **74**.

**Table 19**Electrochemical data for  $[(\beta-diketonate)_2Ni(\mu-L)Ni(\beta-diketonate)_2]$  complexes.

Complex	Peak potential (V)			
Complex _	Ep <sub>1</sub>	Ep <sub>2</sub>	Ep <sub>3</sub>	
[(dbm) <sub>2</sub> Ni(μ-1,3-bpmba)Ni(dbm) <sub>2</sub> ] <b>67</b>	1.26 (I)	1.54(I)	-	
$[(dbm)_2Ni(\mu\text{-}1,4\text{-}bpmba)Ni(dbm)_2]\textbf{68}$	1.24 (I)	1.61(I)	-	
[(dbm) <sub>2</sub> Ni( $\mu$ -1,5-bpmna)Ni(dbm) <sub>2</sub> ] <b>69</b>	1.32 (I)	1.68(I)	-	
[(dbm) <sub>2</sub> Ni(μ-bpmhd)Ni(dbm) <sub>2</sub> ] <b>70</b>	1.32(I)	1.40(I)	1.64(I)	
$[(tmhd)_2Ni(\mu\text{-}1,3\text{-}bpmba)Ni(tmhd)_2]~\textbf{71}$	0.96 (I)	1.54(I)	-	
$[(tmhd)_2Ni(\mu-1,4-bpmba)Ni(tmhd)_2] \ \textbf{72}$	1 03(I)	1.51 (I)	-	
$[(tmhd)_2Ni(\mu\text{-}1,5\text{-}bpmna)Ni(tmhd)_2]~\textbf{73}$	0.94 (I)	1.54(I)	-	
$[(tmhd)_2Ni(\mu\text{-bpmhd})Ni(tmhd)_2]~\textbf{74}$	0.98*	1.23*	1.62(I)	

<sup>\*</sup>  $E_{1/2}$  for reversible process.

A comparison of the oxidation potential of *dbm* complexes with *tmhd* complexes mirrors the trend observed in the  $[Ni(\beta-diketonate)_2(ppa^X)]$  series with the oxidation potential of the *dbm* 

complexes higher than that of *tmhd* complexes. The structure of the bridging ligands also plays an important role in controlling the electron transfer properties of the dimer complexes. The difference in the oxidation potential for the different ligands reveals no trend other than that the bpmhd complexes are always the most difficult to oxidize (Figure 22). The presence of two oxidation peaks in the complexes indicates that there is communication between the two metal centres. The shortest bridge *i.e. bpmhd* appears to display a largest difference in oxidation potentials consistent with the strongest communication between the metal centres.

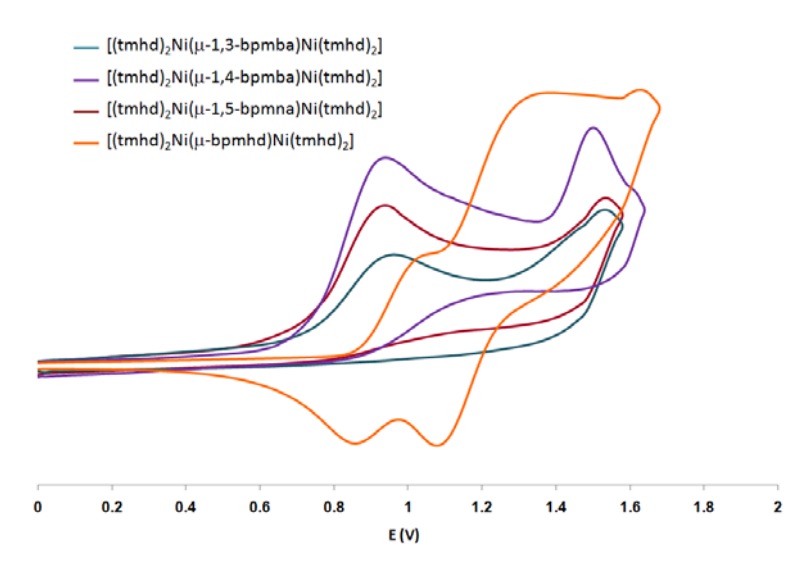


**Figure 22** Cyclic voltammograms of  $[(tmhd)_2Ni(\mu-L)Ni(tmhd)_2]$  **71-74**.

In case of the Co dimers **75-82** the cyclic voltammograms show oxidation peaks followed by returned peaks which are separated from the oxidation peaks by ca. 800-2000 mV indicative of the redox-coupled spin crossover behavior observed in the  $[Co(\beta-diketonate)_2(ppa^X)]$  and  $[Co(\beta-diketonate)_2(N-N)]$  complexes (Figures 23 and 24, Table 20).

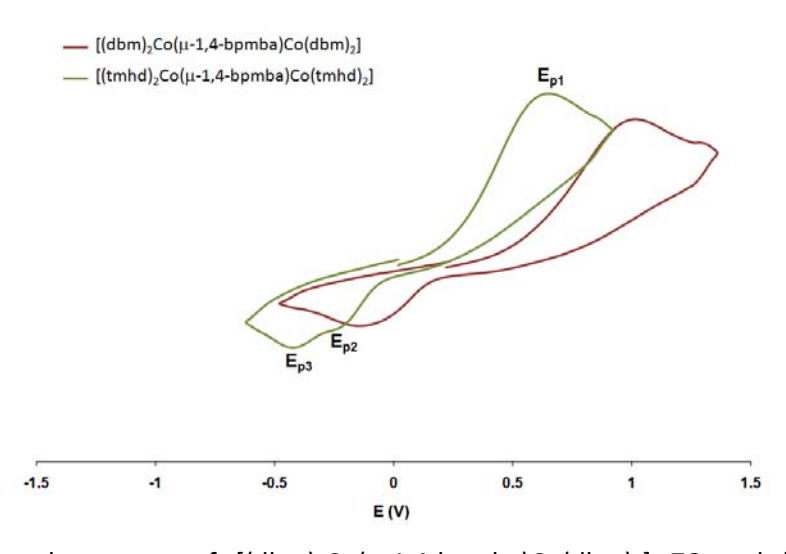


**Figure 23** Cyclic voltammetry of  $[(dbm)_2Co(\mu-1,4-bpmba)Co(dbm)_2]$  **76** and  $[(tmhd)_2Co(\mu-1,4-bpmba)Co(tmhd)_2]$  **80**.

**Table 20** Electrochemical data for  $[(\beta-diketonate)_2Co(\mu-L)Co(\beta-diketonate)_2]$  complexes.

Complex	Peak potential (V)			
Complex	Ep <sub>1</sub>	Ep <sub>2</sub>	Ep <sub>3</sub>	
[(dbm) <sub>2</sub> Co(μ-1,3-bpmba)Co(dbm) <sub>2</sub> ] <b>75</b>	0.96	-	-0.16	
[(dbm) $_2$ Co( $\mu$ -1,4-bpmba)Co(dbm) $_2$ ] <b>76</b>	1.02	-	-0.14	
[(dbm) $_2$ Co( $\mu$ -1,5-bpmna)Co(dbm) $_2$ ] <b>77</b>	0.88	-	0.04	
[(dbm) $_2$ Co( $\mu$ -bpmhd)Co(dbm) $_2$ ] <b>78</b>	1.16	0.22	-0.12	
$[(tmhd)_2Co(\mu-1,3-bpmba)Co(tmhd)_2]$ 79	1.16	-0.72	-0.96	
[ $(tmhd)_2Co(\mu-1,4-bpmba)Co(tmhd)_2$ ] <b>80</b>	0.66	-0.28	-0.42	
[(tmhd) <sub>2</sub> Co( $\mu$ -1,5-bpmna)Co(tmhd) <sub>2</sub> ] <b>81</b>	0.70	-0.38	-	
[(tmhd) <sub>2</sub> Co( $\mu$ -bpmhd)Co(tmhd) <sub>2</sub> ] <b>82</b>	1.28	0.14	-0.32	

When we compare the oxidation peak potential of the complexes in the dbm series we found that the complexes are increasingly easy to oxidize in the order bpmhd > 1,4-bpmba > 1,3-bpmba > 1,5-bpmba. While for the tmhd series the order is bpmhd > 1,3-bpmba > 1,5-bpmba > 1,4-bpmba.

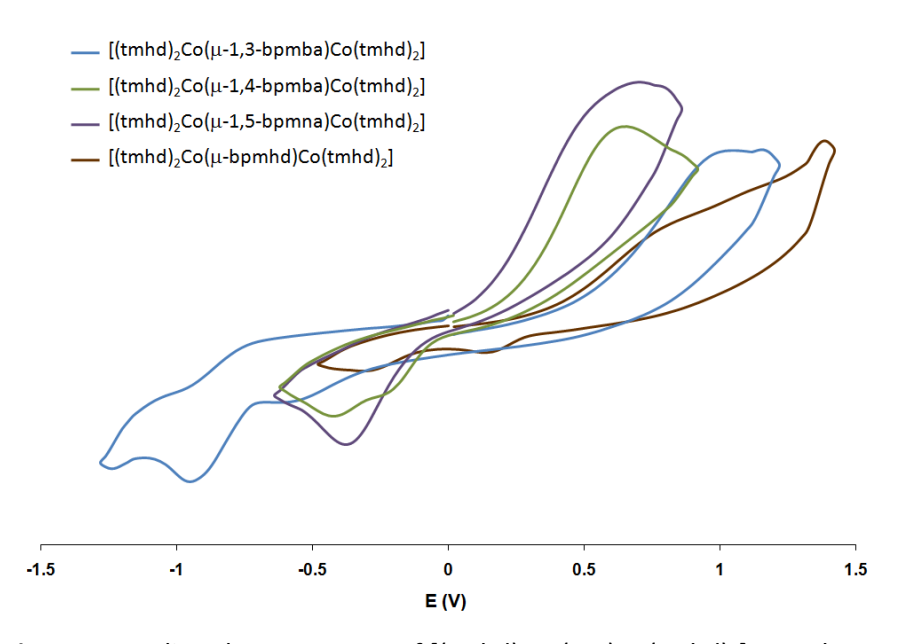


**Figure 24** Cyclic voltammograms of  $[(tmhd)_2Co(\mu-L)Co(tmhd)_2]$  complexes.

The unusual electron transfer behavior might due to the strong communication between the two metal centres through the bridging ligand. It is also possible that the structural reorganization required upon oxidation is more difficult to achieve as a result of increased steric interactions that would be expected in the 1,3-bpmba ligand complexes. Further studies of these complexes need to be conducted by spectroelectrochemistry and structural studies of redox pairs of the cobalt and if possible the nickel complexes.

#### 4.9. Computational calculations of [Co(β-diketonate)<sub>2</sub>(N-N)] complexes

In order to better understand the electronic structure of  $[Co(\beta-diketonate)_2(N-N)]\{N-N = ppa^X$  **33-48**, phen, bpy and dmae **57-62**} and their respective cations, and in particular the role of the electronic structure on the redox coupled-spin crossover process we have undertaken DFT calculations. For a given complex, all possible spin states were considered.

To find the best calculation method for  $[Co(\beta-diketonate)_2(N-N)]$  we initially started with complexes **57-62** as there are less compounds in the series. The fact that  $[Co(dbm)_2(phen)]$  **57** has been structurally characterized by single crystal X-ray crystallography allows a comparison between the computational and experimental geometries (see Figure 24 and Table 21). The computed bond lengths match well with the experimental bond lengths with differences no more than 0.05 Å. The bonds angles show similar agreement between experiment and theory. Good agreements between the X-ray structure and computed geometry of  $[Co(dbm)_2(phen)]$  in the quartet spin state indicates that these complex exists in a high spin state. It also confirms that the B3LYP/SDD model can be used to describe these types of complexes.

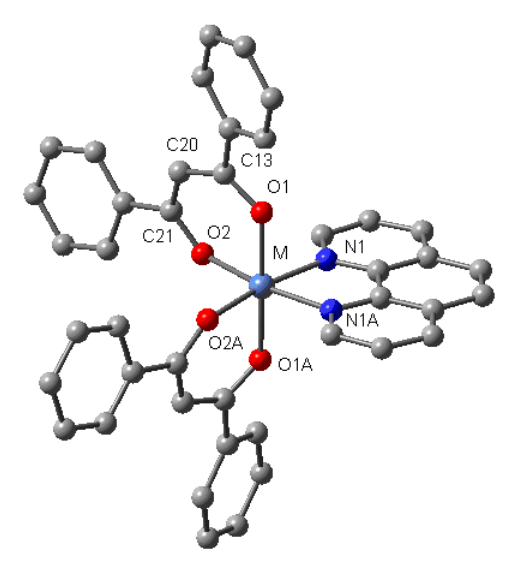


Figure 24 Numbering scheme for [Co(dbm)<sub>2</sub>(phen)] complex as used for structural comparison with the X-ray structures.

**Table 21** Selected computed and X-ray crystallographically determined bond lengths (Å) and bond angles (°) for [Co(dbm)<sub>2</sub>(phen)] **57**. See Figure 24 for the numbering scheme.

[Co(dbm) <sub>2</sub> (phen)]	X-ray <sup>1</sup>	Doublet	diff. <sup>2</sup>	Quartet	diff. <sup>2</sup>
Co-O1	2.07	2.15	0.08	2.0627	0.01
Co-O2	2.07	1.94	0.13	2.0544	0.01
Co-N1	2.15	1.96	0.19	2.1493	0.00

C7-O1	1.28	1.29	0.01	1.3022	0.02
C20-O2	1.27	1.31	0.04	1.3052	0.03
C7-C21	1.41	1.43	0.02	1.4019	0.00
C20-C21	1.41	1.41	0.00	1.4163	0.01
O1-Co-O2	86.29	88.63	2.34	85.73	0.56
O2-Co-O2A	102.54	91.92	10.62	98.69	3.85
O1-Co-O2A	83.67	89.01	5.34	91.96	8.29
O1-Co-N1	101.53	92.85	8.68	96.11	5.42
O1-Co-N1A	91.10	89.67	1.43	86.68	4.42
O2-Co-N1	90.49	92.24	1.75	92.43	1.94
O1-Co-O1A	163.92	176.63	12.71	176.42	12.50
N1-Co-N1A	76.87	83.64	6.77	77.58	0.71

<sup>&</sup>lt;sup>1</sup>From ref. 59.

Our B3LYP/SDD calculations confirm the observation that the HS state is the most stable state for the Co<sup>III</sup> complexes and the LS state is the most stable state for the Co<sup>III</sup> complexes and as such is consistent with the magnetic susceptibility measurements. In contrast, with the previously studied  $[Co(tacn)_2]^{2+/3+}$  redox pair the gas-phase energy difference between the HS and LS states, E(HS)-E(LS), for the neutral Co<sup>II</sup> complexes is between -12.7 and -15.6 kcal/mol (see Table 22) compared with -0.09 kcal/mol for  $[Co(tacn)_2]^{2+}$ . However, in the case of the Co<sup>III</sup> cations the gap is significantly decreased to between 16.1 and 18.1 kcal/mol (*cf.* 45.3 kcal/mol for  $[Co(tacn)_2]^{3+}$ ). Judging from the gas-phase energy, the triplet and quintet states are found to lie close to each other. The differences between E(HS)-E(LS) of  $57^+-62^+$  and  $[Co(tacn)_2]^{3+}$  are simply explained by the presence of the lower field  $\beta$ -diketonate ligands which are better able to stabilize the HS states. The thmd ligand stabilizes the HS state compared to the LS state to a greater extent than the dbm ligand. Moreover, the phen ligand stabilizes the HS state most in comparison with the other N-N ligands. This might be due to a metal d- $\pi$ \* orbital interaction from the low-lying  $\pi$ \* orbital of the phen ligand. The smaller difference in the LS and HS states in  $57^+-62^+$  might also explain why we are able to observe the reduction peak for the HS Co<sup>III</sup> species in some of the electrochemical studies. These

<sup>&</sup>lt;sup>2</sup>Difference between X-ray crystallographic and optimized structure

studies further suggest that the mechanism for the redox coupled-spin crossover involves a HS  $Co^{III}$  intermediate as has also been found in the  $[Co(tacn)_2]^{2+/3+}$  system.

**Table 22** The high-spin and low-spin complex energy difference, E(HS)-E(LS), at B3LYP/SDD level for  $[Co(β-diketonate)_2(N-N)]$  complexes. For  $57^+-62^+$ , the pentet and triplet (in parenthesis) HS states were considered. The E(LUMO)-E(SOMO) gap was estimated from the alpha spin orbital energy of the most stable spin state.

Complex	E(HS)-E(LS)/(kcal.mol <sup>-1</sup> )	E(LUMO)-E(SOMO)/eV
[Co(dbm) <sub>2</sub> (phen)] <b>57</b>	-13.84	3.13
[Co(dbm) <sub>2</sub> (2,2'-bpy)] <b>58</b>	-12.80	2.86
[Co(dbm) <sub>2</sub> (dmae)] <b>59</b>	-13.26	3.75
[Co(tmhd) <sub>2</sub> (phen)] <b>60</b>	-15.63	2.91
[Co(tmhd) <sub>2</sub> (2,2'-bpy)] <b>61</b>	-14.55	2.91
[Co(tmhd) <sub>2</sub> (dmae)] <b>62</b>	-12.67	4.54
[Co(dbm) <sub>2</sub> (phen)] <sup>+</sup> <b>57</b> <sup>+</sup>	16.93 (17.31)	3.29
[Co(dbm) <sub>2</sub> (2,2'-bpy)] <sup>+</sup> <b>58</b> <sup>+</sup>	18.01 (18.16)	3.24
[Co(dbm) <sub>2</sub> (dmae)] <sup>+</sup> <b>59</b> <sup>+</sup>	17.93 (16.61)	3.70
[Co(tmhd) <sub>2</sub> (phen)] <sup>+</sup> <b>60</b> <sup>+</sup>	16.12 (16.38)	3.48
[Co(tmhd) <sub>2</sub> (2,2'-bpy)] <sup>+</sup> <b>61</b> <sup>+</sup>	17.15 (17.19)	3.40
[Co(tmhd) <sub>2</sub> (dmae)] <sup>+</sup> <b>62</b> <sup>+</sup>	17.41 (17.60)	4.27

The molecular orbital analysis reveals that in the case of **59** and **60-62** complexes the SOMO is composed of an antibonding interaction between  $\beta$ -diketonate oxygen p-orbitals and the cobalt  $d_{z2}$  orbital (see Figure 26). The dmae complexes also exhibit an additional antibonding interaction between the metal orbital and a hybrid  $\sigma$  donor orbital on the NMe<sub>2</sub> nitrogen of the dmae ligand. The SOMO of related bipy and phen complexes, **60** and **61** are different from the others with a metal  $d_{xz}$  orbital involved in a weaker antibonding interaction with the  $\beta$ -diketonate ligands. The significant electron density on the  $\beta$ -diketonate ligands in **57-62** is consistent with the strong influence of the  $\beta$ -

diketonate upon the oxidation potentials of the above complexes. In the case of **57**, **58**, **60** and **61**, the LUMO is essentially a low lying phen or bipy  $\pi^*$  orbital while for **59** and **62** the absence of such  $\pi^*$  orbitals results in a LUMO which is dominated by a  $\beta$ -diketonate  $\pi^*$  orbital (Figure 27). Consequently, a much larger SOMO-LUMO gap is observed in the case of the dmae complexes compared with **60**, **61**, **57** and **58** (see Table 22).

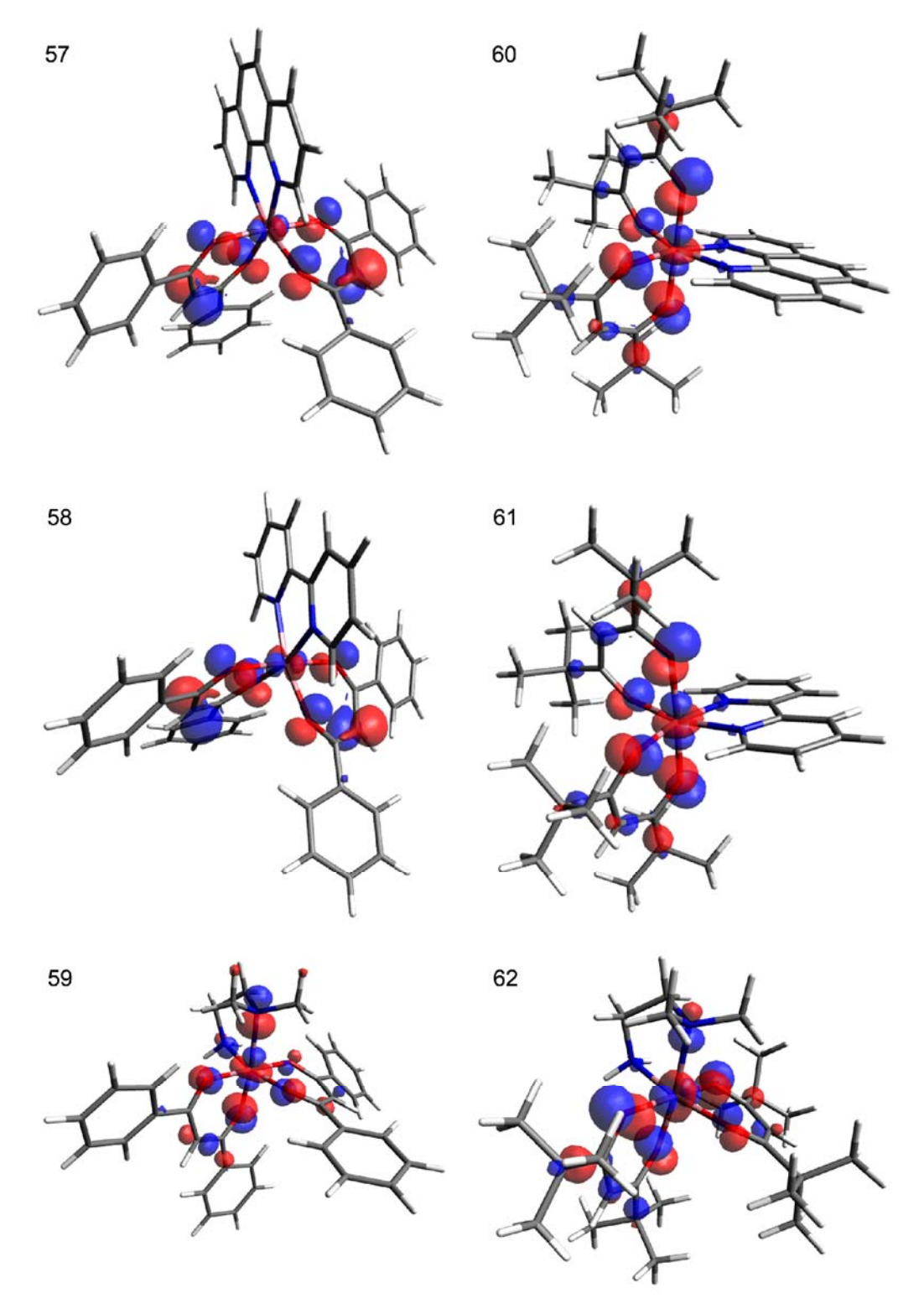


Figure 26 The SOMO orbital of complexes 57-62.

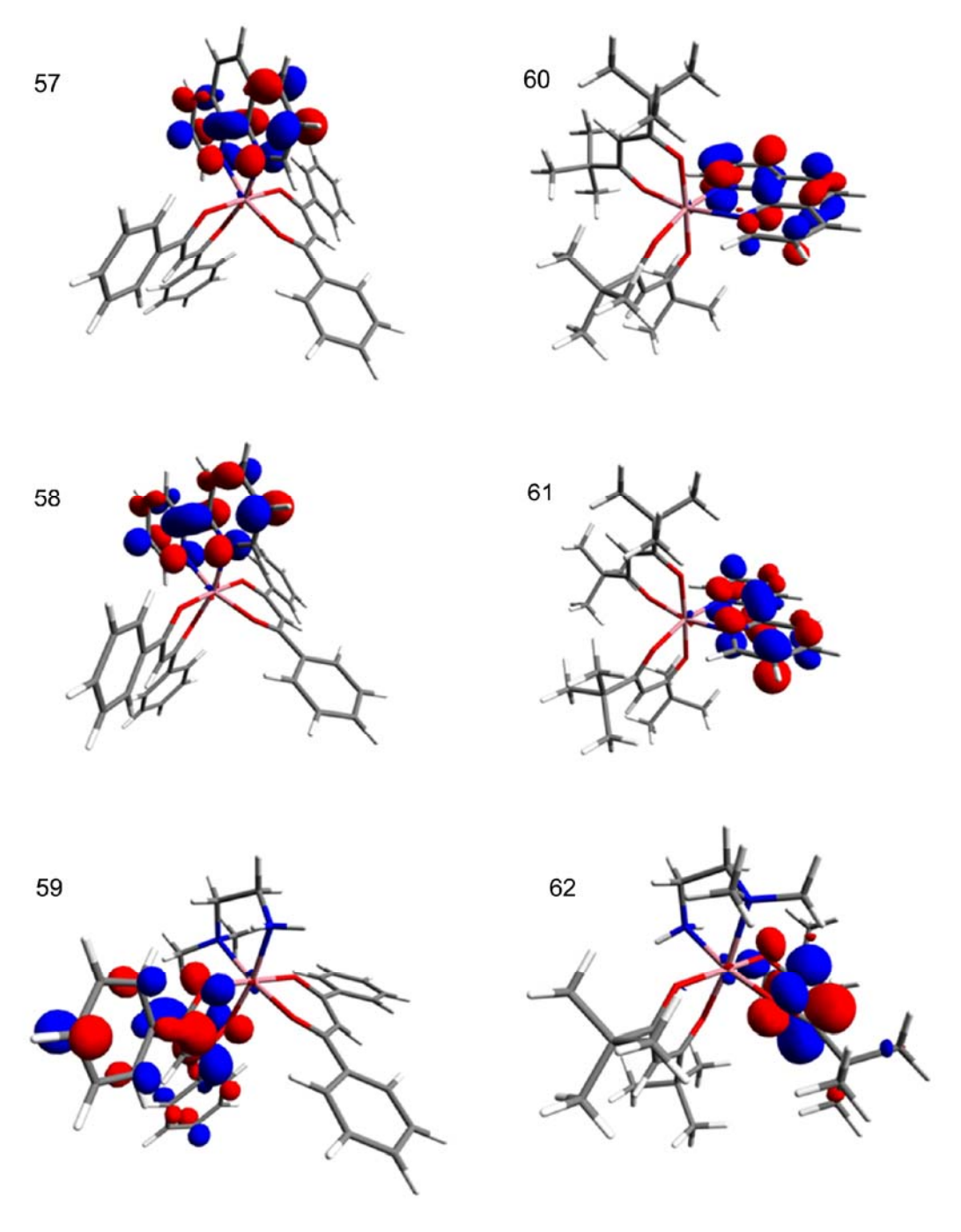


Figure 27 The LUMO orbital of complexes 57-62.

Further DFT calculations have been undertaken on the  $[Co(\beta\text{-diketonate})_2(ppa^X)]$  33-56 series (Tables 23 and 24) and these confirm the findings from electrochemical studies that the SOMO of the complex is dominated by the Co and  $\beta$ -diketonate orbitals with little contribution from the ppa<sup>X</sup> ligand. As with 57-62 the LUMO is based strong on the ppa<sup>X</sup> ligand suggesting that the strong colours observed for these complexes are the result of MLCT bands from an appropriate metal d-orbital into a low lying  $\pi^*$  orbital on the ligand.

**Table 23** The high-spin and low-spin complex energy difference, E(HS)-E(LS), at B3LYP/SDD level for  $[Co(\beta\text{-diketonate})_2(ppa^X)]$  complexes **33-56**. The E(LUMO)-E(SOMO) gap was estimated from the alpha spin orbital energy of the most stable spin state.

Complex	E(HS)-E(LS)/(kcal.mol <sup>-1</sup> )	E(LUMO)-E(SOMO)/eV
[Co(dbm) <sub>2</sub> (ppa <sup>H</sup> )] <b>33</b>	-12.74	2.83
$[Co(dbm)_2(ppa^{Me})]$ 34	-12.74	2.85
$[Co(dbm)_2(ppa^{Et})]$ 35	-12.36	2.84
[Co(dbm) <sub>2</sub> (ppa <sup>OMe</sup> )] <b>36</b>	-12.32	2.86
[Co(dbm) <sub>2</sub> (ppa <sup>F</sup> )] <b>37</b>	-12.38	2.76
[Co(dbm) <sub>2</sub> (ppa <sup>Cl</sup> )] <b>38</b>	-12.31	2.73
[Co(dbm) <sub>2</sub> (ppa <sup>Br</sup> )] <b>39</b>	-14.47	2.73
[Co(dbm) <sub>2</sub> (ppa <sup>l</sup> )] <b>40</b>	-12.36	2.73
[Co(tmhd) <sub>2</sub> (ppa <sup>H</sup> )] <b>41</b>	-13.04	2.62
$[Co(tmhd)_2(ppa^{Me})]$ <b>42</b>	-13.03	2.66
[Co(tmhd) $_2$ (ppa <sup>Et</sup> )] <b>43</b>	-12.49	2.67
$[Co(tmhd)_2(ppa^{OMe})]$ 44	-13.16	2.67
[Co(tmhd) <sub>2</sub> (ppa <sup>F</sup> )] <b>45</b>	-12.42	2.59
[Co(tmhd) <sub>2</sub> (ppa <sup>Cl</sup> )] <b>46</b>	-12.92	2.56
$[Co(tmhd)_2(ppa^{Br})]$ 47	-13.04	2.56
[Co(tmhd) <sub>2</sub> (ppa <sup>l</sup> )] <b>48</b>	-13.10	2.56
[Co(hfac) <sub>2</sub> (ppa <sup>H</sup> )] <b>49</b>	-13.34	3.66
[Co(hfac) <sub>2</sub> (ppa <sup>Me</sup> )] <b>50</b>	-13.36	3.52
[Co(hfac) <sub>2</sub> (ppa <sup>Et</sup> )] <b>51</b>	-13.37	3.50
[Co(hfac) <sub>2</sub> (ppa <sup>OMe</sup> )] <b>52</b>	-13.42	3.21
[Co(hfac) <sub>2</sub> (ppa <sup>F</sup> )] <b>53</b>	-13.46	3.63
[Co(hfac) <sub>2</sub> (ppa <sup>Cl</sup> )] <b>54</b>	-13.13	3.52
[Co(hfac) <sub>2</sub> (ppa <sup>Br</sup> )] <b>55</b>	-13.14	3.50
[Co(hfac) <sub>2</sub> (ppa <sup>l</sup> )] <b>56</b>	-13.39	3.35

**Table 24** The high-spin and low-spin complex energy difference, E(HS)-E(LS), at B3LYP/SDD level for  $[Co(β-diketonate)_2(ppa^X)]^+$  complexes  $33^+-56^+$ . The E(LUMO)-E(SOMO) gap was estimated from the alpha spin orbital energy of the most stable spin state.

Complex	E(HS)-E(LS)/(kcal.mol <sup>-1</sup> )	E(LUMO)-E(SOMO)/eV
[Co(dbm) <sub>2</sub> (ppa <sup>H</sup> )]OTf <b>33</b> <sup>+</sup>	15.98	2.85
$[Co(dbm)_2(ppa^{Me})]OTf$ <b>34</b> <sup>+</sup>	15.97	2.90
$[Co(dbm)_2(ppa^{Et})]OTf$ 35 <sup>+</sup>	16.03	2.90
$[Co(dbm)_2(ppa^{OMe})]OTf$ <b>36</b> <sup>+</sup>	15.93	2.92
$[Co(dbm)_2(ppa^F)]OTf$ 37 <sup>+</sup>	15.80	2.81
[Co(dbm)₂(ppa <sup>Cl</sup> )]OTf <b>38</b> <sup>+</sup>	15.73	2.80
[Co(dbm) <sub>2</sub> (ppa <sup>Br</sup> )]OTf <b>39</b> <sup>+</sup>	15.77	2.80
$[Co(dbm)_2(ppa^l)]OTf$ <b>40</b> <sup>+</sup>	15.74	2.80
[Co(tmhd) <sub>2</sub> (ppa <sup>H</sup> )]OTf <b>41</b> <sup>+</sup>	15.29	3.02
$[Co(tmhd)_2(ppa^{Me})]OTf$ <b>42</b> <sup>+</sup>	15.46	3.01
$[Co(tmhd)_2(ppa^{Et})]OTf$ <b>43</b> <sup>+</sup>	14.19	3.11
$[Co(tmhd)_2(ppa^{OMe})]OTf$ <b>44</b> <sup>+</sup>	14.64	3.01
[Co(tmhd) <sub>2</sub> (ppa <sup>F</sup> )]OTf <b>45</b> <sup>+</sup>	15.79	3.05
[Co(tmhd) <sub>2</sub> (ppa <sup>Cl</sup> )]OTf <b>46</b> <sup>+</sup>	14.50	3.04
$[Co(tmhd)_2(ppa^{Br})]OTf$ 47 <sup>+</sup>	15.16	2.98
[Co(tmhd) <sub>2</sub> (ppa <sup>l</sup> )]OTf <b>48</b> <sup>+</sup>	14.42	3.03
[Co(hfac) <sub>2</sub> (ppa <sup>H</sup> )]OTf <b>49</b> <sup>+</sup>	18.39	3.35
[Co(hfac) <sub>2</sub> (ppa <sup>Me</sup> )]OTf <b>50</b> <sup>+</sup>	18.53	3.03
[Co(hfac) <sub>2</sub> (ppa <sup>Et</sup> )]OTf <b>51</b> <sup>+</sup>	18.49	2.99
[Co(hfac) <sub>2</sub> (ppa <sup>OMe</sup> )]OTf <b>52</b> <sup>+</sup>	15.97	2.94
[Co(hfac) <sub>2</sub> (ppa <sup>F</sup> )]OTf <b>53</b> <sup>+</sup>	19.82	3.28
[Co(hfac) <sub>2</sub> (ppa <sup>Cl</sup> )]OTf <b>54</b> <sup>+</sup>	24.57	3.00
[Co(hfac) <sub>2</sub> (ppa <sup>Br</sup> )]OTf <b>55</b> <sup>+</sup>	18.18	2.80
[Co(hfac)₂(ppa¹)]OTf <b>56</b> <sup>+</sup>	17.86	2.43

The dimers have proved to be much more difficult to model as it is necessary the model the potential communication between the metals. However, preliminary results from these studies indicate that, as expected, the shortest ligand bpmhd, has the strongest degree of communication with the other ligands revealing only weak communication. This is particularly surprising in the case of the 1,5-bpmna ligand as it places the metals very far from each other. Perhaps the large  $\pi$  cloud of

the naphthalene linker aids electronic communication. Further work is still on going to provide more definitive answers into the exact communication process and the orbitals on the metal and ligand that may be used to facilitate it.

#### 5. References

- 1. Létard, J.-F.; Guionneau, P.; Goux-Capes, L. Top. Curr. Chem. 2004, 235, 221.
- 2. Kahn, O. Martinez, C. J. Science 1998, 279, 44.
- 3. Fabbrizzi, L.; Licchelli, M.; Pallavicini, P. Acc. Chem. Rev. 1999, 32, 846.
- 4. Venturi, M.; Credi, A.; Balzani, V. Coord. Chem. Rev. 1999,
- 5. H. A. Goodwin, Coord. Chem. Rev. 1976, 18, 293.
- (a) Real, J. A.; Gaspar, A. B.; Niel, V.; Muñoz, M. C. Coord. Chem. Rev. 2003, 236, 121. (b)
   Garcia, Y.; Niel, V.; Muñoz, M. C. and Real, J. A. Top. Curr. Chem. 2004, 233, 229.
- 7. Murray, K. S.; Kepert, C. J. *Top. Curr. Chem.* **2004**, *233*, 195.
- 8. Gaspar, A. B.; Ksenofontov, V.; Real, J. A.; Gütlich, P. Chem. Phys. Lett. 2003, 373, 385.
- (a) Spiering, H.; Kohlhaas, T.; Romstedt, H.; Hauser, A.; Bruns-Yilmaz, C.; Gütlich, P. Coord. Chem. Rev. 1999, 190–192, 629.
   (b) Gütlich, P.; Hauser, A.; Spiering, H. Angew. Chem., Int. Ed. Engl. 1994, 33, 2024.
- (a) Real, J. A. in *Transition Metals in Supramolecular Chemistry*, ed. Sauvage, J. P. John Wiley and Sons, Ltd., Chichester, 1999, p. 53. (b) Real, J. A.; Gaspar, A. B.; Muñoz, M. C.; Gütlich, P.; Ksenofontov, V.; Spiering, H. *Top. Curr. Chem.* 2004, 233, 167.
- 11. Haasnoot, J. G. Coord. Chem. Rev. 2000, 200, 131.
- 12. Breuning, E.; Ruben, M.; Lehn, J. M.; Renz, F.; Garcia, Y.; Ksenofontov, V.; Gütlich, P.; Wegelius, E.; Rissanen, K. *Angew. Chem., Int. Ed.* **2000**, *39*, 2504.
- 13. Real, J. A.; Andres, E.; Muñoz, M. C.; Julve, M.; Granier, T.; Bousseksou, A.; Varret, F. *Science* **1995**, *268*, 265.
- 14. Halder, G. J.; Kepert, C. J.; Moubaraki, B.; Murray, K. S.; Cashion, J. D. *Science* **2002**, *298*, 1762.
- 15. Madeja, K.; König, E. J. Inorg. Nucl. Chem. 1963, 25, 377.
- 16. Sieber, R.; Decurtins, S.; Stoeckli, H.; Evans, C.; Wilson, D.; Yufit, J. A. K.; Howard, S. C.; Capelli, A.; Hauser, A. *Chem. Eur. J.* **2000**, *6*, 361.
- 17. (a) Zerara, M.; Hauser, A. *Chem. Phys. Chem.* **2004**, *5*, 395. (b) Hauser A.; Amstutz, N.; Delahaye, S.; Schenker, S.; Sadki, A.; Sieber, R.; Zerara, M. *Struct. Bond.* **2004**, *106*, 81.
- (a) Hogg, R.; Wilkins, R. G. J. Chem. Soc. 1962, 341. (b) Judge, J. S.; Baker, W. A. Inorg. Chim. Acta 1967, 1, 68.

- 19. Figgis, B. N.; Kucharski, E. S.; White, A.H. Aust. J. Chem. 1983, 36, 1537.
- 20. Scheidt, W. R.; Reed, C. A. Chem. Rev. 1981, 81, 543.
- 21. Bertani, I.; Gray, H. B.; Lippard, S. J.; Valentine, J. S. *Bioinorganic Chemistry*, University Science Books, Sausalito, CA, **1994**.
- 22. Lippard, S. J.; Berg, J. M. *Principles of Bioinorganic Chemistry*, University Science Books, Mill Balley, CA, **1995**.
- 23. Kaim, W.; Schwederski, B. *Bioinorganic Chemistry: Inorganic Elements in the Chemistry of Life*, Wiley, New York, **1995**.
- 24. Sligar, S. C. Biochemistry **1976**, *15*, 5399.
- 25. Mueller, E. J.; Lioda, P. J.; Sligar, S. C. in *Cytochrome P450: Structure, Mechanism and Biochemistry*, ed. Ortiz de Montellano, P.R. 2<sup>nd</sup> ed., Plenum Press, New York, 1995, Chap.
   3.
- 26. Rees, D. C.; Chan, M. K.; Kim, J. Adv. Inorg. Chem. 1993, 40, 89.
- 27. Burgess, B. K.; Lowe, D. J. Chem. Rev. 1996, 96, 2983.
- 28. Lopes, H.; Pettigrew, G. W.; Moura, I.; Moura, J. J. G. J. Biol. Inorg. Chem. 1998, 3, 632.
- 29. Hendry, P.; Ludi, A. Adv. Inorg. Chem. 1990, 35, 117.
- 30. Stynes, H.C.; Ibers, J.A. *Inorg. Chem.* **1971**, *10*, 2304.
- 31. Buhks, E.; Bixon, M.; Jortner, J.; Navon, G. Inorg. Chem. 1979, 18, 2014.
- 32. Geselowitz, D.A., Taube, H. Adv. Inorg. Bioinorg. Mech. 1982, 1, 391.
- 33. Larsson, S.; Ståhl, K.; Zerner, M.C. Inorg. Chem. 1986, 25, 3033.
- 34. Geselowitz, D.A. Inorg. Chim. Acta 1988, 154, 225.
- 35. Newton, M.D. J. Phys. Chem. 1991, 95, 30.
- 36. Shalders, R.D.; Swaddle, T.W. Inorg. Chem. 1995, 34, 4815.
- 37. Swaddle, T.W. Can. J. Chem. 1996, 74, 631.
- 38. Turner, J. W.; Schultz, F. A. Inorg. Chem. 1999, 38, 358.
- 39. Turner, J. W.; Schultz, F. A. J. Phys. Chem. B 2002, 106, 2009.
- 40. Lord, R. L.; Schultz, F. A., Baik, M.-H. J. Am. Chem. Soc. 2009, 131, 6189.
- 41. Nakamoto, K. in *Infrared and Raman Spectra of Inorganic and Coordination Compounds:*Part B, 6<sup>th</sup> ed., Wiley, New York, **2009**, pp. 96-104.
- 42. Harding, P.; Harding, D. J.; Phonsri, W.; Saithong, S.; Phetmung, H. *Inorg. Chim. Acta* **2009**, *362*, 78.
- 43. Cotton, F.A.; Wilkinson, G.; Murillo, C.A.; Bochmann, M. in *Advanced Inorganic Chemistry*, 6<sup>th</sup> ed.; John Wiley & Sons, New York, **1999**, pp. 817-822.

- 44. Bandoli, G.; Barreca, D.; Gasparotto, A.; Maccato, C.; Seraglia, R.; Tondello, E.; Devi, A.; Fischer, R. A.; Winter, M. *Inorg. Chem.* **2009**, *48*, 82.
- 45. Nagashima, N.; Kudoh, S.; Nakata, M. Chem. Phys. Lett. 2003, 374, 59.
- 46. Sankhla, D. S.; Mathur, R. C.; Misra, S. N. J. Inorg. Nuc. Chem. 1980, 42, 489.
- 47. Chassot, P.; Emmenegger, F. *Inorg. Chem.* **1996**, *35*, 5931.
- 48. Archer, R. D.; Cotsoradis, B. P. Inorg. Chem. 1965, 4, 1584.
- 49. York, R. J.; Bonds, W.D. Jr.; Cotsoradis, B. P.; Archer, R. A. Inorg. Chem. 1969, 8, 789.
- 50. Izumi, F.; Kurosawa, R.; Kawamoto, H.; Akaiwa, H. Bull. Chem. Soc. Jpn. 1975, 48, 3188.
- 51. Turner, J. W.; Schultz, F. A. Coord. Chem. Rev. 2001, 219-221, 81.
- 52. For examples of other Co complexes exhibiting RCSCO see (a) Buhks, E.; Dixon, M.; Jortner, J.; Navon, G. *Inorg. Chem.* 1979, 18, 2014. (b) Endicott, J. F.; Brubaker, G. R.; Ramasami, T.; Kumar, K.; Dwarakanath, K.; Cassel, J.; Johnson, D. *Inorg. Chem.* 1983, 22, 3754. (c) Hammershøi, A.; Geselowitz, D.; Taube, H. *Inorg. Chem.* 1984, 32, 979. (d) Bernhardt, P. V.; Jones, L. A.; Sharpe, P. C. *Inorg. Chem.* 1997, 36, 2420.
- 53. Johansson, F. B.; Bond, A. D.; Nielson, U. G.; Moubaraki, B.; Murray, K. S.; Berry, K. J.; Larrabee, J. A.; McKenzie, C. J. *Inorg. Chem.* **2008**, *47*, 5079.
- 54. De Alwis, D. C. L.; Schultz, F. A. *Inorg. Chem.* **2003**, *42*, 3616.
- 55. Wieghardt, K.; Schmidt, W.; Herrmann, W.; Kueppers, H. J. Inorg. Chem. 1983, 22, 2953.
- 56. Kueppers, H. J.; Neves, A.; Pomp, C.; Ventur, D.; Wieghardt, K.; Nuber, B.; Weiss, J. *Inorg. Chem.* **1986**, *25*, 2400.
- 57. Richards, T. C.; Geiger, W.E. J. Am. Chem. Soc. 1994, 116, 2028.
- Gaussian O3, Revision D.O1, Frisch, M. J.; Trucks, G. W.; Schlegel, H. B.; Scuseria, G. E.; Robb, M. A.; Cheeseman, J. R.; Montgomery, Jr., J. A.; Vreven, T.; Kudin, K. N.; Burant, J. C.; Millam, J. M.; Iyengar, S. S.; Tomasi, J.; Barone, V.; Mennucci, B.; Cossi, M.; Scalmani, G.; Rega, N.; Petersson, G. A.; Nakatsuji, H.; Hada, M.; Ehara, M.; Toyota, K.; Fukuda, R.; Hasegawa, J.; Ishida, M.; Nakajima, T.; Honda, Y.; Kitao, O.; Nakai, H.; Klene, M.; Li, X.; Knox, J. E.; Hratchian, H. P.; Cross, J. B.; Bakken, V.; Adamo, C.; Jaramillo, J.; Gomperts, R.; Stratmann, R. E.; Yazyev, O.; Austin, A. J.; Cammi, R.; Pomelli, C.; Ochterski, J. W.; Ayala, P. Y.; Morokuma, K.; Voth, G. A.; Salvador, P.; Dannenberg, J. J.; Zakrzewski, V. G.; Dapprich, S.; Daniels, A. D.; Strain, M. C.; Farkas, O.; Malick, D. K.; Rabuck, A. D.; Raghavachari, K.; Foresman, J. B.; Ortiz, J. V.; Cui, Q.; Baboul, A. G.; Clifford, S.; Cioslowski, J.; Stefanov, B. B.; Liu, G.; Liashenko, A.; Piskorz, P.; Komaromi, I.; Martin, R. L.; Fox, D. J.; Keith, T.; Al-Laham, M. A.; Peng, C. Y.; Nanayakkara, A.; Challacombe, M.; Gill, P. M. W.; Johnson, B.;

- Chen, W.; Wong, M. W.; Gonzalez, C.; and Pople, J. A.; Gaussian, Inc., Wallingford CT, 2004.
- 59. Meštrović, E; Kaitner, B. J. Chem. Crystallogr. 2006, 36, 599.
- 60. Barreca, D.; Massignan, C.; Daolio, S.; Fabrizio, M.; Piccirillo, C.; Armelao, L.; Tondello, E. *Chem. Mater.* **2001**, *13*, 588.
- 61. Barrios, L. A.; Ribas, J.; Aromí, G.; Ribas-Ariño, J.; Gamez, P.; Roubeau, O.; Teat, S. J. *Inorg. Chem.* **2007**, *46*, 7154.
- 62. Evans, D. F. J. Chem. Soc. 1959, 2003–2005.
- 63. Shaw, M. J., Henson, R. L., Houk, S. E., Westhoff, J. W., Richter-Addo, G. B., Jones, M. W. *J. Electroanal. Chem.* **2002**, *534*, 47
- 64. Becke, A. D. J. Chem. Phys. 1993, 98, 1372.
- 65. Stephens, P. J.; Devlin, F. J.; Frisch, M. J.; Chabalowski, C. F. *J. Phys. Chem.* **1994**, *98*, 11623.
- 66. Dunning Jr., T. H.; Hay, P. J. in *Modern Theoretical Chemistry*, ed. H. F. Schaefer III, Vol. 3 Plenum, New York, **1976**, pp. 1-28.
- 67. Dolg, M.; Wedig, U.; Stoll, H.; Preuss, H. J. Chem. Phys. 86, 1987, 866.

#### 6. Project Outcomes

#### 6.1. Publications

Two international papers have been published in *Australian Journal of Chemistry* and *Acta Crystallographica Section E*, one has been accepted and a further paper is in the final stages of preparation for submission.

- 1. P. Harding, D. J. Harding, K. Tinpun, S. Samuadnuan, N. Sophonrat and H. Adams, Synthesis and electrochemical studies of nickel  $\beta$ -diketonate complexes incorporating asymmetric diimine ligands, *Aust. J. Chem*, 2010, **63**, 75.
- 2. P. Harding, D. J. Harding, N. Sophonrat and H. Adams, Bis(1,1,1,5,5,5-hexafluoropentane-2,4-dionato- $\kappa^2$ -O,O')[(4-bromo-phenyl)pyridin-2-ylmethyleneamine- $\kappa^2$ -N,N']cobalt(II), Acta Cryst. Section E, 2010, E**66**, m1138.
- 3. P. Harding, D.J. Harding, N. Soponrat and H. Adams, Bis(1,1,1,5,5,5-hexafluoropentane-2,4-dionato- $\kappa^2$ -O,O')[(4-bromo-phenyl)pyridin-2-ylmethylene amine– $\kappa^2$ -N,N']nickel(II), submitted to *Acta Cryst. Section E.*
- 4. P. Harding, D. J. Harding, R. Daengngern, T. Thurakitsaree, B. M. Schutte, M. J. Shaw and Y. Tantirungrotechai, Redox Coupled-Spin Crossover in Cobalt β-Diketonate Complexes: Observation of the High Spin Co<sup>III</sup> Intermediate, to be submitted to *Eur. J. Inorg. Chem.*

Two more publications on the nickel dimer complexes  $[(\beta\text{-diketonate})_2\text{Ni}(\mu\text{-L})\text{Ni}(\beta\text{-diketonate})_2]$  and the redox coupled spin crossover  $[\text{Co}(\beta\text{-diketonate})_2(\text{ppa}^X)]$  complexes will be prepared shortly. Further DFT calculations of  $[(\beta\text{-diketonate})_2\text{Co}(\mu\text{-L})\text{Co}(\beta\text{-diketonate})_2]$  should also provide another publication in a high impact factor journal.

#### **6.2.** Presentations

Four oral and three poster presentations have been made upon this work.

- P. Harding and D.J. Harding, Electronic Communication Between Two Metal β-Diketonate Complexes Bridged by Diimine Linkers, the Pure and Applied Chemistry International Conference 2011 (PACCON 2011), January 2011, Bangkok, Thailand.
- 2. P. Harding, D.J. Harding, R. Daengngern, T. Thurakitsaree, B.M. Schutte, M.J. Shaw and Y. Tantirungrotechai, Redox Coupled-Spin Crossover in  $[Co(\beta\text{-diketonate})_2(N\text{-N})]^{0/+}$  Complexes, the Pure and Applied Chemistry International Conference 2010 (PACCON 2010), February 2010, Ubon Ratchathani, Thailand.
- 3. P. Harding, D.J. Harding, Y. Tantirungrotechai and A. Sayananon, Redox Coupled-Spin Crossover Cobalt  $\beta$ -Diketonate Complexes: Synthesis, Electron Transfer Studies and DFT Calculations, TRF Annual Meeting, October 2010, Phetchaburi, Thailand.
- 4. P. Harding, Simultaneous UV-Vis Spectroelectrochemistry, Metrohm Siam Ltd. Seminar, August 2009, Bangkok, Thailand.
- 5. P. Harding, D.J. Harding, N. Soponrat, K. Tinpun, S. Samuadnuan and H. Adams, Synthesis and Electrochemical Studies of Nickel  $\beta$ -Diketonate Complexes Incorporating Asymmetric Diimine Ligands, The  $8^{th}$  Conference of the Inorganic Chemistry Division, December 2008, Christchurch, New Zealand.
- 6. P. Harding and D.J. Harding, Electronic Communication in Redox Coupled-Spin Crossover Cobalt Dimers, TRF Annual Meeting, October 2009, Phetchaburi, Thailand.
- 7. P. Harding, D.J. Harding, N. Soponrat, K. Tinpun, S. Samuadnuan and H. Adams, Electron Transfer Studies of  $[Ni(\beta-Diketonate)_2(ppa^R)]$ , TRF Annual Meeting, October 2008, Phetchaburi, Thailand.

#### 6.3. Collaborations with International/national Institutes and Awards

As a result of this project we have developed two new collaborations:

 Professor Mike Shaw at Southern Illinois University Edwardsville, USA is working with us on developing spectroelectrochemistry here in Thailand.

- 2. Assoc. Prof. Dr. Supa Hannongbau at Kasedsart University, Thailand was supervised undergraduate student from Computational Science program, Walailak University on the DFT calculations of [Ni(β-diketonate)<sub>2</sub>(ppa<sup>x</sup>)] complexes.
- 3. Assist. Prof. Dr. Yuthana Tantirungrotechai, NANOTEC, Thailand is working with us on the DFT calculations of the Co spin-crossover system.
- 4. Won the UMAP travelling grant to study the Co spin crossover by using spectroelectrochemistry at Southern Illinois University Edwardsville, USA during May 2009-June 2009.

#### 6.4. Training new generation of Thai researchers in Inorganic Chemistry

There are three schemes for training the young researchers in our laboratory: through "Young researcher training summer project", the undergraduate senior projects and the master thesis project.

Young	researcher	training	1.	Miss Kittiya Tinpun, Thaksin University
summer	project		2.	Miss Sirirat Samuadnuan, Thaksin University
			3.	Mr. Nitisart Soponrat, Thaksin University
			4.	Miss Sirikan Thongmeang, Rangsit University
			5.	Miss Angkana Kongbunkeaw, Thammasat University
			6.	Miss Tuanjai Somboon, Walailak University
Undergr	aduate senior	projects	1.	Miss Tuanjai Somboon, Walailak University
			2.	Mr. Rathawat Daengngern, Walailak University
Master t	hesis project		1.	Miss Apiraya Sayananon, MSc student, Thammasat University

Appendix One
International Publication

www.publish.csiro.au/journals/ajc

# Synthesis and Electrochemical Studies of Nickel $\beta$ -Diketonate Complexes Incorporating Asymmetric Diimine Ligands

Phimphaka Harding, A,D David J. Harding, A,D Nitisastr Soponrat, B Kittiya Tinpun, B Sirirat Samuadnuan, and Harry Adams C

The reaction of  $ppa^X$  {(4-X-phenyl)-pyridin-2-ylmethylene-amine; X = H, Me, Et, OMe, F, Cl, Br, and I} with [Ni( $\beta$ -diketonate)<sub>2</sub>(H<sub>2</sub>O)<sub>2</sub>] { $\beta$ -diketonate = 1,3-diphenylpropanedionate (dbm), 2,2,6,6-tetramethyl-3,5-heptadionate (tmhd), or hexafluoroacetylacetonate (hfac)} yields a series of nickel complexes. X-ray crystallography reveals octahedral coordinated nickel centres with a cis arrangement of the  $\beta$ -diketonate ligands. The  $\beta$ -diketonate ligands adopt 'planar' or 'bent' coordination modes, whereas the aryl ring of the ppa<sup>X</sup> ligand is twisted with respect to the pyridylimine unit. The electrochemical behaviour of the complexes reveals quasi-reversible or irreversible one-electron oxidation to Ni(III) in the case of the [Ni(tmhd)<sub>2</sub>(ppa<sup>X</sup>)] and [Ni(dbm)<sub>2</sub>(ppa<sup>X</sup>)] complexes, respectively. The peak potential for oxidation is dependent on the type of  $\beta$ -diketonate ligand but essentially independent of the substituent, X, on the ppa<sup>X</sup> ligand. The [Ni( $\beta$ -diketonate)<sub>2</sub>(ppa<sup>X</sup>)] complexes (X = F, Cl, Br, and I) also undergo ligand based reduction.

Manuscript received: 20 April 2009. Manuscript accepted: 15 July 2009.

#### Introduction

Metal β-diketonates represent an important class of complexes and have been extensively studied due to their ease of synthesis, ready modification, and multiple applications.<sup>[1-3]</sup> In the case of divalent metal ions, the  $[M(\beta-diketonate)_2]$  complexes are able to coordinate additional ligands forming octahedral metal complexes.<sup>[4]</sup> The nature of the chelating ligands can have a significant effect on the properties of the complexes and therefore their subsequent application. Thus, chelating alkyl diamines are used to synthesize volatile precursors for the preparation of metal-oxide thin films<sup>[5,6]</sup> whereas organic radicals may be used to construct single molecule magnets. [7-10] However, in much of the reported literature on such octahedral metal-β-diketonate adducts only acac or hfac ligands (acac = acetylacetonate, hfac = hexafluoroacetyl-acetonate) are used with the larger dbm and tmhd ligands (dbm = 1,3-diphenylpropanedionate, tmhd = 2,2,6,6-tetramethylheptanedionate) remaining poorly represented.

While metal- $\beta$ -diketonate adducts have found many applications, to date little research has been concerned with the redox chemistry of these systems. [11–13] However, recent studies in our group have shown that the complexes, [Ni( $\beta$ -diketonate)<sub>2</sub>(L)] ( $\beta$ -diketonate = dbm, tmhd; L = bipy, phen), which incorporate the less widely used dbm and tmhd ligands and diimines are electrochemically active oxidizing to rare Ni(III) species. [14] In an attempt to develop this area of chemistry we have undertaken a course of research into the chemistry of [M( $\beta$ -diketonate)<sub>2</sub>(L)] complexes. The bipyridine and phenanthroline ligands used in this preliminary study, while commercially available, are

difficult to derivatize. In contrast, iminopyridines are easy to prepare and readily modified. Moreover, the different substituents on the aryl group might be expected to allow subtle changes in the steric and electronic properties of the ligands, which may in turn, affect the structure and redox chemistry of the complexes. A further point is that unlike bipy and phen, iminopyridines are asymmetric, which may also influence the chemistry of the system. In the following paper we report the synthesis, structural characterization, and redox chemistry of a series of novel  $[Ni(\beta-diketonate)_2(ppa^X)]$  complexes.

#### **Results and Discussion**

Synthesis and Characterization

The synthesis of the (4-X-phenyl)-pyridin-2-ylmethylene-amine  $(ppa^{X})$  ligands, where X = H(1), Me (2), Et (3), OMe (4), F (5), Cl (6), Br (7), and I (8), was achieved by a simple condensation reaction between pyridine-2-carboxaldehyde and the appropriate substituted aniline in diethyl or diisopropyl ether (Scheme 1). While many of these ligands have been reported previously, [15,16] we found that in most cases the reported procedure did not give the expected ppa<sup>X</sup> cleanly. Instead considerable quantities of the starting materials remained. Hannon et al. recently reported the use of molecular sieves in an improved preparation of ppa<sup>H</sup>, to remove the water produced during the course of the reaction.<sup>[17]</sup> We therefore added molecular sieves to the reaction mixture and found that this simple addition significantly increased yields, purity, and also reduced reaction times. The molecular sieves are readily removed by filtration once the reaction is complete. The ligands have been characterized by IR, UV-vis, and <sup>1</sup>H NMR

<sup>&</sup>lt;sup>A</sup>Molecular Technology Research Unit, School of Science, Walailak University, Thasala, Nakhon Si Thammarat, 80161, Thailand.

<sup>&</sup>lt;sup>B</sup>Department of Chemistry, Faculty of Science, Taksin University, Songkhla, 90000, Thailand.

<sup>&</sup>lt;sup>C</sup>Department of Chemistry, University of Sheffield, Brook Hill, Sheffield S3 7HF, UK.

<sup>&</sup>lt;sup>D</sup>Corresponding authors. Email: kphimpha@wu.ac.th; hdavid@wu.ac.th

76 P. Harding et al.

**Scheme 1.** Synthesis of ppa<sup>X</sup> ligands.

**Scheme 2.** Synthesis of  $[Ni(\beta-diketonate)_2(ppa^X)]$  complexes.

spectroscopy. IR spectroscopy of the ligands revealed a medium intensity imine stretch between 1623 and 1626 cm<sup>-1</sup> in line with those for previously reported ppa<sup>X</sup> compounds.<sup>[15–17]</sup> The <sup>1</sup>H NMR spectra were recorded in CDCl<sub>3</sub> showing a singlet between 8.58 and 8.68 ppm for the imino proton confirming the formation of the desired ppa<sup>X</sup> ligands. The peaks for the pyridyl and phenylene groups are assigned on the basis of their splitting patterns, coupling constants, and intergration values and are typical of such iminopyridine ligands.

The reaction of  $[Ni(dbm)_2(H_2O)_2]$ ,  $[Ni(tmhd)_2(H_2O)_2]$ , or [Ni(hfac)<sub>2</sub>(H<sub>2</sub>O)<sub>2</sub>] with the eight ppa<sup>X</sup> ligands, in CH<sub>2</sub>Cl<sub>2</sub>, THF or acetone affords red, brown, and yellow solids of the octahedral complexes [Ni(dbm)<sub>2</sub>(ppa<sup>X</sup>)]  $\{X = H(9), Me(10), Me(10),$ Et (11), OMe (12), F (13), Cl (14), Br (15), and I (16)}, [Ni(tmhd)<sub>2</sub>(ppa<sup>X</sup>)] {X = H (17), Me (18), Et (19), OMe (20), F (21), Cl (22), Br (23), and I (24)}, and  $[Ni(hfac)_2(ppa^X)]$  $\{X = H(25), Me(26), Et(27), OMe(28), F(29), Cl(30), Br$ (31), and I (32)} (Scheme 2). The red, brown, and yellow colours of these compounds are in marked contrast with the related [Ni( $\beta$ -diketonate)<sub>2</sub>(L)] (L = bpy, phen) complexes, which are green<sup>[14]</sup> and indicative of absorption by the ppa<sup>X</sup> ligand. The expected d-d transitions are unfortunately obscured by these strong UV bands. IR spectroscopy of complexes 9-24 shows a C=O stretch from 1588 to 1595 cm<sup>-1</sup>, similar to that reported for the  $[Ni(\beta-diketonate)_2(L)]$  (L = bpy, phen) complexes (1582– 1595 cm<sup>-1</sup>),<sup>[14]</sup> and indicative of a chelating coordination mode for the β-diketonate ligand. [18] The C=O stretch for the hfac compounds, 25–32, is on average 60 cm<sup>-1</sup> higher than that observed for complexes 9-24, consistent with the strong electron withdrawing effect of the CF3 groups. The imine stretches of coordinated ppaX ligands which are expected to be between 1580 and 1590 cm<sup>-1</sup> are not observed as they masked by the strong C=O stretch of the  $\beta$ -diketonate ligand.

#### Crystallographic Studies

The molecular structures of complexes 10, 12, and 14 were determined by X-ray crystallography (Table 1). The structures of 10 and 12 are shown in Figs 1 and 2, respectively. Crystals of all complexes were grown by allowing hexane to diffuse slowly into a concentrated solution of the complex in  $CH_2Cl_2$  at room temperature.

Table 1. Selected bond lengths [Å] and angles [°] of 10, 12, and 14

	10	12	14
Ni-O(1)	2.013(3)	2.0349(12)	2.0091(16)
Ni-O(2)	2.005(3)	2.0135(12)	2.0205(17)
Ni-O(3)	2.027(3)	2.0479(12)	2.0165(16)
Ni-O(4)	2.010(4)	2.0163(12)	2.0128(16)
Ni-N(1)	2.090(4)	2.0812(14)	2.091(2)
Ni-N(2)	2.180(4)	2.1096(14)	2.189(2)
O(1)-Ni-O(2)	89.05(14)	88.93(5)	90.66(6)
O(3)-Ni-O(4)	90.58(14)	88.18(5)	89.29(6)
N(1)-Ni-N(2)	76.81(16)	78.60(6)	77.31(8)
$\beta^{\mathrm{A}}$	2.98	31.94	16.57
	17.06	24.72	1.51
$\gamma^{ m B}$	22.87	39.50	23.99
Intermolecular distances <sup>C</sup>			
O(1)-H(8)	2.439		
O(3)-H(8)		2.615	2.396
O(3)-H(6)		2.578	

 $<sup>^{</sup>A}\beta$  is the angle between the plane defined by the carbon and oxygen atoms of the  $\beta$ -diketonate ligand and the plane defined by the nickel and two oxygen atoms.

Complexes **10**, **12**, and **14** assume slightly distorted octahedral coordination geometries. The  $\beta$ -diketonate ligands exhibit a *cis* arrangement enforced by the chelating ppa<sup>X</sup> ligand. The Ni–O bond lengths vary between 2.005 and 2.048 Å for the three complexes and are similar to other previously reported nickel  $\beta$ -diketonate adducts, [Ni(dbm)<sub>2</sub>(en)] {2.009(6), 2.060(7) Å}, [19] and [Ni(dbm)<sub>2</sub>(phen)] {2.035(1), 2.041(1) Å}. [14]

The nickel bond to the pyridine of the ppa<sup>X</sup> ligand of complexes **10** and **14** is considerably shorter than the bond to the imine nitrogen, differing by  $\sim$ 0.1 Å. In contrast, the Ni–N bond lengths for **12** are different by only 0.03 Å. It is also interesting to note that in [Cu(ppa<sup>2Me,3Me</sup>)<sub>2</sub>]ClO<sub>4</sub><sup>[16]</sup> and [Ru(bipy)<sub>2</sub>(ppa<sup>H</sup>)][PF<sub>6</sub>]<sub>2</sub>, [17] the imine nitrogen metal bond is

 $<sup>^{\</sup>mathrm{B}}\gamma$  is the angle between the plane of the pyridylimine unit and the plane of the substituted phenyl ring.

<sup>&</sup>lt;sup>C</sup>Non-bonded metrics and those involving centroids were not included in the structure refinement, and thus do not have an estimated standard deviation.

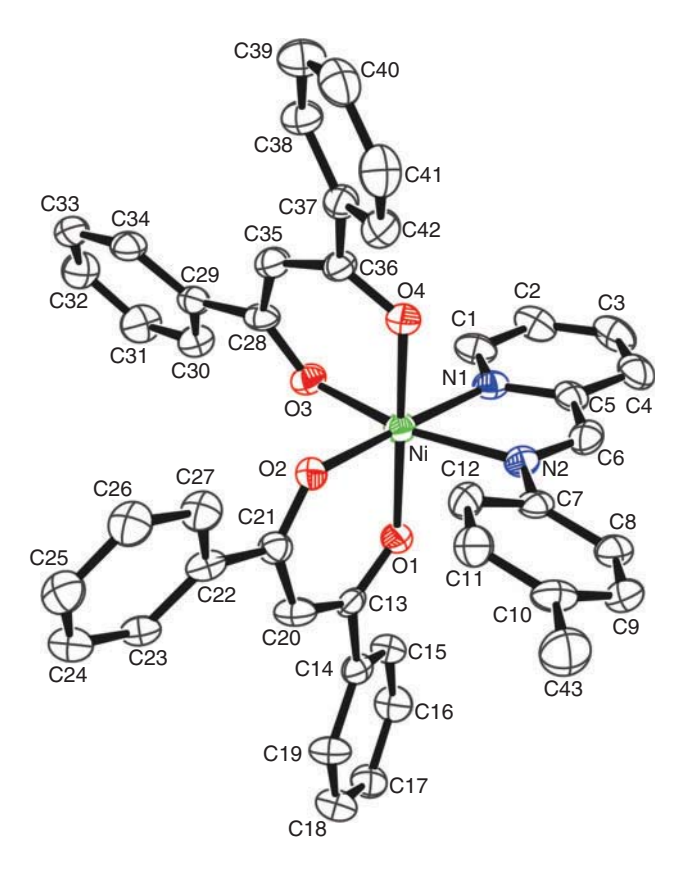


Fig. 1. *ORTEP* diagram of  $[Ni(dbm)_2(ppa^{Me})]$  10. The thermal ellipsoids are drawn to 50% probability level. Hydrogen atoms are omitted for clarity.

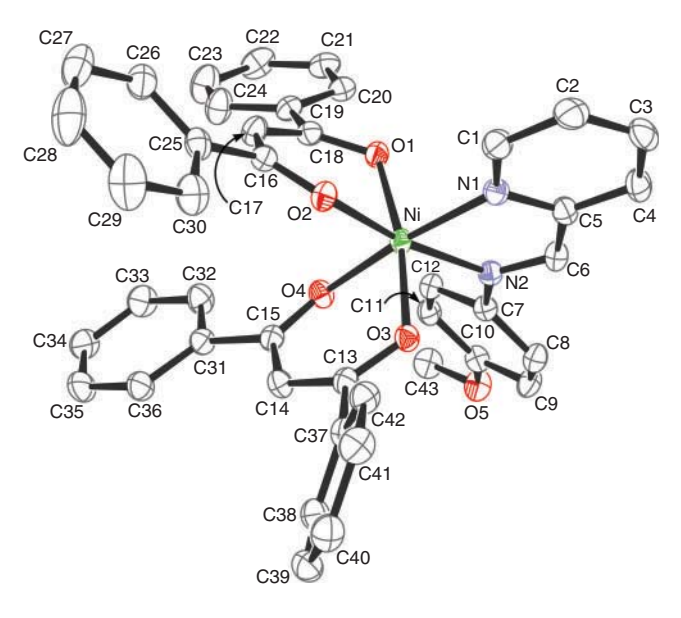
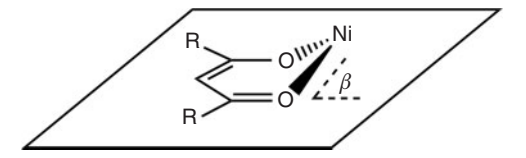


Fig. 2. ORTEP diagram of [Ni(dbm)<sub>2</sub>(ppa<sup>OMe</sup>)] 12. The thermal ellipsoids are drawn to 50% probability level. Hydrogen atoms are omitted for clarity.

shorter than the pyridine nitrogen metal bond. The reason for this difference remains unclear. The phenyl ring in all the complexes is twisted with respect to the pyridylimine unit. Interestingly, the angle for 12 is  $39.5^\circ$ , whereas those of 10 and 14 are  $22.9^\circ$  and  $24.0^\circ$ , respectively. By comparison [Cu(ppa^2Me,3Me)\_2]ClO4 and [Ru(bipy)\_2(ppa^H)][PF\_6]\_2 exhibit angles of  $69^\circ$  and  $45^\circ$ , respectively.  $^{[16,17]}$  The phenyl ring is positioned above the



**Fig. 3.** Schematic diagram showing the angle  $\beta$  between the  $\beta$ -diketonate and NiO<sub>2</sub> planes.

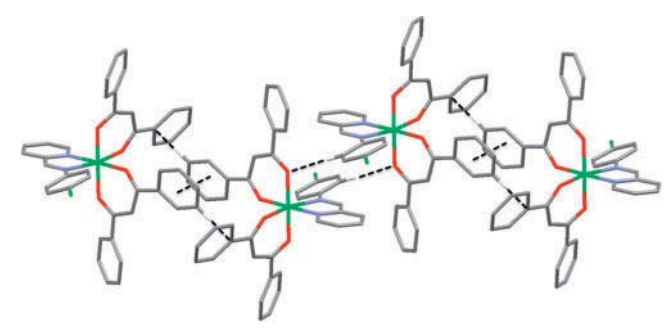


Fig. 4. Mercury plot showing the  $CH\cdots O$  and  $\pi$ - $\pi$  interactions in  $[Ni(dbm)_2(ppa^{Cl})]$  14. For clarity, only hydrogen atoms involved in interactions are shown.

pyridyl ring of a neighbouring ppa<sup>X</sup> ligand but is neither co-planar with, nor perpendicular to, that pyridyl ring.

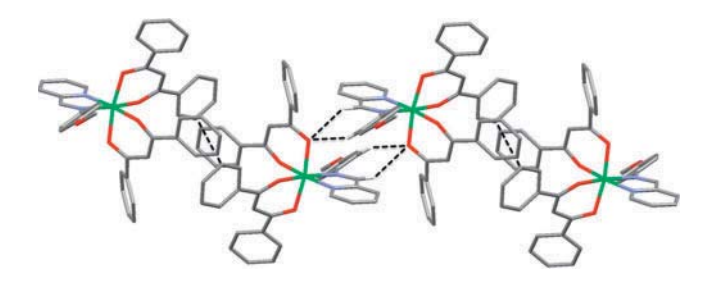
The  $\beta$ -diketonate ligand is essentially planar and symmetric suggesting that the negative charge is delocalized over the  $\beta$ -diketonate framework. As noted in other nickel  $\beta$ -diketonate adducts the nickel centre lies above the plane of the dbm ligand in a 'bent' coordination mode. [14] The extent of this displacement has been determined by calculating the angle between the plane of the  $\beta$ -diketonate framework and the plane defined by the nickel and two oxygen atoms (Fig. 3). For complex 12 both dbm ligands exhibit a 'bent' coordination mode, whereas for 10 and 14 only one of the dbm ligands is 'bent' with the other assuming a 'planar' coordination mode. This is probably the result of the different substituents on the ppa ligands.

The complexes are packed into chiral columns with each column exhibiting the same helicity and adjacent columns of alternate helicity as shown in Figs 4 and 5. The molecules are arranged so that the ppa<sup>X</sup> ligands are positioned above one another with the substituent alternately pointing 'in' and 'out'. The interaction principally involved here is between a C-H group from the phenyl ring of the ppaX ligand and a coordinated oxygen atom from the dbm ligand. The structure of 12 is slightly different revealing a further interaction from the imino C-H to the same oxygen atom. As a result of the stacking of the ppa<sup>X</sup> ligands, the dbm ligands are also stacked in columns. As might be expected, this leads to  $\pi$ - $\pi$  interactions between two adjacent dbm phenyl rings (centroid-centroid 3.653 and 3.651 Å for 10 and 14, respectively). The absence of this interaction in the structure of 12 once again seems to stem from the extra space needed to accommodate the ppa<sup>OMe</sup> ligand and the subsequent 'bent' coordination mode of both dbm ligands which preclude this interaction. Surprisingly, the  $\pi\text{-}\pi$  interaction is not replaced by any face to edge CH- $\pi$  interactions.

#### Electrochemical Studies

The redox properties of the complexes **9–32** were studied by cyclic voltammetry (CV) in CH<sub>2</sub>Cl<sub>2</sub> at 25°C (Table 2). The CVs of **13**, **21**, and **29** are shown in Fig. 6 as representative examples. Complexes **9–16** exhibit an irreversible oxidation wave, whereas

78 P. Harding et al.



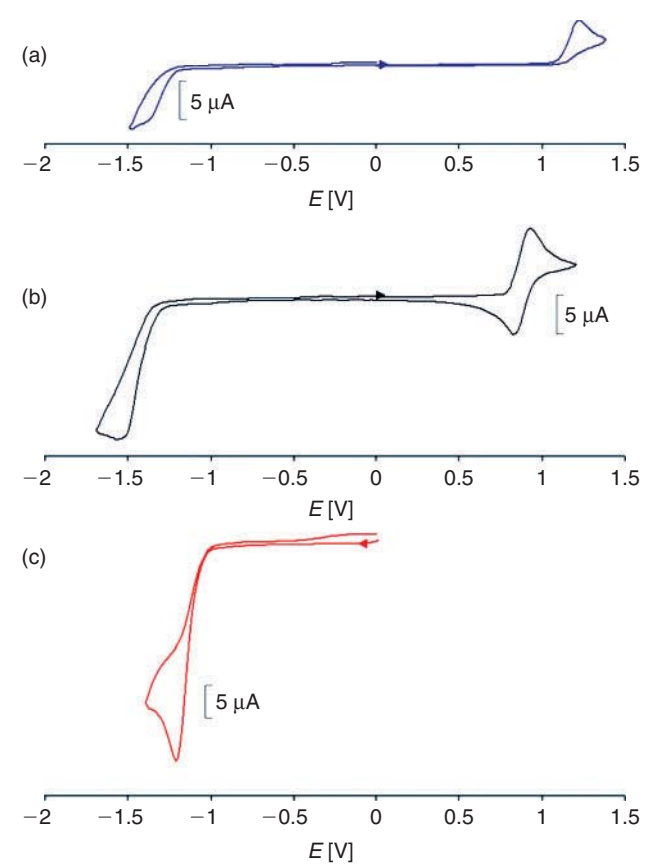
**Fig. 5.** Mercury plot showing the  $CH\cdots O$  interactions in  $[Ni(dbm)_2(ppa^{OMe})]$  **12.** For clarity, only hydrogen atoms involved in interactions are shown.

Table 2. Electrochemical data of  $[Ni(\beta-diketonate)_2(ppa^X)]$  complexes<sup>A</sup>

Complex	Oxidation process $E^{o'}/E_p [V]^B$	Reduction process $E_p$ [V]
9	0.67 (I)	_
10	0.66 (I)	_
11	0.66 (I)	_
12	0.66 (I)	_
13	0.68 (I)	-1.94 (I)
14	0.72 (I)	-1.84 (I)
15	0.68 (I)	-1.85 (I)
16	0.70 (I)	-1.83 (I)
17	0.33	- ` `
18	0.32	_
19	0.31	_
20	0.32, 0.97 (I)	_
21	0.35	-2.09 (I)
22	0.35	-2.01(I)
23	0.36	-1.98 (I)
24	0.37	-2.00 (I)
25	_	-1.76 (I)
26	_	$-1.79  (I)^{C}$
27	_	-1.69 (I)
28	_	-1.74 (I)
29	_	$-1.73  (I)^{C}$
30	_	-1.57 (I)
31	_	-1.61 (I)
32	0.58 (I)	-1.61 (I)

<sup>&</sup>lt;sup>A</sup>All measurements were performed at 298 K, in dried and degassed  $CH_2Cl_2$  0.1 M [NBu<sub>4</sub><sup>n</sup>][PF<sub>6</sub>] solution; scan rate 100 mV s<sup>-1</sup>; calibrated with [FeCp<sub>2</sub>], and reported relative to the [FeCp<sub>2</sub>]<sup>0/+</sup> couple.

those of 17–24 undergo quasi-reversible oxidation, albeit only at scan rates above 200 mV s $^{-1}$ . Comparison with the related cobalt complexes  $[Co(\beta\text{-}diketonate)_2(L)]$  ( $\beta\text{-}diketonate = dbm, tmhd, L=bpy, phen), which oxidize between <math display="inline">-0.15$  and  $0.06\,\mathrm{V}$  (versus  $[FeCp_2]^{0/+}$ ) to give the isolable  $Co(\mathrm{III})$  cations, suggest that the oxidation is to Ni(III) and, as such, represent rare examples of Ni(III) species (P. Harding and D. J. Harding, unpubl. data). As expected the [Ni( $\beta$ -diketonate)\_2(ppa^X)] complexes are oxidized at potentials very similar to the analogous [Ni( $\beta$ -diketonate)\_2(L)] ( $\beta$ -diketonate = dbm, tmhd; L = bpy, phen) complexes.  $^{[14]}$  This is unsurprising given the structural similarity between the ligands. Attempts to chemically oxidize the complexes have thus far proved unsuccessful.



**Fig. 6.** Cyclic voltammogram of (a)  $[Ni(dbm)_2(ppa^F)]$  **13**, (b)  $[Ni(tmhd)_2(ppa^F)]$  **21**, and (c)  $[Ni(hfac)_2(ppa^F)]$  **29**. All potentials are versus  $[FeCp_2]^{0/+}$ .

The peak potentials for oxidation of **9–16** are between 0.32 and 0.37 V more positive than those of **17–24**. It is clear that the tmhd ligands are considerably more electron donating than the dbm ligands, presumably as a result of the inductive effect of the *t*-butyl groups on the tmhd ligands. The hfac ligands also have a significant effect on the peak potential for oxidation with no oxidation observed within the solvent window, with the exception of **32**. This is consistent with the findings of Villamena et al., in which the oxidation potential for [Ni(hfac)<sub>2</sub>(2-pyBN)] (2-pyBN = N-*tert*-butyl- $\alpha$ -(2-pyridyl)nitrone) is observed at 1.80 V (versus Ag/AgCl). [11]

In contrast to the considerable effect that the  $\beta$ -diketonate ligand has on the peak potential for oxidation, the different ppa<sup>X</sup> ligands result in only minor changes in the peak potential for oxidation. A similar insensitivity to the substituent has been observed in a series of Cu(I) compounds, [Cu(ppa<sup>X</sup>)<sub>2</sub>]ClO<sub>4</sub> (X = F, Cl, Br, and I). It is possible that the substituent on the ppa<sup>X</sup> ligand is simply too remote to significantly affect the peak potential for oxidation. Moreover, the twist between the phenyl ring and the pyridylimine unit seen in the solid state will reduce the degree of conjugation between the rings, thereby limiting the effect of the substituent on the oxidation potential. However, in the case of [Ni(tmhd)<sub>2</sub>(ppa<sup>OMe</sup>)] a second irreversible oxidation is also observed, although whether this is metal-based or ligand-based remains unclear. Further spectroelectrochemical studies are currently underway to determine the nature of this second oxidation and will be reported in a later publication.

<sup>&</sup>lt;sup>B</sup>For an irreversible (I) process the oxidation peak potential,  $(E_p)_{ox}$ , is given. <sup>C</sup>Uncalibrated as the compound reacts with [FeCp<sub>2</sub>].

Fig. 7. Hydrogen labels of the  $ppa^X$  ligands.

In addition to the metal-based oxidation noted above, the complexes also undergo irreversible reduction. In the case of the complexes with dbm or tmhd ligands, only when X = F, Cl, Br, and I, are reduction peaks observed. Given the absence of any reduction peaks for the other complexes; i.e. where X = H, Me, Et, and OMe; it seems likely that these reductions are ligand based. Despite this, the reductions show considerable variation, with differences between the hfac and dbm complexes being on average 235 mV, whereas those between the dbm and tmhd complexes are 155 mV. The reason for this variation may be the result of the differing degrees of  $\pi$ -backbonding from the metal centre to the ppa<sup>X</sup> ligand. Thus, the [Ni(tmhd)<sub>2</sub>(ppa<sup>X</sup>)] compounds are the most electron rich, resulting in considerable  $\pi$ -backbonding and are therefore, the most difficult to reduce. Conversely, the [Ni(hfac)<sub>2</sub>(ppa<sup>X</sup>)] complexes are the most electron poor, resulting in minimal  $\pi$ -backbonding, making the ppa<sup>X</sup> ligand easier to reduce. It is also noteworthy that when X = F the complexes are more difficult to reduce by  $\sim 0.1 \,\mathrm{V}$  than for [Ni( $\beta$ diketonate)<sub>2</sub>(ppa<sup>X</sup>)] ( $\beta$ -diketonate = dbm, tmhd, hfac; X = Cl, Br, I). A final point of interest is that 25-28 also exhibit irreversible reduction waves. Whether this results from the reduction of the hfac or ppaX ligands remains unclear.

#### Conclusions

In conclusion, we have prepared a series of [Ni(βdiketonate)<sub>2</sub>(ppa<sup>X</sup>)] complexes and have shown that the ppa<sup>X</sup> ligands are convenient alternatives to substituted bipyridine or phenanthroline ligands. The crystal structures reveal octahedral coordinated nickel centres, with the β-diketonate ligands exhibiting both 'bent' and 'planar' bidentate coordination modes dependent upon the type of ppa<sup>X</sup> ligand present. The aryl rings of the ppa<sup>X</sup> ligands are found to be non-coplanar with the pyridylimine unit, the degree of twisting dependent on the substituent, X. The complexes are irreversibly or quasi-reversibly oxidized to Ni(III) in the case of [Ni(dbm)<sub>2</sub>(ppa<sup>X</sup>)] and [Ni(tmhd)<sub>2</sub>(ppa<sup>X</sup>)], respectively. With the exception of [Ni(hfac)<sub>2</sub>(ppa<sup>I</sup>)] the hfac complexes show no oxidation processes. The [Ni(tmhd)<sub>2</sub>(ppa<sup>X</sup>)] complexes are more easily oxidized by ~350 mV than the [Ni(dbm)<sub>2</sub>(ppa<sup>X</sup>)] complexes indicating that the  $\beta$ -diketonate ligand has a significant effect on the redox potential. In contrast, the ppa<sup>X</sup> ligands have only a very minor effect on the redox potential with a difference of  $\sim 50 \,\mathrm{mV}$  between the various ppa<sup>X</sup> ligands.

#### **Experimental**

General Remarks

All reactions were conducted in air using HPLC grade solvents. [Ni(tmhd)<sub>2</sub>(H<sub>2</sub>O)<sub>2</sub>], [Ni(hfac)<sub>2</sub>(H<sub>2</sub>O)<sub>2</sub>], and [Ni(dbm)<sub>2</sub>(H<sub>2</sub>O)<sub>2</sub>] were prepared by literature methods. [1,20] Although the ppa ligands are known, our synthesis differs from that previously reported and thus, their syntheses are included in the interests

of completeness. All other chemicals were purchased from Fluka Chemical Co. and used as received. Infrared spectra were recorded on a Perkin-Elmer Spectrum One infrared spectrophotometer as KBr discs, in the range 400–4000 cm<sup>-1</sup>. Electronic spectra were recorded in CH<sub>2</sub>Cl<sub>2</sub> on a Unicam UV300 UV-Visible spectrometer. Elemental analyses were carried out on a Eurovector EA3000 analyzer. <sup>1</sup>H NMR spectra were recorded on a Bruker 300 MHz FT-NMR spectrometer at 298 K in CDCl<sub>3</sub> with SiMe<sub>4</sub> added as an internal standard. Hydrogen atoms are labelled according to Fig. 7. ESI-MS were carried out on a Bruker Daltonics 7.0T Apex 4 FTICR Mass Spectrometer. Electrochemical studies were carried out using a PalmsensPC Vs 2.11 Potentiosat in conjunction with a three electrode cell. The auxiliary electrode was a platinum rod and the working electrode was a platinum disc (2.0 mm diameter). The reference electrode was a Ag-AgCl electrode (2 M LiCl). Solutions were  $5 \times 10^{-4} \, \mathrm{mol} \, \mathrm{dm}^{-3}$  in the test compound and  $0.1 \, \mathrm{mol} \, \mathrm{dm}^{-3}$  in [NBu<sub>4</sub><sup>n</sup>][PF<sub>6</sub>] as the supporting electrolyte. Under these conditions, E<sup>o'</sup> for the one-electron oxidation of [FeCp<sub>2</sub>] added to the test solutions for internal calibration is 0.52 V.

Synthesis

Synthesis of (Phenyl)-pyridine-2-ylmethylene-amine  $(ppa^H)$  **1** 

To a solution of aniline (274  $\mu$ L, 3 mmol) in diethylether (10 mL) over molecular sieves, was added pyridine-2-carboxaldehyde (266  $\mu$ L, 3 mmol). The yellow solution was stirred overnight. The solution was filtered and the molecular sieves washed with CH<sub>2</sub>Cl<sub>2</sub> (5 mL). The solvent was removed under vacuum, yielding a bright yellow oil (0.273 g, 50%).  $\nu_{\rm max}$ (CH<sub>2</sub>Cl<sub>2</sub>)/cm<sup>-1</sup> 1630 ( $\nu_{\rm C=N}$ ).  $\lambda_{\rm max}$ (CH<sub>2</sub>Cl<sub>2</sub>)/nm (log  $\varepsilon$ /M<sup>-1</sup> cm<sup>-1</sup>) 236 (4.07), 278 (3.82), 318 (3.50).  $\delta_{\rm H}$  = 8.70 (1H, d,  $^{1}$ J<sub>HH</sub> 4.8, H<sub>a</sub>), 8.58 (1H, s, H<sub>e</sub>), 8.19 (1H, d,  $^{1}$ J<sub>HH</sub> 7.8, H<sub>d</sub>), 7.79 (1H, m,  $^{1}$ J<sub>HH</sub> 7.8, H<sub>c</sub>), 7.35 (3H, m, H<sub>f</sub>, H<sub>b</sub>), 7.20 (3H, m, H<sub>g</sub>, H<sub>H</sub>).

Ligands 2–8 were synthesized using the same procedure. Analytical and spectroscopic data are given for each compound.

Synthesis of (4-Methylphenyl)-pyridine-2-ylmethyleneamine ( $ppa^{Me}$ ) **2** 

Yellow crystalline solid (0.360 g, 62%).  $\nu_{max}(KBr)/cm^{-1}$  1625 ( $\nu_{C=N}$ ).  $\lambda_{max}(CH_2Cl_2)/nm$  (log  $\varepsilon/M^{-1}$  cm<sup>-1</sup>) 234 (4.23), 280 (4.12), 324 (4.00 sh).  $\delta_H = 8.71$  (1H, d,  $^1J_{HH}$  6.3,  $H_a$ ), 8.62 (1H, s,  $H_e$ ), 8.19 (1H, d,  $^1J_{HH}$  7.8,  $H_d$ ), 7.80 (1H, m,  $^1J_{HH}$  7.8,  $H_c$ ), 7.35 (1H, m,  $^1J_{HH}$  6.3,  $H_b$ ), 7.24 (4H, m,  $H_f$ ,  $H_g$ ), 2.36 (3H, s,  $CH_3$ ).

Synthesis of (4-Ethylphenyl)-pyridine-2-ylmethyleneamine ( $ppa^{Et}$ ) **3** 

Dull orange oil (0.375 g, 59%).  $\nu_{max}(CH_2Cl_2)/cm^{-1}$  1630 ( $\nu_{C=N}$ ).  $\lambda_{max}(CH_2Cl_2)/nm$  (log  $\varepsilon/M^{-1}$  cm<sup>-1</sup>) 234 (4.10), 280 (4.03), 324 (3.93 sh).  $\delta_H = 8.73$  (1H, d,  $^1J_{HH}$  4.8, H<sub>a</sub>), 8.68 (1H, s, H<sub>e</sub>), 8.24 (1H, d,  $^1J_{HH}$  7.8, H<sub>d</sub>), 7.85 (1H, m,  $^1J_{HH}$  7.5, H<sub>c</sub>), 7.23 (5H, m, H<sub>b</sub>, H<sub>f</sub>, H<sub>g</sub>), 2.69 (2H, q,  $^1J_{HH}$  7.2, CH<sub>2</sub>), 1.23 (3H, t,  $^1J_{HH}$  7.2, CH<sub>3</sub>).

Synthesis of (4-Methoxyphenyl)-pyridine-2-ylmethyleneamine (ppa $^{\mathrm{OMe}}$ ) 4

Light orange solid (0.423 g, 67%).  $\nu_{max}(KBr)/cm^{-1}$  1626 ( $\nu_{C=N}$ ).  $\lambda_{max}(CH_2Cl_2)/nm$  (log  $\varepsilon/M^{-1}$  cm<sup>-1</sup>) 238 (4.11), 286 (4.01), 340 (4.08).  $\delta_H=8.70$  (1H, d,  $^1J_{HH}$  7.2, Ha), 8.65 (1H, s, He), 8.20 (1H, d,  $^1J_{HH}$  7.8, Hd), 7.81 (1H, dd,  $^1J_{HH}$  8.1, 7.8,

80 P. Harding et al.

 $H_c$ ), 7.36 (3H, m,  $H_b$ ,  $H_g$ ), 6.94 (2H, m,  $^1J_{HH}$  8.7,  $H_f$ ), 3.83 (3H, s,  $CH_3$ ).

Synthesis of (4-Fluorophenyl)-pyridine-2-ylmethyleneamine  $(ppa^F)$  **5** 

Bright yellow crystalline solid (0.491 g, 82%).  $\nu_{max}(KBr)/cm^{-1}$  1627 ( $\nu_{C=N}$ ).  $\lambda_{max}(CH_2Cl_2)/nm$  (log  $\varepsilon/M^{-1}$  cm<sup>-1</sup>) 236 (3.91), 282 (3.91), 318 (3.75 sh).  $\delta_H = 8.80$  (1H, d,  $^1J_{HH}$  4.8, H<sub>a</sub>), 8.60 (1H, s, H<sub>e</sub>), 8.20 (1H, d,  $^1J_{HH}$  7.8, H<sub>d</sub>), 7.85 (1H, dd,  $^1J_{HH}$  7.5, 7.8, H<sub>c</sub>), 7.38 (1H, dd,  $^1J_{HH}$  7.5, 4.8, H<sub>b</sub>), 7.31 (2H, dd,  $^1J_{HH}$  8.1, 7.9, H<sub>f</sub>), 7.09 (2H, dd,  $^1J_{HH}$  7.9, 8.1, H<sub>g</sub>).

Synthesis of (4-Chlorophenyl)-pyridine-2-ylmethyleneamine ( $ppa^{Cl}$ ) **6** 

Pale yellow crystalline solid (0.452 g, 70%).  $\nu_{max}(KBr)/cm^{-1}$  1624 ( $\nu_{C=N}$ ).  $\lambda_{max}(CH_2Cl_2)/nm$  (log  $\varepsilon/M^{-1}$  cm<sup>-1</sup>) 238 (4.12), 280 (4.09), 320 (3.95 sh).  $\delta_H = 8.80$  (1H, d,  $^1J_{HH}$  5.1, Ha), 8.66 (1H, s, He), 8.30 (1H, d,  $^1J_{HH}$  8.1, Hd), 7.89 (1H, dd,  $^1J_{HH}$  8.1, 7.8, Hc), 7.44 (1H, dd,  $^1J_{HH}$  5.1, 7.8, Hb), 7.30 (2H, d,  $^1J_{HH}$  8.7, Hf), 7.01 (2H, d,  $^1J_{HH}$  8.7, Hg).

Synthesis of (4-Bromophenyl)-pyridine-2-ylmethyleneamine ( $ppa^{Br}$ ) 7

Brown solid (0.596 g, 76%).  $\nu_{max}(KBr)/cm^{-1}$  1623 ( $\nu_{C=N}$ ).  $\lambda_{max}(CH_2Cl_2)/nm$  (log  $\varepsilon/M^{-1}$  cm<sup>-1</sup>) 232 (4.12), 280 (4.12), 324 (3.97 sh).  $\delta_H = 8.73$  (1H, d,  $^1J_{HH}$  4.8, H<sub>a</sub>), 8.62 (1H, s, H<sub>e</sub>), 8.21 (1H, d,  $^1J_{HH}$  7.5, H<sub>d</sub>), 7.86 (1H, t,  $^1J_{HH}$  7.5, 6.9, H<sub>c</sub>), 7.53 (2H, d,  $^1J_{HH}$  7.8, H<sub>f</sub>), 7.42 (1H, dd,  $^1J_{HH}$  6.9, 4.8, H<sub>b</sub>), 7.18 (2H, d,  $^1J_{HH}$  7.8, H<sub>g</sub>).

Synthesis of (4-lodophenyl)-pyridine-2-ylmethyleneamine ( $ppa^{l}$ ) **8** 

Pale green solid (prepared in  $\it i\text{-}Pr_2O$ ) (0.605 g, 65%).  $\nu_{max}(KBr)/cm^{-1}$  1625 ( $\nu_{C=N}$ ).  $\lambda_{max}(CH_2Cl_2)/nm$  (log  $\it \epsilon/M^{-1}$  cm  $^{-1}$ ) 242 (4.21), 282 (4.07), 320 (4.00 sh).  $\delta_H=8.72$  (1H, dd,  $^1J_{HH}$  1.5, 4.8,  $H_a$ ), 8.58 (1H, s,  $H_e$ ), 8.15 (1H, d,  $^1J_{HH}$  8.1,  $H_d$ ), 7.96 (1H, ddd,  $^1J_{HH}$  1.5, 7.8, 8.1,  $H_c$ ), 7.54 (1H, ddd,  $^1J_{HH}$  0.9, 4.8, 7.8,  $H_b$ ), 7.31 (2H, d,  $^1J_{HH}$  8.4,  $H_f$ ), 7.09 (2H, d,  $^1J_{HH}$  8.4,  $H_g$ ).

#### Synthesis of $[Ni(dbm)_2(ppa^H)]$ **9**

To a lime green suspension of [Ni(dbm)<sub>2</sub>(H<sub>2</sub>O)<sub>2</sub>] (0.135 g, 0.25 mmol) in acetone (10 mL), was added a solution of ppa<sup>H</sup> (0.046 g, 0.25 mmol) in acetone (3 mL). The brown orange solution was stirred overnight then concentrated under vacuum. n-Hexane (10 mL) was added to precipitate a brown solid, which was washed with additional n-hexane (2 × 5 mL) and dried under vacuum, yielding a brown solid (0.106 g, 61%) (Found: C 73.4, H 4.6, N 3.9. Calc. for C<sub>42</sub>H<sub>32</sub>N<sub>2</sub>NiO<sub>4</sub>: C 73.4, H 4.7, N 4.1%). m/z (ESI) 463 (100%, [M-dbm<sup>-</sup>]<sup>+</sup>).  $\nu_{\rm max}$ (KBr)/cm<sup>-1</sup> 1595 ( $\nu_{\rm C=O}$ ).  $\lambda_{\rm max}$ (CH<sub>2</sub>Cl<sub>2</sub>)/nm (log  $\varepsilon$ /M<sup>-1</sup> cm<sup>-1</sup>) 259 (4.84), 277 (4.81), 352 (4.60).

Complexes 10–32 were synthesized by the same general procedure using acetone, THF, or  $CH_2Cl_2$  in the case of  $[Ni(dbm)_2(H_2O)_2]$ ,  $[Ni(tmhd)_2(H_2O)_2]$ , and  $[Ni(hfac)_2(H_2O)_2]$ , respectively. They were crystallized from the solvents indicated.

#### Synthesis of [Ni(dbm)<sub>2</sub>(ppa<sup>Me</sup>)] **10**

Dull green microcrystals (CH<sub>2</sub>Cl<sub>2</sub>/n-hexane) (0.207 g, 55%) (Found: C 73.5, H 4.9, N 4.1. Calc. for C<sub>43</sub>H<sub>34</sub>N<sub>2</sub>NiO<sub>4</sub>: C 73.6, H 4.9, N 4.0%). m/z (ESI) 477 (100%, [M-dbm<sup>-</sup>]<sup>+</sup>).

 $\nu_{max}(KBr)/cm^{-1}$  1595  $(\nu_{C=O}).~\lambda_{max}(CH_2Cl_2)/nm~(log~\epsilon/~M^{-1}~cm^{-1})$  248 (4.63), 358 (4.51).

#### Synthesis of [Ni(dbm)<sub>2</sub>(ppa<sup>Et</sup>)] **11**

Brown-yellow solid (acetone/n-hexane) (0.115 g, 64%) (Found: C 73.5, H 5.1, N 4.0. Calc. for C<sub>44</sub>H<sub>36</sub>N<sub>2</sub>NiO<sub>4</sub>: C 73.9, H 5.1, N 3.9%). m/z (ESI) 701 (100%, [M-dbm $^-$ +ppa<sup>Et</sup>] $^+$ ), 491 (28%, [M-dbm $^-$ ] $^+$ ).  $\nu_{\rm max}$ (KBr)/cm $^-$ 1 1595 ( $\nu_{\rm C=O}$ ).  $\lambda_{\rm max}$ (CH<sub>2</sub>Cl<sub>2</sub>)/nm (log  $\varepsilon$ /M $^-$ 1 cm $^-$ 1) 246 (4.45), 284 (4.23 sh), 356 (4.48).

#### Synthesis of $[Ni(dbm)_2(ppa^{OMe})]$ **12**

Brown-yellow solid (acetone/n-hexane) (0.122 g, 68%) (Found: C 72.2 H 5.0, N 3.9. Calc. for  $C_{43}H_{34}N_2NiO_5$ : C 72.0 H 4.8, N 3.9%). m/z (ESI) 493 (100%, [M-dbm<sup>-</sup>]+).  $\nu_{max}(KBr)/cm^{-1}$  1595 ( $\nu_{C=O}$ ).  $\lambda_{max}(CH_2Cl_2)/nm$  (log  $\varepsilon/M^{-1}$  cm<sup>-1</sup>) 250 (4.60), 282 (4.21 sh), 358 (4.54).

#### Synthesis of [Ni(dbm)<sub>2</sub>(ppa<sup>F</sup>)] **13**

Brown-yellow microcrystals (CH<sub>2</sub>Cl<sub>2</sub>/n-hexane) (0.222 g, 59%) (Found: C 71.2, H 4.6, N 4.2. Calc. for C<sub>42</sub>H<sub>31</sub>FN<sub>2</sub>NiO<sub>4</sub>: C 71.5, H 4.4, N 4.0%). m/z (ESI) 481 (100%, [M-dbm<sup>-</sup>]+).  $\nu_{max}$ (KBr)/cm<sup>-1</sup> 1595 ( $\nu_{C=O}$ ).  $\lambda_{max}$ (CH<sub>2</sub>Cl<sub>2</sub>)/nm (log  $\varepsilon$ /M<sup>-1</sup> cm<sup>-1</sup>) 246 (4.66), 284 (4.33 sh), 356 (4.53).

#### Synthesis of [Ni(dbm)<sub>2</sub>(ppa<sup>Cl</sup>)] **14**

Yellow solid (acetone/n-hexane) (0.114 g, 63%) (Found: C 71.2, H 4.7, N 3.9. Calc. for  $C_{42}H_{31}ClN_2NiO_4$ : C 69.9, H 4.3, N 3.9%). m/z (ESI) 497 (100%, [M-dbm $^-$ ] $^+$ ).  $\nu_{max}(KBr)/cm^{-1}$  1594 ( $\nu_{C=O}$ ).  $\lambda_{max}(CH_2Cl_2)/nm$  (log  $\varepsilon/M^{-1}$  cm $^{-1}$ ) 246 (4.61), 358 (4.50).

#### Synthesis of $[Ni(dbm)_2(ppa^{Br})]$ **15**

Yellow solid (acetone/n-hexane) (0.158 g, 82%) (Found: C 65.9, H 4.0, N 3.9. Calc. for  $C_{42}H_{31}BrN_2NiO_4$ : C 65.8, H 4.1, N 3.6%). m/z (ESI) 543 (100%, [M-dbm $^-$ ] $^+$ ).  $\nu_{max}(KBr)/cm^{-1}$  1593 ( $\nu_{C=O}$ ).  $\lambda_{max}(CH_2Cl_2)/nm$  (log  $\varepsilon/M^{-1}$  cm $^{-1}$ ) 247 (4.66), 355 (4.47).

#### Synthesis of [Ni(dbm)<sub>2</sub>(ppa<sup>1</sup>)] **16**

Brown solid (THF/n-hexane) (0.091 g, 44%) (Found: C 61.9, H 4.2, N 3.2. Calc. for  $C_{42}H_{31}IN_2NiO_4$ : C 62.0, H 3.8, N 3.4%). m/z (ESI) 897 (100%, [M-dbm $^-$ +ppa $^1$ ] $^+$ ), 589 (85%, [M-dbm $^-$ ] $^+$ ).  $\nu_{max}$  (KBr)/cm $^-$ 1 1594 ( $\nu_{C=O}$ ).  $\lambda_{max}$  (CH $_2$ Cl $_2$ )/nm (log  $\varepsilon/M^{-1}$  cm $^{-1}$ ) 248 (4.66), 286 (4.28 sh), 354 (4.50).

#### Synthesis of [Ni(tmhd)<sub>2</sub>(ppa<sup>H</sup>)] **17**

Brown solid (THF/*n*-hexane) (0.063 g, 41%) (Found: C 67.8, H 7.9, N 4.8. Calc. for  $C_{34}H_{48}N_2NiO_4$ : C 67.2, H 8.0, N 4.6%). m/z (ESI) 605 (37%, [M-tmhd<sup>-</sup> + ppa<sup>H</sup>]<sup>+</sup>), 423 (100%, [M-tmhd<sup>-</sup>]<sup>+</sup>).  $\nu_{max}(KBr)/cm^{-1}$  1591 ( $\nu_{C=O}$ ).  $\lambda_{max}(CH_2Cl_2)/nm$  (log  $\varepsilon/M^{-1}$  cm<sup>-1</sup>) 240 (4.36), 294 (4.28).

#### Synthesis of [Ni(tmhd)<sub>2</sub>(ppa<sup>Me</sup>)] **18**

Brown needles (slow evaporation of  $CH_2Cl_2$ ) (0.080 g, 52%) (Found: C 67.0, H 7.9, N 4.4. Calc. for  $C_{35}H_{50}N_2NiO_4$ : C 67.6, H 8.1, N 4.5%). m/z (ESI) 633 (100%, [M-tmhd<sup>-</sup> + ppa<sup>Me</sup>]<sup>+</sup>), 437 (88%, [M-tmhd<sup>-</sup>]<sup>+</sup>).  $\nu_{max}(KBr)/cm^{-1}$  1586 ( $\nu_{C=O}$ ).  $\lambda_{max}(CH_2Cl_2)/nm$  (log  $\varepsilon/M^{-1}$  cm<sup>-1</sup>) 240 (4.46), 272 (4.26 sh), 308 (4.42).

#### Synthesis of [Ni(tmhd)<sub>2</sub>(ppa<sup>Et</sup>)] **19**

Brown oil (0.066 g, 40%) (Found: C 67.8, H 8.0, N 4.1. Calc. for  $C_{36}H_{52}N_2NiO_4$ : C 68.0, H 8.2, N 4.4%). m/z (ESI) 451 (100%, [M-tmhd<sup>-</sup>]<sup>+</sup>).  $\nu_{max}(KBr)/cm^{-1}$  1591 ( $\nu_{C=O}$ ).  $\lambda_{max}(CH_2Cl_2)/nm$  (log  $\varepsilon/M^{-1}$  cm<sup>-1</sup>) 240 (4.40), 308 (4.35).

#### Synthesis of [Ni(tmhd)<sub>2</sub>(ppa<sup>OMe</sup>)] **20**

Red-brown solid (THF/*n*-hexane) (0.079 g, 37%) (Found: C 65.7, H 7.4, N 4.5. Calc. for  $C_{35}H_{50}N_2NiO_5$ : C 65.9, H 7.9, N 4.4%). m/z (ESI) 665 (100%, [M-tmhd $^-$  + ppa $^{OMe}]^+$ ), 453 (73%, [M-tmhd $^-]^+$ ).  $\nu_{max}$  (KBr)/cm $^{-1}$  1592 ( $\nu_{C=O}$ ).  $\lambda_{max}$  (CH $_2$ Cl $_2$ )/nm (log  $\varepsilon$ /M $^{-1}$  cm $^{-1}$ ) 242 (4.51), 316 (4.42) 354 (4.31 sh).

#### Synthesis of [Ni(tmhd)<sub>2</sub>(ppa<sup>F</sup>)] **21**

Brown needles (slow evaporation of CH<sub>2</sub>Cl<sub>2</sub>) (0.048 g, 32%) (Found: C 65.3, H 7.5, N 4.8. Calc. for C<sub>34</sub>H<sub>47</sub>FN<sub>2</sub>NiO<sub>4</sub>: C 65.3, H 7.6, N 4.5%).  $\emph{m/z}$  (ESI) 641 (13%, [M-tmhd<sup>-</sup> + ppa<sup>F</sup>]<sup>+</sup>), 441 (100%, [M-tmhd<sup>-</sup>]<sup>+</sup>).  $\nu_{max}(KBr)/cm^{-1}$  1591 ( $\nu_{C=O}$ ).  $\lambda_{max}(CH_2Cl_2)/nm$  (log  $\varepsilon/M^{-1}$  cm<sup>-1</sup>) 238 (4.46), 272 (4.27), 308 (4.45).

#### Synthesis of [Ni(tmhd)<sub>2</sub>(ppa<sup>Cl</sup>)] **22**

Red-brown solid (THF/n-hexane) (0.068 g, 42%) (Found: C 63.3, H 7.3, N 4.7. Calc. for  $C_{34}H_{47}ClN_2NiO_4$ : C 63.6, H 7.4, N 4.4%). m/z (ESI) 675 (13%, [M-tmhd $^-$  + ppa $^{Cl}$ ] $^+$ ), 457 (100%, [M-tmhd $^-$ ] $^+$ ).  $\nu_{\rm max}(KBr)/{\rm cm}^{-1}$  1588 ( $\nu_{\rm C=O}$ ).  $\lambda_{\rm max}(CH_2Cl_2)/{\rm nm}$  (log  $\varepsilon/{\rm M}^{-1}$  cm $^{-1}$ ) 240 (4.27), 303 (4.24).

#### Synthesis of [Ni(tmhd)<sub>2</sub>(ppa<sup>Br</sup>)] **23**

Brown solid (THF/*n*-hexane) (0.051 g, 29%) (Found: C 59.2, H 6.6, N 4.3. Calc. for  $C_{34}H_{47}BrN_2NiO_4$ : C 59.5, H 6.9, N 4.1%). *m/z* (ESI) 763 (100%, [M-tmhd<sup>-</sup> + ppa<sup>Br</sup>]<sup>+</sup>), 503 (88%, [M-tmhd<sup>-</sup>]<sup>+</sup>).  $\nu_{max}(KBr)/cm^{-1}$  1592 ( $\nu_{C=O}$ ).  $\lambda_{max}(CH_2Cl_2)/nm$  (log  $\varepsilon/M^{-1}$  cm<sup>-1</sup>) 244 (4.39).

#### Synthesis of [Ni(tmhd)<sub>2</sub>(ppa<sup>l</sup>)] **24**

Brown solid (THF/*n*-hexane) (0.091 g, 49%) (Found: C 55.2, H 6.5, N 3.7. Calc. for C<sub>34</sub>H<sub>47</sub>IN<sub>2</sub>NiO<sub>4</sub>: C 55.7, H 6.5, N 3.8%). *m/z* (ESI) 857 (100%, [M-tmhd<sup>-</sup> + ppa<sup>I</sup>]<sup>+</sup>), 549 (90%, [M-tmhd<sup>-</sup>]<sup>+</sup>).  $\nu_{max}$ (KBr)/cm<sup>-1</sup> 1592 ( $\nu_{C=O}$ ).  $\lambda_{max}$ (CH<sub>2</sub>Cl<sub>2</sub>)/nm (log  $\varepsilon$ /M<sup>-1</sup> cm<sup>-1</sup>) 252 (4.50), 276 (4.38).

#### Synthesis of [Ni(hfac)<sub>2</sub>(ppa<sup>H</sup>)]-0.5THF **25**

Yellow solid (THF/n-hexane) (0.076 g, 46%) (Found: C 41.3, H 2.2, N 4.3. Calc. for  $C_{24}H_{16}F_{12}N_2NiO_{4.5}$ : C 41.7, H 2.3, N 4.0%). m/z (ESI) 447 (100%, [M-hfac $^-$ ] $^+$ ).  $\nu_{max}$ (KBr)/cm $^-$ 1 1652 ( $\nu_{C=O}$ ).  $\lambda_{max}$ (CH $_2$ Cl $_2$ )/nm (log  $\varepsilon$ /M $^-$ 1 cm $^-$ 1) 243.5 (4.26), 285 (4.36), 315 (4.35).

#### Synthesis of [Ni(hfac)<sub>2</sub>(ppa<sup>Me</sup>)] $\cdot 0.5$ CH<sub>2</sub>Cl<sub>2</sub> **26**

Green-brown solid (CH<sub>2</sub>Cl<sub>2</sub>/n-hexane) (0.181 g, 98%) (Found: C 40.3, H 2.6, N 3.6. Calc. for C<sub>23.5</sub>H<sub>15</sub>ClF<sub>12</sub>N<sub>2</sub>NiO<sub>4</sub>: C 40.0, H 2.1, N 3.9%). m/z (ESI) 657 (100%, [M-hfac<sup>-</sup> + ppa<sup>Me</sup>]<sup>+</sup>), 461 (26%, [M-hfac<sup>-</sup>]<sup>+</sup>).  $\nu_{max}$ (KBr)/cm<sup>-1</sup> 1653 ( $\nu_{C=O}$ ).  $\lambda_{max}$ (CH<sub>2</sub>Cl<sub>2</sub>)/nm (log  $\varepsilon$ /M<sup>-1</sup> cm<sup>-1</sup>) 242 (4.20), 318 (4.40).

#### Synthesis of [Ni(hfac)<sub>2</sub>(ppa<sup>Et</sup>)] **27**

Brown solid (THF/n-hexane) (0.055 g, 31%) (Found: C 42.5, H 2.5, N 4.2. Calc. for  $C_{24}H_{16}F_{12}N_2NiO_4$ : C 42.2, H 2.4, N 4.1%). m/z (ESI) 685 (100%, [M-hfac $^-$  + ppa $^{Et}$ ] $^+$ ), 475 (84%,

[M-hfac<sup>-</sup>]<sup>+</sup>).  $\nu_{max}$ (KBr)/cm<sup>-1</sup> 1654 ( $\nu_{C=O}$ ).  $\lambda_{max}$ (CH<sub>2</sub>Cl<sub>2</sub>)/nm (log  $\varepsilon$ /M<sup>-1</sup> cm<sup>-1</sup>) 247 (4.23), 320 (4.31).

#### Synthesis of [Ni(hfac)<sub>2</sub>(ppa<sup>OMe</sup>)] **28**

Deep yellow solid (THF/n-hexane) (0.098 g, 54%) (Found: C 40.3, H 2.4, N 4.3. Calc. for  $C_{23}H_{14}F_{12}N_2NiO_5$ : C 40.3, H 2.1, N 4.1%). m/z (ESI) 477 (100%, [M-hfac $^-$ ]+).  $\nu_{max}(KBr)/cm^{-1}$  1647 ( $\nu_{C=O}$ ).  $\lambda_{max}(CH_2Cl_2)/nm$  (log  $\varepsilon/M^{-1}$  cm $^{-1}$ ) 255 (4.27), 325 (4.26).

#### Synthesis of $[Ni(hfac)_2(ppa^F)] \cdot 0.5C_6H_{14}$ **29**

Brown solid (CH<sub>2</sub>Cl<sub>2</sub>/*n*-hexane) (0.131 g, 78%) (Found: C 41.6, H 2.3, N 3.7. Calc. for C<sub>25</sub>H<sub>18</sub>F<sub>13</sub>N<sub>2</sub>NiO<sub>4</sub>: C 41.9, H 2.5, N 3.9%). m/z (ESI) 665 (100%, [M-hfac + ppa<sup>F</sup>] +), 465 (27%, [M-hfac ] +).  $\nu_{max}$  (KBr)/cm <sup>-1</sup> 1651 ( $\nu_{C=O}$ ).  $\lambda_{max}$  (CH<sub>2</sub>Cl<sub>2</sub>)/nm (log  $\varepsilon$ /M <sup>-1</sup> cm <sup>-1</sup>) 238 (4.26), 318 (4.45).

#### Synthesis of [Ni(hfac)<sub>2</sub>(ppa<sup>Cl</sup>)] **30**

Golden brown solid (CH<sub>2</sub>Cl<sub>2</sub>/n-hexane) (0.101 g, 58%) (Found: C 38.5, H 1.7, N 4.2. Calc. for C<sub>22</sub>H<sub>11</sub>ClF<sub>12</sub>N<sub>2</sub>NiO<sub>4</sub>: C 38.3, H 1.6, N 4.1%). m/z (ESI) 481 (100%, [M-hfac<sup>-</sup>]<sup>+</sup>).  $\nu_{max}$ (KBr)/cm<sup>-1</sup> 1651 ( $\nu_{C=O}$ ).  $\lambda_{max}$ (CH<sub>2</sub>Cl<sub>2</sub>)/nm (log  $\varepsilon$ /M<sup>-1</sup> cm<sup>-1</sup>) 240 (4.25), 319 (4.38).

#### Synthesis of [Ni(hfac)<sub>2</sub>(ppa<sup>Br</sup>)] **31**

Deep yellow solid (CH<sub>2</sub>Cl<sub>2</sub>/n-hexane) (0.096 g, 52%) (Found: C 36.2, H 1.7, N 3.9. Calc. for C<sub>22</sub>H<sub>11</sub>BrF<sub>12</sub>N<sub>2</sub>NiO<sub>4</sub>: C 36.0, H 1.5, N 3.8%). m/z (ESI) 527 (100%, [M-hfac<sup>-</sup>]<sup>+</sup>).  $\nu_{max}$ (KBr)/cm<sup>-1</sup> 1651 ( $\nu_{C=O}$ ).  $\lambda_{max}$ (CH<sub>2</sub>Cl<sub>2</sub>)/nm (log  $\varepsilon$ /M<sup>-1</sup> cm<sup>-1</sup>) 319 (4.46), 342 (4.34).

#### Synthesis of [Ni(hfac)<sub>2</sub>(ppa<sup>I</sup>)] **32**

Yellow solid (THF/n-hexane) (0.107 g, 54%) (Found: C 33.6, H 1.9, N 3.6. Calc. for  $C_{22}H_{11}F_{12}IN_2NiO_4$ : C 33.8, H 1.4, N 3.6%). m/z (ESI) 881 (100%, [M-hfac $^-$ +ppa $^I$ ] $^+$ ), 573 (82%, [M-hfac $^-$ ] $^+$ ).  $\nu_{max}$ (KBr)/cm $^-$ 1 1654 ( $\nu_{C=O}$ ).  $\lambda_{max}$ (CH<sub>2</sub>Cl<sub>2</sub>)/nm (log  $\varepsilon$ /M $^-$ 1 cm $^-$ 1) 244 (4.40), 320 (4.41).

#### Crystal Structure Determinations

Crystal data for the structures of 10, 12, and 14 are given in Table 1. X-ray quality crystals of 10, 12, and 14 were grown by allowing hexane to diffuse into a concentrated solution of the complex in CH<sub>2</sub>Cl<sub>2</sub>. Crystals were mounted on a glass fibre using perfluoropolyether oil and cooled rapidly to 150 K for 10 and 12 and 100 K for 14 in a stream of cold nitrogen. All diffraction data were collected on a Bruker Smart CCD area detector with graphite monochromated Mo  $K\alpha$  ( $\lambda = 0.71073 \text{ Å}$ ). After data collection, in each case an empirical absorption correction (SADABS) was applied,[21] and the structures were then solved by direct methods and refined on all  $F^2$  data using the SHELX suite of programs. [22] In all cases non-hydrogen atoms were refined with anisotropic thermal parameters; hydrogen atoms were included in calculated positions and refined with isotropic thermal parameters, which were  $\sim 1.2 \times (aromatic CH)$ or  $1.5 \times (Me)$  the equivalent isotropic thermal parameters of their parent carbon atoms.

**10**: C<sub>43</sub>H<sub>34</sub>N<sub>2</sub>NiO<sub>4</sub>, *M* 701.43, yellow needle, triclinic, space group *P-1*, *a* 9.6344(15), *b* 11.9506(18), *c* 16.267(3) Å, α 85.726(12), β 87.747(11), γ 66.802(10)°, *U* 1716.6(5) Å<sup>3</sup>, *Z* 2, *D* 1.357 Mg m<sup>-3</sup>,  $\mu$ (Mo<sub>Kα</sub>) 0.612 mm<sup>-1</sup>, F(000) 732, T 150 K, 20118 reflections, 6429 unique ( $R_{\rm int}$  0.0806),  $R_1$  0.0655 (6429 reflections,  $I > 2.0\sigma(I)$ ),  $wR_2$  0.1449,  $R_1$  0.1316 (all data),  $wR_2$  0.1796 (all data), S 1.008.

82 P. Harding et al.

12:  $C_{43}H_{34}N_2NiO_5$ , M 717.43, yellow plate, triclinic, space group P-I, a 9.9252(3), b 11.2859(3), c 17.4359(4) Å,  $\alpha$  73.2240(10),  $\beta$  86.0220(10),  $\gamma$  68.8910(10)°, U 1743.17(8) ų, Z 2, D 1.367 Mg m $^{-3}$ ,  $\mu$ (Mo<sub>K $\alpha$ </sub>) 0.607 mm $^{-1}$ , F(000) 748, T 150 K, 23492 reflections, 7901 unique ( $R_{\rm int}$  0.0318),  $R_1$  0.0372 (7901 reflections, I >2.0 $\sigma$ (I)),  $wR_2$  0.0922,  $R_1$  0.0480 (all data),  $wR_2$  0.0987 (all data), S 1.037.

**14**:  $C_{42}H_{31}CIN_2NiO_4$ , M 721.85, red needle, triclinic, space group P-I, a 9.6098(4), b 12.0443(5), c 16.1292(7) Å,  $\alpha$  85.154(2),  $\beta$  86.882(2),  $\gamma$  66.725(2)°, U 1708.34(12) ų, Z 2, D 1.403 Mg m $^{-3}$ ,  $\mu(Mo_{K\alpha})$  0.693 mm $^{-1}$ , F(000) 748, T 100 K, 31160 reflections, T710 unique ( $R_{\rm int}$  0.0334),  $R_1$  0.0466 (7710 reflections, I >2.0 $\sigma(I)$ ),  $wR_2$  0.1209,  $R_1$  0.0626 (all data),  $wR_2$  0.1278 (all data), S 1.094.

#### Acknowledgements

We gratefully acknowledge the Thailand Research Fund and Walailak University (Grant No. RSA5080007) for funding this research. We also thank the School of Chemistry, University of Bristol for elemental analysis and MS services.

#### References

- F. A. Cotton, G. Wilkinson, C. A. Murillo, M. Bochmann, in *Advanced Inorganic Chemistry*, 6th edn 1999, pp. 479–482 (John Wiley Sons: New York, NY).
- [2] N. S. Nandurkar, D. S. Patil, B. M. Bhanage, *Inorg. Chem. Commun.* 2008, 11, 733. doi:10.1016/J.INOCHE.2008.03.014
- [3] (a) R. G. Miller, T. J. Kealy, A. L. Barney, J. Am. Chem. Soc. 1967, 89, 3756. doi:10.1021/JA00991A013
  - (b) T. Yamada, O. Rhode, T. Takai, T. Mukaiyama, *Chem. Lett.* **1991**, *20*. 5. doi:10.1246/CL.1991.5
  - (c) T. Yamada, T. Takai, O. Rhode, T. Mukaiyama, *Bull. Chem. Soc. Jpn.* **1991**, *64*, 2109. doi:10.1246/BCSJ.64.2109
  - (d) Y. Nishida, T. Fujimoto, N. Tanaka, *Chem. Lett.* **1992**, *21*, 1291. doi:10.1246/CL.1992.1291
- [4] (a) P. Chassot, F. Emmenegger, *Inorg. Chem.* 1996, 35, 5931. doi:10.1021/IC9605130
  - (b) F. Emmenegger, C. W. Schlaepfer, H. Stoeckli-Evans, M. Piccand, H. Piekarski, *Inorg. Chem.* **2001**, *40*, 3884. doi:10.1021/IC0014540
- [5] (a) S. Pasko, L. G. Hubert-Pfalzgraf, A. Abrutis, J. Vaissermann, *Polyhedron* 2004, 23, 735. doi:10.1016/J.POLY.2003.11.044
   (b) L. G. Hubert-Pfalzgraf, *Inorg. Chem. Commun.* 2003, 6, 102. doi:10.1016/S1387-7003(02)00664-0
- [6] D. Barreca, C. Massignan, S. Daolio, M. Fabrizio, C. Piccirillo, L. Armelao, E. Tondello, *Chem. Mater.* 2001, 13, 588. doi:10.1021/ CM001041X

- [7] (a) M. H. Dickman, Acta Crystallogr. C 1997, 53, 1192.
   doi:10.1107/S0108270197005945
   (b) M. H. Dickman, J. P. Ward, F. A. Villamena, D. R. Crist, Acta
  - (b) M. H. Dickman, J. P. Ward, F. A. Villamena, D. R. Crist, *Acta Crystallogr. C* **1998**, *54*, 929. doi:10.1107/S0108270198000730
  - (c) F. A. Villamena, M. H. Dickman, D. R. Crist, *Inorg. Chem.* **1998**, *37*, 1446. doi:10.1021/IC9709741
  - (d) F. A. Villamena, M. H. Dickman, D. R. Crist, *Inorg. Chem.* 1998, 37, 1454. doi:10.1021/IC971215L
- [8] (a) R. G. Hicks, M. T. Lemaire, L. K. Thompson, T. M. Barclay, J. Am. Chem. Soc. 2000, 122, 8077. doi:10.1021/JA001627K
   (b) T. M. Barclay, R. G. Hicks, M. T. Lemaire, L. K. Thompson, Inorg.
- [9] (a) L. M. Field, P. M. Lahti, *Inorg. Chem.* 2003, 42, 7447. doi:10.1021/IC0349050

Chem. 2001, 40, 5581. doi:10.1021/IC010542X

- (b) M. Baskett, P. M. Lahti, A. Paduan-Filho, N. F. Oliveira, Jr, *Inorg. Chem.* **2005**, *44*, 6725, doi:10.1021/IC050435T
- [10] (a) A. Caneschi, D. Gatteschi, J. Laugier, P. Rey, R. Sessoli, *Inorg. Chem.* 1988, 27, 1553. doi:10.1021/IC00282A009
  - (b) A. Caneschi, D. Gatteschi, J. P. Renard, P. Rey, R. Sessoli, *Inorg. Chem.* 1989, 28, 2940. doi:10.1021/IC00314A013
  - (c) D. Luneau, G. Risoan, P. Rey, A. Caneschi, D. Gatteschi, J. Laugier, Inorg. Chem. 1993, 32, 5616. doi:10.1021/IC00076A032
- [11] F. A. Villamena, V. Horak, D. R. Crist, *Inorg. Chim. Acta* 2003, 342, 125. doi:10.1016/S0020-1693(02)01154-4
- [12] S. Kudo, A. Iwase, N. Tanaka, *Inorg. Chem.* 1985, 24, 2388. doi:10.1021/IC00209A015
- [13] G. M. Denison, A. O. Evans, C. A. Bessel, D. W. Skaf, R. W. Murray, J. M. DeSimone, J. Electrochem. Soc. 2005, 152, B435. doi:10.1149/1.2047387
- [14] P. Harding, D. J. Harding, W. Phonsri, S. Saithong, H. Phetmung, *Inorg. Chim. Acta* 2009, 362, 78. doi:10.1016/J.ICA.2008.03.014
- [15] S. Dehghanpour, A. Mahmoudi, Main Group Chemistry 2007, 6, 121. doi:10.1080/10241220801889025
- [16] S. Dehghanpour, N. Bouslimani, R. Welter, F. Mojahed, *Polyhedron* 2007, 26, 154. doi:10.1016/J.POLY.2006.08.011
- [17] A. C. G. Hotze, J. A. Faiz, N. Mourtzis, G. I. Pascu, P. R. A. Webber, G. J. Clarkson, K. Yannakopoulou, Z. Pikramenou, M. J. Hannon, *Dalton Trans.* 2006, 3025. doi:10.1039/B518027A
- [18] K. Nakamoto, in *Infrared and Raman Spectra of Inorganic and Coordination Compounds: Part B, 5th edn* 1997, pp. 91–99 (Wiley: New York, NY).
- [19] A. J. Jircitano, R. F. Henry, R. R. Hammond, Acta Crystallogr. C 1990, 46, 1799. doi:10.1107/S0108270190000944
- [20] D. V. Soldatov, A. T. Henegouwen, G. D. Duright, C. I. Ratcliffe, J. A. Ripmeester, *Inorg. Chem.* 2001, 40, 1626. doi:10.1021/IC000981G
- [21] SMART Bruker, XSCANS, SHEXTL and SADABS 2005 (Bruker AXS Inc.: Madison, WI).
- [22] G. M. Sheldrick, SHELXS97 and SHELXL97 1997 (University of Göttingen: Germany).

Appendix Two
International Publication

Acta Crystallographica Section E

#### **Structure Reports**

Online

ISSN 1600-5368

Editors: W.T.A. Harrison, J. Simpson and M. Weil

# [(4-Bromophenyl)(2-pyridylmethylidene)amine- $\kappa^2 N$ , N']bis-(1,1,1,5,5,5-hexafluoropentane-2,4-dionato- $\kappa^2 O$ , O')cobalt(II)

# Phimphaka Harding, David J. Harding, Nitisastr Soponrat and Harry Adams

Acta Cryst. (2010). E66, m1138-m1139

This open-access article is distributed under the terms of the Creative Commons Attribution Licence http://creativecommons.org/licenses/by/2.0/uk/legalcode, which permits unrestricted use, distribution, and reproduction in any medium, provided the original authors and source are cited.





Acta Crystallographica Section E: Structure Reports Online is the IUCr's highly popular open-access structural journal. It provides a simple and easily accessible publication mechanism for the growing number of inorganic, metal-organic and organic crystal structure determinations. The electronic submission, validation, refereeing and publication facilities of the journal ensure very rapid and high-quality publication, whilst key indicators and validation reports provide measures of structural reliability. In 2007, the journal published over 5000 structures. The average publication time is less than one month.

## Crystallography Journals Online is available from journals.iucr.org

### metal-organic compounds

Acta Crystallographica Section E

**Structure Reports** 

**Online** 

ISSN 1600-5368

# [(4-Bromophenyl)(2-pyridylmethylidene)amine- $\kappa^2 N, N'$ ]bis(1,1,1,5,5,5-hexafluoropentane-2,4-dionato- $\kappa^2 O, O'$ )-cobalt(II)

## Phimphaka Harding, a\* David J. Harding, A Nitisastr Soponrat and Harry Adams Adams

<sup>a</sup>Molecular Technology Research Unit, Department of Chemistry, Walailak University, Thasala, Nakhon Si Thammarat 80161, Thailand, <sup>b</sup>Department of Chemistry, Faculty of Science, Taksin University, Songkhla 90000, Thailand, and <sup>c</sup>Department of Chemistry, Faculty of Science, University of Sheffield, Brook Hill, Sheffield S3 7HF, England

Correspondence e-mail: kphimpha@wu.ac.th

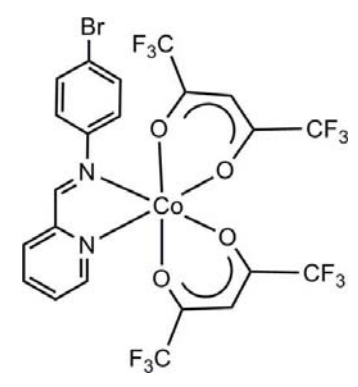
Received 3 August 2010; accepted 14 August 2010

Key indicators: single-crystal X-ray study; T = 150 K; mean  $\sigma(C-C) = 0.005 \text{ Å}$ ; R factor = 0.035; wR factor = 0.090; data-to-parameter ratio = 13.7.

In the title complex,  $[\text{Co}(\text{C}_5\text{HF}_6\text{O}_2)_2(\text{C}_{12}\text{H}_9\text{BrN}_2)]$ , the  $\text{Co}^{\text{II}}$  atom exhibits a pseudo-octahedral coordination geometry, comprising two N-donor atoms from a bidentate chelate (4-bromophenyl)(2-pyridylmethylidene)amine (ppa^{Br}) ligand [Co-N=2.098~(2)~and~2.209~(2)~Å] and four O-donor atoms from two bidentate chelate 1,1,1,5,5,5-hexafluoropentane-2,4-dionate (hfac) ligands [Co-O~range=~2.0452~(19)-2.0796~(19)~Å]. The packing of the structure involves weak  $\pi$ - $\pi$  interactions between the pyridyl and benzene rings of neighbouring ppa<sup>Br</sup> ligands [centroid-centroid~distance=~3.928~(2)~Å] and interactions between the Br atom on the ppa<sup>Br</sup> ligand and the hfac ligand  $[\text{Br}\cdot\cdot\cdot\text{C}=~3.531~(2)~\text{Å}]$ .

#### **Related literature**

For a review of halogen bonding, see: Corradi *et al.* (2000); Walsh *et al.* (2001); Liantonio *et al.* (2003). For an introduction to crystal engineering, see: Braga *et al.* (2002). For related structures, see: Harding, Harding, Sophonrat & Adams (2010); Harding, Harding, Tinpun *et al.* (2010); Aäkeroy *et al.* (2004, 2007). For a description of the Cambridge Structural database, see: Allen *et al.* (2002).



#### **Experimental**

Crystal data

$[Co(C_5HF_6O_2)_2(C_{12}H_9BrN_2)]$	$\gamma = 77.080 \ (1)^{\circ}$
$M_r = 734.17$	$V = 1269.51 (5) \text{ Å}^3$
Triclinic, $P\overline{1}$	Z = 2
a = 8.3568 (2)  Å	Mo $K\alpha$ radiation
b = 10.9420 (2)  Å	$\mu = 2.37 \text{ mm}^{-1}$
c = 14.8151 (3)  Å	T = 150  K
$\alpha = 74.042 \ (1)^{\circ}$	$0.60 \times 0.30 \times 0.03 \text{ mm}$
$\beta = 86.510 \ (1)^{\circ}$	

Data collection

Bruker SMART CCD area-detector diffractometer 21525 measured reflections 5176 independent reflections 4508 reflections with  $I > 2\sigma(I)$   $T_{\rm min} = 0.330, T_{\rm max} = 0.932$  21525 measured reflections 5176 independent reflections 4508 reflections with  $I > 2\sigma(I)$   $T_{\rm min} = 0.330, T_{\rm max} = 0.932$ 

Refinement

 $\begin{array}{ll} R[F^2 > 2\sigma(F^2)] = 0.035 & 379 \text{ parameters} \\ wR(F^2) = 0.090 & \text{H-atom parameters constrained} \\ S = 1.08 & \Delta\rho_{\text{max}} = 1.23 \text{ e Å}^{-3} \\ 5176 \text{ reflections} & \Delta\rho_{\text{min}} = -0.91 \text{ e Å}^{-3} \end{array}$ 

Data collection: *SMART* (Bruker, 1997); cell refinement: *SAINT* (Bruker, 1997); data reduction: *SAINT*; program(s) used to solve structure: *SHELXS97* (Sheldrick, 2008); program(s) used to refine structure: *SHELXL97* (Sheldrick, 2008); molecular graphics: *SHELXTL* (Sheldrick, 2008); software used to prepare material for publication: *SHELXTL*.

We thank the Thailand Research Fund (Grant No.: RSA5080007) for funding this research.

Supplementary data and figures for this paper are available from the IUCr electronic archives (Reference: ZS2056).

#### References

Aäkeroy, C. B., Desper, J. & V.-Martínez, J., (2004). CrystEngComm, 6, 413–418.

Aäkeroy, C. B., Schultheiss, N., Desper, J. & Moore, C. (2007). CrystEng-Comm. 9, 421–426.

Allen, F. H. (2002). Acta Cryst. B58, 380-388.

Braga, D., Desiraju, G. R., Miller, J. S., Orpen, A. G. & Price, S. L. (2002). CrystEngComm, 4, 500–509.

Bruker (1997). SMART, SAINT and SADABS. Bruker AXS Inc., Madison, Wisconsin, USA.

Corradi, E., Meille, M. T., Messina, S. V., Metrangolo, P. & Resnati, R. (2000). Angew. Chem. Int. Ed. 39, 1782–1786.

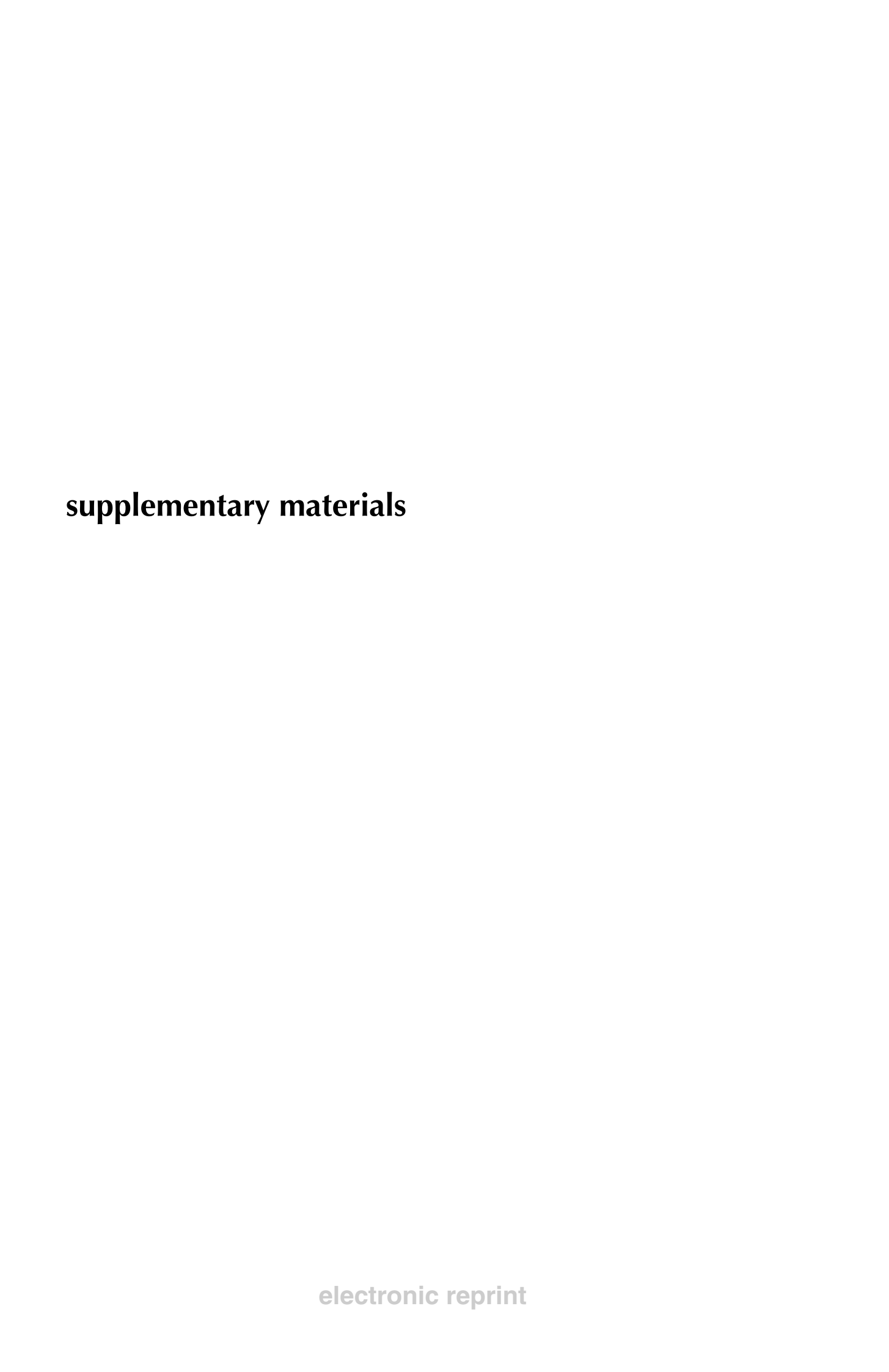
## metal-organic compounds

Harding, P., Harding, D. J., Sophonrat, N. & Adams, H. (2010). Unpublished results.

Harding, P., Harding, D. J., Tinpun, K., Samuadnuan, S., Sophonrat, N. & Adams, H. (2010). Aust. J. Chem. 63, 75–82.

Liantonio, R., Metrangolo, P., Pilati, T., Resnati, G. & Stevenazzi, A. (2003). Cryst. Growth Des. 3, 799-803.

Cryst. Growth Des. 3, 799–805.
Sheldrick, G. M. (2008). Acta Cryst. A64, 112–122.
Walsh, R. B., Padgett, C. W., Metrangolo, P., Resnati, G., Hanks, T. W. & Pennington, W. T. (2001). Cryst. Growth Des. 1, 165–175.



Acta Cryst. (2010). E66, m1138-m1139 [doi:10.1107/S1600536810032757]

[(4-Bromophenyl)(2-pyridylmethylidene)amine- $\kappa^2 N$ , N'] bis(1,1,1,5,5,5-hexafluoropentane-2,4-dionato- $\kappa^2 O$ , O') cobalt(II)

## P. Harding, D. J. Harding, N. Soponrat and H. Adams

#### Comment

The construction of supramolecular networks with designed architectures still remains the goal of crystal engineering and represents a significant challenge (Braga *et al.*, 2002). Although complementary hydrogen-bonding ligands have been successfully used (Aäkeroy *et al.*, 2004) in the construction of a number of networks, halogen-bonding (Walsh *et al.*, 2001; Liantonio *et al.*, 2003) and halogen-halogen interactions remain less well represented despite the fact that these interactions can be as strong as hydrogen-bonding interactions (Corradi *et al.*, 2000). In this paper we report the synthesis and structure of  $[Co(hfac)_2(ppa^{Br})]$  [hfac = 1,1,1,5,5,5-hexafluoropentane-2,4-dionato;  $ppa^{Br} = (4-bromo-phenyl)pyridin-2-yl-methyleneamine].$ 

The reaction of  $[Co(hfac)_2(H_2O)_2]$  with ppa<sup>Br</sup> in  $CH_2Cl_2$  yields  $[Co(hfac)_2(ppa^{Br})]$  (I) (Fig. 1) which crystallizes from  $CH_2Cl_2$ /hexane. In (I) the cobalt metal centre is six-coordinate with a distorted octahedral geometry, the hfac ligands adopting a *cis* arrangement enforced by the chelating ppa<sup>Br</sup> ligand. The  $CF_3$  groups of the hfac ligand in some cases exhibit large thermal ellipsoids due to thermal motion of these groups. The Co—N and Co—O bond lengths are comparable with related cobalt hfac and diimine complexes reported in the CSD (Allen, 2002) (mean Co—O distance = 2.01 Å, Co—N distance = 2.11 Å). The  $\beta$ -diketonate ligands exhibit a *bent* coordination mode in which the angles between the planes defined by the Co and oxygen atoms and the carbon and oxygen atoms of the  $\beta$ -diketonate ligand are 18.9° and 24.7°. In contrast, in *trans-*[ $M(hfac)_2(py-CH=CH—C_6F_4Br)_2$ ] (M=Co, Cu) the  $\beta$ -diketonate ligands exhibit a *planar* coordination mode (Aäkeroy *et al.*, 2007). In addition, the phenyl ring is twisted with respect to the pyridylimine unit by 17.6° and is similar to the angle observed in [Ni(dbm)<sub>2</sub>(ppa<sup>X</sup>)] [X=Me, 22.9°; Cl, 24.0° (Harding, Harding, Tinpun *et al.*, 2010)].

The packing in the structure of (I) involves a weak  $\pi$ – $\pi$  interaction between the pyridyl and phenyl rings of neighbouring ppa<sup>Br</sup> ligands as shown in Fig. 2 ( $Cg1\cdots Cg2=3.928$  (2) Å where Cg1 and Cg2 are the centroids of the rings C1—C6 and C8—C12—N2). A further weak interaction occurs between the Br atom on the ppa<sup>Br</sup> ligand and the β-diketonate ligand creating discrete dimers within the structure [Br···C20, 3.531 (2) Å, see Fig. 3]. These dimers are then connected via the  $\pi$ – $\pi$  interaction mentioned above resulting in one-dimensional chains. A similar interaction is also observed in the structure of trans-[M(hfac)<sub>2</sub>(py-CH=CH—C<sub>6</sub>F<sub>4</sub>Br)<sub>2</sub>] (Aäkeroy et al., 2007). Interestingly, the corresponding Ni analogue, [Ni(hfac)<sub>2</sub>(ppa<sup>Br</sup>)] has a completely different set of interactions with Br····CH interactions clearly evident (Harding, Harding, Sophonrat & Adams, 2010), once again highlighting the difficulties involved in attempting to use specific interactions in the design of supramolecular networks.

## **Experimental**

To an orange red solution of  $[\text{Co(hfac)}_2(\text{H}_2\text{O})_2]$  (0.127 g, 0.25 mmol) in  $\text{CH}_2\text{Cl}_2$  (5 cm<sup>3</sup>) was added a solution of ppa<sup>Br</sup> (0.065 g, 0.25 mmol) in  $\text{CH}_2\text{Cl}_2$  (3 cm<sup>3</sup>). The deep orange solution was stirred for 1 h and then concentrated *in vacuo*. *n*-Hexane (15 cm<sup>3</sup>) was added to precipitate an orange solid which was washed with *n*-hexane (2 *x* 5 cm<sup>3</sup>) and dried *in vacuo*: yield 0.142 g (77%). IR in KBr disc  $v_{\text{C}=\text{O}}$  1647 cm<sup>-1</sup>. UV-Vis (in CH<sub>2</sub>Cl<sub>2</sub>, log  $\varepsilon$  mol.dm<sup>-3</sup>cm<sup>-1</sup>) 243 (4.24), 309 (4.42).  $C_{22}\text{H}_{11}\text{O}_4\text{N}_2\text{F}_{12}\text{BrCo}$ ; calc. C 36.0, H 1.5, N 3.8%; found C 36.5, H 1.5, N 3.8%.

#### Refinement

Hydrogen atoms were placed geometrically and refined using a riding model with C-H = 0.95 Å and  $U_{iso}$  constrained to be 1.2 times  $U_{eq}$  of the carrier atom.

### **Figures**

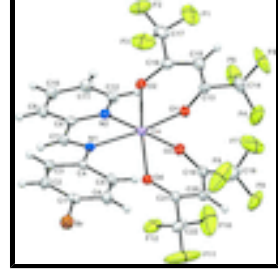


Fig. 1. The molecular structure of (I) showing the atom-labelling scheme. Displacement ellipsoids are drawn at the 50% probability level.

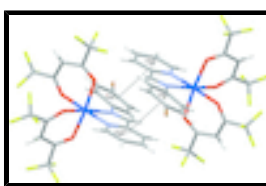


Fig. 2. The molecular packing in (I) showing the  $\pi$ – $\pi$  interactions between the phenyl and pyridyl rings of the ppa<sup>Br</sup> ligand. Only selected atoms are labelled for clarity. [Symmetry code: (i) -x + 2, -y, -z + 2].

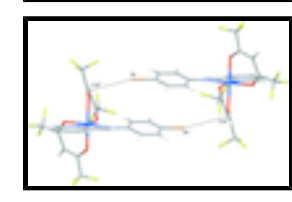


Fig. 3. The molecular packing in (I) showing the Br··· $\beta$ -diketonate interactions of the discrete dimers. Only selected atoms are labelled for clarity. [Symmetry code: (i) -x + 1, -y + 1, -z + 2].

# [(4-Bromophenyl)(2-pyridylmethylidene)amine- $\kappa^2 N, N'$ ]bis(1,1,1,5,5,5-hexafluoropentane-2,4-dionato- $\kappa^2 O, O'$ )cobalt(II)

Crystal data

$$\begin{split} & [\text{Co}(\text{C}_5\text{HF}_6\text{O}_2)_2(\text{C}_{12}\text{H}_9\text{BrN}_2)] & Z = 2 \\ & M_r = 734.17 & F(000) = 718 \\ & \text{Triclinic}, P\overline{1} & D_x = 1.921 \text{ Mg m}^{-3} \end{split}$$

Hall symbol: -P 1 Mo  $K\alpha$  radiation,  $\lambda = 0.71073 \text{ Å}$ a = 8.3568 (2) Å Cell parameters from 9953 reflections

b = 10.9420 (2) Å  $\theta = 2.9-32.8^{\circ}$ c = 14.8151 (3) Å  $\mu = 2.37 \text{ mm}^{-1}$  $\alpha = 74.042 (1)^{\circ}$ T = 150 K $\beta = 86.510 (1)^{\circ}$ Plate, orange

 $\gamma = 77.080 (1)^{\circ}$  $0.60\times0.30\times0.03~mm$ 

 $V = 1269.51 (5) \text{ Å}^3$ 

Data collection

Bruker SMART CCD area-detector 5176 independent reflections diffractometer

4508 reflections with  $I > 2\sigma(I)$ Radiation source: fine-focus sealed tube

 $R_{\rm int} = 0.021$ graphite

 $\theta_{\text{max}} = 26.4^{\circ}, \ \theta_{\text{min}} = 2.0^{\circ}$  $\phi$  and  $\omega$  scans

Absorption correction: multi-scan  $h = -10 \rightarrow 10$ (SADABS; Bruker, 1997)  $T_{\min} = 0.330, T_{\max} = 0.932$  $k = -13 \rightarrow 13$ 

21525 measured reflections  $l = -18 \rightarrow 18$ 

Refinement

Primary atom site location: structure-invariant direct Refinement on  $F^2$ methods

Least-squares matrix: full Secondary atom site location: difference Fourier map

Hydrogen site location: inferred from neighbouring  $R[F^2 > 2\sigma(F^2)] = 0.035$ sites

 $wR(F^2) = 0.090$ H-atom parameters constrained

 $w = 1/[\sigma^2(F_0^2) + (0.0399P)^2 + 2.417P]$ S = 1.08

where  $P = (F_0^2 + 2F_c^2)/3$ 

 $(\Delta/\sigma)_{\text{max}} = 0.001$ 5176 reflections  $\Delta \rho_{\text{max}} = 1.23 \text{ e Å}^{-3}$ 379 parameters

 $\Delta \rho_{\min} = -0.91 \text{ e Å}^{-3}$ 0 restraints

#### Special details

Geometry. All e.s.d.'s (except the e.s.d. in the dihedral angle between two l.s. planes) are estimated using the full covariance matrix. The cell e.s.d.'s are taken into account individually in the estimation of e.s.d.'s in distances, angles and torsion angles; correlations between e.s.d.'s in cell parameters are only used when they are defined by crystal symmetry. An approximate (isotropic) treatment of cell e.s.d.'s is used for estimating e.s.d.'s involving l.s. planes.

**Refinement**. Refinement of  $F^2$  against ALL reflections. The weighted R-factor wR and goodness of fit S are based on  $F^2$ , conventional R-factors R are based on F, with F set to zero for negative  $F^2$ . The threshold expression of  $F^2 > \sigma(F^2)$  is used only for calculating Rfactors(gt) etc. and is not relevant to the choice of reflections for refinement. R-factors based on  $F^2$  are statistically about twice as large as those based on F, and R- factors based on ALL data will be even larger.

		_		2.
Fractional atomic coor	rdinates and isotropic o	r eauivalent isotropic	displacement	parameters $(A^2)$

	x	y	z	$U_{\rm iso}*/U_{\rm eq}$
Br1	0.24966 (4)	0.40512 (3)	1.12788 (2)	0.02627 (10)
C1	0.4059 (3)	0.3017(3)	1.0652 (2)	0.0190(6)
C2	0.4540 (4)	0.1698 (3)	1.1069 (2)	0.0234 (6)
H2	0.4096	0.1318	1.1659	0.028*
C3	0.5671 (4)	0.0937(3)	1.0621 (2)	0.0220(6)
Н3	0.6002	0.0028	1.0903	0.026*
C4	0.6331 (3)	0.1491 (3)	0.97587 (19)	0.0165 (5)
C5	0.5813 (3)	0.2824(3)	0.93439 (19)	0.0198 (6)
H5	0.6237	0.3208	0.8750	0.024*
C6	0.4680 (4)	0.3591 (3)	0.9796 (2)	0.0218 (6)
Н6	0.4337	0.4500	0.9519	0.026*
C7	0.8328 (3)	-0.0354(3)	0.96759 (19)	0.0182 (5)
H7	0.8186	-0.0694	1.0331	0.022*
C8	0.9486 (3)	-0.1115 (3)	0.91526 (19)	0.0172 (5)
C9	1.0341 (4)	-0.2363 (3)	0.9576 (2)	0.0221 (6)
Н9	1.0201	-0.2753	1.0225	0.027*
C10	1.1404 (4)	-0.3031 (3)	0.9032 (2)	0.0240 (6)
H10	1.1991	-0.3896	0.9301	0.029*
C11	1.1601 (4)	-0.2431 (3)	0.8099 (2)	0.0242 (6)
H11	1.2336	-0.2869	0.7718	0.029*
C12	1.0707 (4)	-0.1171 (3)	0.7723 (2)	0.0217 (6)
H12	1.0847	-0.0757	0.7078	0.026*
C13	0.8228 (4)	0.1729 (3)	0.5708 (2)	0.0215 (6)
C14	0.9068 (4)	0.2216 (3)	0.4767 (2)	0.0322 (7)
C15	0.6657 (4)	0.1503 (3)	0.5689 (2)	0.0258 (6)
H15	0.6125	0.1698	0.5102	0.031*
C16	0.5849 (4)	0.0998 (3)	0.6508 (2)	0.0246 (6)
C17	0.4252 (4)	0.0581 (4)	0.6393 (2)	0.0361 (8)
C18	0.7556 (4)	0.4215 (3)	0.6922 (2)	0.0223 (6)
C19	0.6383 (5)	0.5432 (3)	0.6348 (3)	0.0414 (9)
C20	0.9177 (4)	0.4284 (3)	0.7033 (2)	0.0231 (6)
H20	0.9542	0.5051	0.6707	0.028*
C21	1.0267 (4)	0.3261 (3)	0.7608 (2)	0.0203 (6)
C22	1.1961 (4)	0.3521 (3)	0.7732 (3)	0.0330 (8)
Co1	0.82077 (4)	0.13568 (3)	0.77538 (2)	0.01482 (10)
F1	0.3604 (3)	0.1057 (3)	0.55597 (18)	0.0696 (8)
F2	0.4576 (3)	-0.0730 (2)	0.65283 (19)	0.0578 (7)
F3	0.3172 (3)	0.0779 (3)	0.70502 (19)	0.0578 (7)
F4	0.9544 (4)	0.3293 (3)	0.47281 (18)	0.0768 (10)
F5	0.8123 (3)	0.2441 (3)	0.40289 (14)	0.0636 (8)
F6	1.0401 (3)	0.1358 (2)	0.46507 (15)	0.0508 (6)
F7	0.5963 (6)	0.5260(3)	0.5585 (3)	0.130(2)
F8	0.5029 (3)	0.5703 (2)	0.6848 (3)	0.0862 (11)
F9	0.6978 (3)	0.64976 (19)	0.61453 (18)	0.0505 (6)
F10	1.2729 (3)	0.3815 (4)	0.6912 (2)	0.0974 (13)

F11	1.1845 (4)	0.4500(3)	0.8083 (3)	0.1054 (15)
F12	1.2953 (2)	0.25146 (19)	0.82617 (16)	0.0406 (5)
N1	0.7503(3)	0.0775 (2)	0.92465 (16)	0.0159 (5)
N2	0.9660(3)	-0.0524 (2)	0.82359 (16)	0.0171 (5)
O1	0.9099(2)	0.15687 (19)	0.64017 (13)	0.0195 (4)
O2	0.6285 (2)	0.07571 (19)	0.73472 (14)	0.0207 (4)
O3	0.6895 (2)	0.32603 (18)	0.72450 (13)	0.0194 (4)
04	1.0045 (2)	0.21558 (18)	0.80721 (13)	0.0192 (4)

Atomic displacement parameters  $(\mathring{A}^2)$ 

monic displacer	nome displacement parameters (11)						
	$U^{11}$	$U^{22}$	$U^{33}$	$U^{12}$	$U^{13}$	$U^{23}$	
Br1	0.02487 (16)	0.02549 (16)	0.02822 (17)	-0.00312 (12)	0.00920 (12)	-0.01065 (12)	
C1	0.0152 (13)	0.0234 (14)	0.0211 (14)	-0.0036 (11)	0.0022 (11)	-0.0116 (11)	
C2	0.0295 (16)	0.0212 (14)	0.0213 (14)	-0.0111 (12)	0.0086 (12)	-0.0061 (12)	
C3	0.0280 (15)	0.0158 (13)	0.0219 (14)	-0.0066 (12)	0.0031 (12)	-0.0036 (11)	
C4	0.0159 (13)	0.0189 (13)	0.0166 (13)	-0.0056 (11)	-0.0007 (10)	-0.0061 (10)	
C5	0.0201 (14)	0.0212 (14)	0.0152 (13)	-0.0026 (11)	0.0008 (11)	-0.0021 (11)	
C6	0.0222 (14)	0.0179 (13)	0.0214 (14)	0.0010 (11)	-0.0018 (11)	-0.0026 (11)	
C7	0.0207 (14)	0.0194 (13)	0.0140 (13)	-0.0048 (11)	-0.0011 (11)	-0.0032 (10)	
C8	0.0172 (13)	0.0169 (13)	0.0179 (13)	-0.0040 (11)	-0.0035 (10)	-0.0044 (10)	
C9	0.0240 (15)	0.0202 (14)	0.0192 (14)	-0.0010 (12)	-0.0058 (11)	-0.0026 (11)	
C10	0.0232 (15)	0.0190 (13)	0.0269 (15)	0.0036 (12)	-0.0074 (12)	-0.0063 (12)	
C11	0.0207 (14)	0.0244 (14)	0.0270 (15)	0.0004 (12)	-0.0010 (12)	-0.0102 (12)	
C12	0.0224 (14)	0.0227 (14)	0.0195 (14)	-0.0036 (12)	-0.0001 (11)	-0.0057 (11)	
C13	0.0279 (15)	0.0176 (13)	0.0181 (14)	-0.0028 (12)	0.0005 (12)	-0.0050 (11)	
C14	0.0380 (19)	0.0381 (18)	0.0193 (15)	-0.0089 (15)	0.0039 (13)	-0.0058 (13)	
C15	0.0278 (16)	0.0287 (15)	0.0206 (15)	-0.0050 (13)	-0.0044 (12)	-0.0060 (12)	
C16	0.0245 (15)	0.0239 (14)	0.0269 (16)	-0.0075 (12)	-0.0044 (12)	-0.0065 (12)	
C17	0.0330 (18)	0.050(2)	0.0322 (18)	-0.0197 (16)	-0.0029 (15)	-0.0127 (16)	
C18	0.0281 (16)	0.0191 (14)	0.0175 (14)	-0.0024 (12)	-0.0025 (12)	-0.0030 (11)	
C19	0.041(2)	0.0228 (16)	0.054(2)	-0.0067 (15)	-0.0224 (18)	0.0045 (16)	
C20	0.0279 (15)	0.0195 (14)	0.0218 (14)	-0.0095 (12)	0.0018 (12)	-0.0025 (11)	
C21	0.0216 (14)	0.0208 (14)	0.0206 (14)	-0.0074 (11)	0.0005 (11)	-0.0069 (11)	
C22	0.0295 (17)	0.0220 (15)	0.048 (2)	-0.0120 (14)	-0.0081 (15)	-0.0028 (14)	
Co1	0.01588 (19)	0.01408 (18)	0.01382 (18)	-0.00367 (14)	-0.00033 (14)	-0.00219 (14)	
F1	0.0544 (16)	0.104(2)	0.0513 (15)	-0.0445 (16)	-0.0281 (12)	0.0049 (14)	
F2	0.0614 (16)	0.0504 (14)	0.0774 (18)	-0.0309 (12)	0.0001 (13)	-0.0281 (13)	
F3	0.0297 (11)	0.0890 (19)	0.0739 (17)	-0.0283 (12)	0.0120 (11)	-0.0436 (15)	
F4	0.141 (3)	0.0613 (16)	0.0414 (14)	-0.0620 (18)	0.0404 (16)	-0.0119 (12)	
F5	0.0408 (13)	0.118 (2)	0.0176 (10)	-0.0071 (14)	-0.0015 (9)	-0.0019 (12)	
F6	0.0361 (12)	0.0704 (16)	0.0345 (12)	0.0019 (11)	0.0130 (9)	-0.0088 (11)	
F7	0.238 (5)	0.0398 (15)	0.102(3)	0.010(2)	-0.137 (3)	-0.0037 (16)	
F8	0.0272 (13)	0.0385 (14)	0.159 (3)	0.0060 (11)	0.0007 (16)	0.0188 (17)	
F9	0.0464 (13)	0.0239 (10)	0.0674 (16)	-0.0076 (9)	-0.0113 (11)	0.0128 (10)	
F10	0.0476 (16)	0.158 (3)	0.0688 (19)	-0.062 (2)	-0.0036 (14)	0.031 (2)	
F11	0.0547 (17)	0.0586 (17)	0.230 (4)	0.0108 (14)	-0.065 (2)	-0.088 (2)	
F12	0.0260 (10)	0.0309 (10)	0.0644 (14)	-0.0070 (8)	-0.0163 (10)	-0.0077 (10)	

N1	0.0160 (11)	0.0154 (11)	0.0174 (11)	-0.0043 (9)	-0.0008(9)	-0.0055 (9)
N2	0.0179 (11)	0.0164 (11)	0.0174 (11)	-0.0047 (9)	-0.0002 (9)	-0.0040 (9)
O1	0.0210 (10)	0.0214 (10)	0.0155 (9)	-0.0057 (8)	0.0001 (8)	-0.0031 (8)
O2	0.0224 (10)	0.0206 (10)	0.0195 (10)	-0.0090(8)	-0.0007(8)	-0.0025 (8)
O3	0.0192 (10)	0.0179 (9)	0.0194 (10)	-0.0035 (8)	-0.0010 (8)	-0.0026 (8)
O4	0.0209 (10)	0.0181 (9)	0.0190 (10)	-0.0064(8)	-0.0022(8)	-0.0031 (8)
Geometric para	ameters (Å, °)					
Br1—C1		1.902 (3)	C14-	-F6	1.32	22 (4)
C1—C6		1.378 (4)	C14-			22 (4)
C1—C2		1.382 (4)	C15—			91 (4)
C2—C3		1.379 (4)	C15—		0.9:	
C2—H2		0.9500	C16-			56 (4)
C3—C4		1.394 (4)	C16-			37 (4)
С3—Н3		0.9500	C17—			00 (4)
C4—C5		1.397 (4)	C17—			16 (4)
C4—N1		1.429 (3)	C17—			58 (4)
C5—C6		1.388 (4)	C18-			55 (4)
C5—H5		0.9500	C18-			96 (4)
C6—H6		0.9500	C18-			34 (4)
C7—N1		1.284 (4)	C19-			78 (5)
C7—C8		1.461 (4)	C19-	-F9		21 (4)
C7—H7		0.9500	C19-			36 (5)
C8—N2		1.349 (4)	C20-	-C21		37 (4)
C8—C9		1.384 (4)	C20-		0.93	
C9—C10		1.385 (4)	C21-	-O4	1.20	64 (3)
C9—H9		0.9500	C21-	-C22		37 (4)
C10—C11		1.375 (4)	C22-	-F11		96 (4)
C10—H10		0.9500	C22-	-F12	1.30	08 (4)
C11—C12		1.392 (4)	C22-	-F10	1.33	32 (5)
C11—H11		0.9500	Co1-	-O2	2.04	152 (19)
C12—N2		1.335 (4)	Co1-	-O4	2.00	539 (19)
C12—H12		0.9500	Co1-	-O1	2.00	544 (19)
C13—O1		1.246 (3)	Co1-	-O3	2.0	796 (19)
C13—C15		1.392 (4)	Co1-	-N2	2.09	98 (2)
C13—C14		1.537 (4)	Co1-	-N1	2.20	09 (2)
C14—F4		1.312 (4)				
C6—C1—C2		121.5 (3)	F1—0	C17—F2	104	.7 (3)
C6—C1—Br1		119.8 (2)		C17—F2		.7 (3)
C2—C1—Br1		118.7 (2)		C17—C16		.6 (3)
C3—C2—C1		119.3 (3)		C17—C16		.2 (3)
C3—C2—H2		120.4		C17—C16		.1 (3)
C1—C2—H2		120.4		C18—C20		.0 (3)
C2—C3—C4		120.5 (3)		C18—C19		.7 (3)
C2—C3—H3		119.7		-C18—C19		.3 (3)
C4—C3—H3		119.7		C19—F9		.7 (4)
C3—C4—C5		119.2 (3)		C19—F8		.4 (4)
C3—C4—N1		124.2 (2)		C19—F8		.6 (3)

C5—C4—N1	116.6 (2)	F7—C19—C18	111.1 (3)
C6—C5—C4	120.3 (3)	F9—C19—C18	114.0 (3)
C6—C5—H5	119.9	F8—C19—C18	109.6 (3)
C4—C5—H5	119.9	C21—C20—C18	121.5 (3)
C1—C6—C5	119.2 (3)	C21—C20—H20	119.3
C1—C6—H6	120.4	C18—C20—H20	119.3
C5—C6—H6	120.4	O4—C21—C20	129.1 (3)
N1—C7—C8	119.7 (2)	O4—C21—C22	115.2 (3)
N1—C7—H7	120.1	C20—C21—C22	115.7 (3)
C8—C7—H7	120.1	F11—C22—F12	108.3 (3)
N2—C8—C9	122.5 (3)	F11—C22—F10	106.4 (4)
N2—C8—C7	115.7 (2)	F12—C22—F10	105.6 (3)
C9—C8—C7	121.7 (3)	F11—C22—C21	111.6 (3)
C10—C9—C8	118.5 (3)	F12—C22—C21	113.1 (3)
С10—С9—Н9	120.7	F10—C22—C21	111.3 (3)
C8—C9—H9	120.7	O2—Co1—O4	173.89 (8)
C11—C10—C9	119.3 (3)	O2—Co1—O1	87.88 (8)
C11—C10—H10	120.3	O4—Co1—O1	89.87 (8)
C9—C10—H10	120.3	O2—Co1—O3	87.74 (8)
C10—C11—C12	119.0 (3)	O4—Co1—O3	86.41 (8)
C10—C11—H11	120.5	O1—Co1—O3	85.05 (8)
C12—C11—H11	120.5	O2—Co1—N2	94.96 (8)
N2—C12—C11	122.3 (3)	O4—Co1—N2	90.82 (8)
N2—C12—H12	118.9	O1—Co1—N2	92.91 (8)
C11—C12—H12	118.9	O3—Co1—N2	176.56 (8)
O1—C13—C15	128.6 (3)	O2—Co1—N1	91.80 (8)
O1—C13—C14	113.3 (3)	O4—Co1—N1	91.41 (8)
C15—C13—C14	118.1 (3)	O1—Co1—N1	169.94 (8)
F4—C14—F6	106.5 (3)	O3—Co1—N1	104.98 (8)
F4—C14—F5	107.8 (3)	N2—Co1—N1	77.10 (9)
F6—C14—F5	106.3 (3)	C7—N1—C4	119.2 (2)
F4—C14—C13	111.0 (3)	C7—N1—Co1	111.94 (18)
F6—C14—C13	111.4 (3)	C4—N1—Co1	128.79 (17)
F5—C14—C13	113.5 (3)	C12—N2—C8	118.4 (2)
C16—C15—C13	121.6 (3)	C12—N2—Co1	126.20 (19)
C16—C15—H15	119.2	C8—N2—Co1	115.41 (18)
C13—C15—H15	119.2	C13—O1—Co1	123.71 (19)
O2—C16—C15	129.1 (3)	C16—O2—Co1	123.95 (19)
O2—C16—C17	114.0 (3)	C18—O3—Co1	123.68 (19)
C15—C16—C17	116.7 (3)	C21—O4—Co1	122.51 (18)
F1—C17—F3	111.6 (3)	C21—0 <del>1</del> —C01	122.31 (10)
	. ,	G5 G4 N4 G5	1.60.6.(0)
C6—C1—C2—C3	0.2 (4)	C5—C4—N1—C7	162.6 (3)
Br1—C1—C2—C3	179.9 (2)	C3—C4—N1—Co1	163.1 (2)
C1—C2—C3—C4	0.4 (4)	C5—C4—N1—Co1	-15.6 (3)
C2—C3—C4—C5	-1.1 (4)	O2—Co1—N1—C7	97.18 (19)
C2—C3—C4—N1	-179.8 (3)	O4—Co1—N1—C7	-88.02 (19)
C3—C4—C5—C6	1.4 (4)	O1—Co1—N1—C7	9.2 (6)
N1—C4—C5—C6	-179.8 (2)	O3—Co1—N1—C7	-174.68 (18)
C2—C1—C6—C5	0.1 (4)	N2—Co1—N1—C7	2.50 (18)

P-1 C1 CC C5	170.7 (2)	02 C-1 N1 C4	04.5 (2)
Br1—C1—C6—C5	-179.7 (2)	O2—Co1—N1—C4	-84.5 (2)
C4—C5—C6—C1	-0.9 (4)	O4—Co1—N1—C4	90.3 (2)
N1—C7—C8—N2	3.1 (4)	01—Co1—N1—C4	-172.5 (4)
N1—C7—C8—C9	-176.7 (3)	O3—Co1—N1—C4	3.6 (2)
N2—C8—C9—C10	-0.5 (4)	N2—Co1—N1—C4	-179.2 (2)
C7—C8—C9—C10	179.2 (3)	C11—C12—N2—C8	0.8 (4)
C8—C9—C10—C11	1.2 (4)	C11—C12—N2—Co1	-178.8(2)
C9—C10—C11—C12	-0.9(4)	C9—C8—N2—C12	-0.5(4)
C10—C11—C12—N2	-0.2 (4)	C7—C8—N2—C12	179.8 (2)
O1—C13—C14—F4	-55.7 (4)	C9—C8—N2—Co1	179.2 (2)
C15—C13—C14—F4	125.5 (3)	C7—C8—N2—Co1	-0.6(3)
O1—C13—C14—F6	62.7 (4)	O2—Co1—N2—C12	88.0 (2)
C15—C13—C14—F6	-116.0 (3)	O4—Co1—N2—C12	-90.1 (2)
O1—C13—C14—F5	-177.3 (3)	O1—Co1—N2—C12	-0.2 (2)
C15—C13—C14—F5	3.9 (4)	N1—Co1—N2—C12	178.7 (2)
O1—C13—C15—C16	-2.0 (5)	O2—Co1—N2—C8	-91.62 (19)
C14—C13—C15—C16	176.6 (3)	O4—Co1—N2—C8	90.35 (19)
C13—C15—C16—O2	5.1 (5)	O1—Co1—N2—C8	-179.74 (19)
C13—C15—C16—C17	-170.3 (3)	N1—Co1—N2—C8	-0.91 (18)
O2—C16—C17—F1	166.4 (3)	C15—C13—O1—Co1	-16.6(4)
C15—C16—C17—F1	-17.5 (5)	C14—C13—O1—Co1	164.79 (19)
O2—C16—C17—F3	37.7 (4)	O2—Co1—O1—C13	23.0(2)
C15—C16—C17—F3	-146.2 (3)	O4—Co1—O1—C13	-151.3 (2)
O2—C16—C17—F2	-76.6 (4)	O3—Co1—O1—C13	-64.9 (2)
C15—C16—C17—F2	99.4 (3)	N2—Co1—O1—C13	117.9 (2)
O3—C18—C19—F7	-67.9 (5)	N1—Co1—O1—C13	111.4 (5)
C20—C18—C19—F7	112.6 (4)	C15—C16—O2—Co1	11.3 (4)
O3—C18—C19—F9	168.8 (3)	C17—C16—O2—Co1	-173.2 (2)
C20—C18—C19—F9	-10.7 (5)	O1—Co1—O2—C16	-20.5 (2)
O3—C18—C19—F8	51.9 (4)	O3—Co1—O2—C16	64.7 (2)
C20—C18—C19—F8	-127.5 (3)	N2—Co1—O2—C16	-113.2 (2)
O3—C18—C20—C21	-5.0 (5)	N1—Co1—O2—C16	169.6 (2)
C19—C18—C20—C21	174.4 (3)	C20—C18—O3—Co1	-16.7 (4)
C18—C20—C21—O4	2.5 (5)	C19—C18—O3—Co1	163.9 (2)
C18—C20—C21—C22	-174.7 (3)	O2—Co1—O3—C18	-150.4 (2)
O4—C21—C22—F11	-118.6 (4)	O4—Co1—O3—C18	27.8 (2)
C20—C21—C22—F11	59.0 (4)	O1—Co1—O3—C18	-62.3 (2)
O4—C21—C22—F12	3.9 (4)	N1—Co1—O3—C18	118.3 (2)
C20—C21—C22—F12	-178.4 (3)	C20—C21—O4—Co1	21.0 (4)
O4—C21—C22—F10	122.6 (3)	C22—C21—O4—Co1	-161.8 (2)
C20—C21—C22—F10	-59.7 (4)	O1—Co1—O4—C21	55.7 (2)
C8—C7—N1—C4	177.8 (2)	O3—Co1—O4—C21	-29.4 (2)
C8—C7—N1—Co1	-3.7 (3)	N2—Co1—O4—C21	148.6 (2)
C3—C4—N1—C7	-18.7 (4)	N1—Co1—O4—C21	-134.3 (2)
	<b>\</b> /		· /

Fig. 1

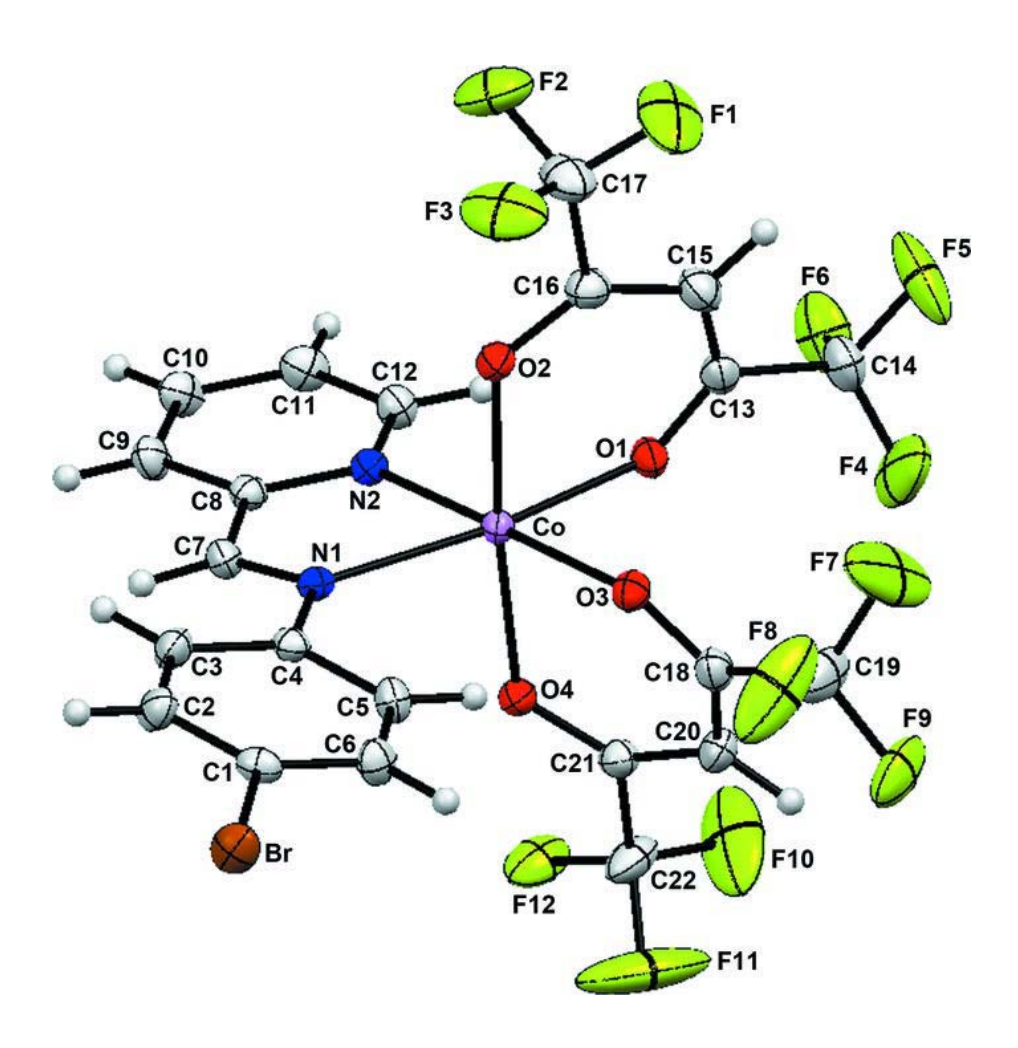


Fig. 2

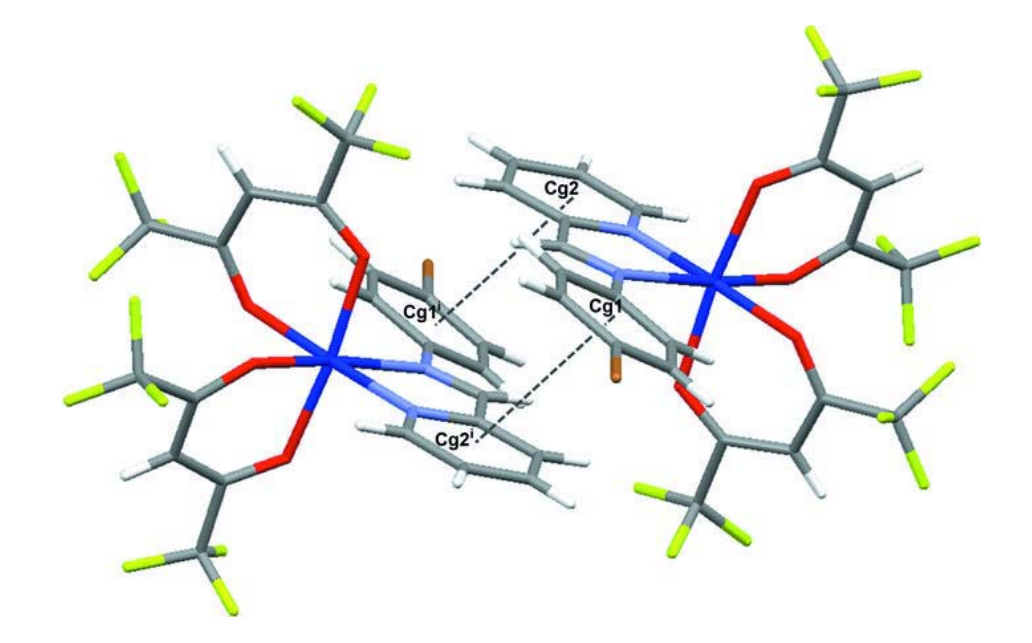
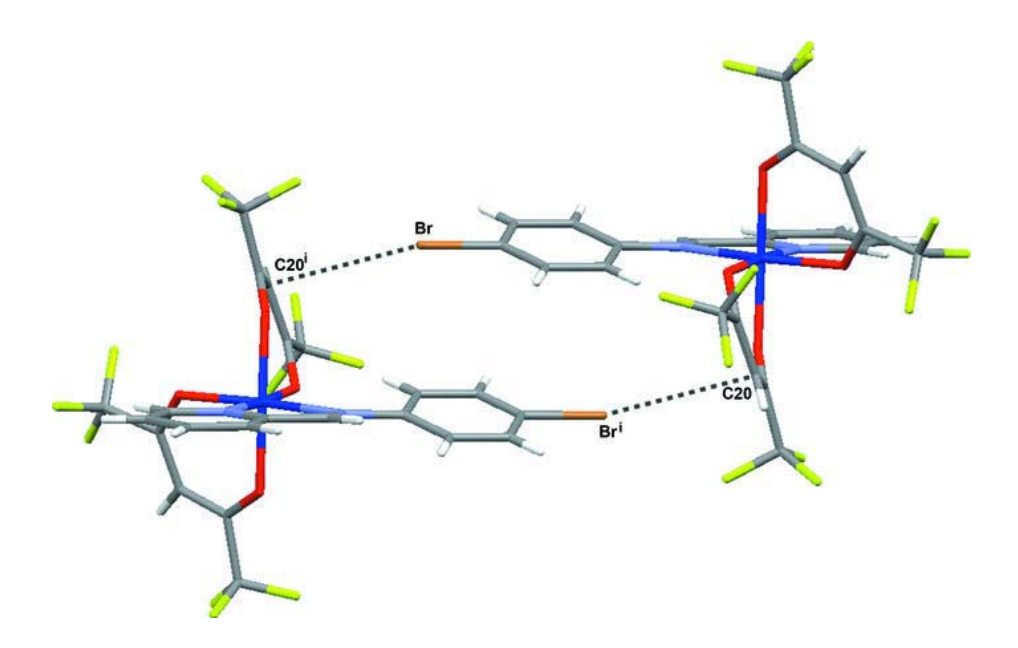


Fig. 3



Appendix Three

Manuscript I

## manuscript zb2010 for review

Acta Crystallographica Section E

#### **Structure Reports**

#### **Online**

ISSN 1600-5368

Editors: W.T.A. Harrison, J. Simpson and

M. Weil

# Bis(1,1,1,5,5,5-hexafluoropentane-2,4-dionato- $\kappa^2$ -O,O')[(4-bromophenyl)pyridin-2-ylmethylene amine- $\kappa^2$ -N,N']nickel(II)

Phimphaka Harding, David J. Harding, Nitisastr Soponrat and Harry Adams

# CONFIDENTIAL – NOT TO BE REPRODUCED, QUOTED NOR SHOWN TO OTHERS SCIENTIFIC MANUSCRIPT

For review only.

Saturday 14 August 2010

Category: metal-organic compounds

#### **Co-editor:**

David Billing

School of Chemistry, University of the Witwatersrand, Private Bag 3, PO Wits, Johannesburg 2050, South Africa

Telephone: 27(11)717659 Fax: 27(11)7176749

Email: dave.billing@wits.ac.za

## **Contact author:**

Assistant Phimphaka Harding

Thailand

Telephone: ++66-75-672100

Fax: ++66-75-672004 Email: kphimpha@wu.ac.th

## checkCIF/PLATON results for paper zb2010

checkCIF/PLATON results Ellipsoid plot

## checkCIF/PLATON results

No syntax errors found. CIF dictionary Interpreting this report Bond precision: C-C = 0.0065 A Wavelength=0.71073 Cell: a=31.251(8) b=10.006(3) c=17.653(5)alpha=90 beta=103.952(5) gamma=90 Temperature: 150 K

Calculated Reported Volume 5357(3) 5358(2) Space group C 2/c C2/c Hall group -C 2yc -C2yc

Moiety formula C22 H11 Br F12 N2 Ni O4 Sum formula

733.92 733.95 1.820 1.820 Dx,g cm-3 8 Mu (mm-1) 2.332 F000 2880.0 2880.0 F000'

2882.74

h,k,lmax 40,12,22 40,12,22 5988 6149

Tmin, Tmax 0.722,0.774 0.628,0.784

Tmin' 0.593

Correction method= MULTI-SCAN Data completeness= 0.974 Theta(max) = 27.500

R(reflections) = 0.0542( 3422) wR2(reflections) = 0.1322( 5988)

S = 0.909 Npar = 379

## Alert level C

```
RINTA01_ALERT_3_C The value of Rint is greater than 0.12
            Rint given 0.145
                                           has ADP max/min Ratio .....
PLAT213 ALERT 2 C Atom F5
                                                                                3.10 prola
PLAT230_ALERT_2_C Hirshfeld Test Diff for C5 -- C6 ..
PLAT230 ALERT 2 C Hirshfeld Test Diff for C7 -- C8 ..
                                                                                5.48 su
PLAT230_ALERT_2_C Hirshfeld Test Diff for C7
                                                                                6.28 su
PLAT242_ALERT_2_C Check Low Ueq as Compared to Neighbors for
                                                                                 C14
                                Ueq as Compared to Neighbors for Ueq as Compared to Neighbors for
PLAT242_ALERT_2_C Check Low
                                                                                   C17
PLAT242_ALERT_2_C Check Low Ueq as Compared to Neighbors for PLAT341_ALERT_3_C Low Bond Precision on C-C Bonds (x 1000) Ang ..
                                                                                   C19
PLAT601 ALERT 2 C Structure Contains Solvent Accessible VOIDS of .
                                                                                 42.00 A
PLAT911 ALERT 3 C Missing # FCF Refl Between THmin & STh/L= 0.600
                                                                                 83
PLAT912 ALERT 4 C Missing # of FCF Reflections Above STh/L= 0.600
```

```
0 ALERT level A = In general: serious problem
0 ALERT level B = Potentially serious problem
```

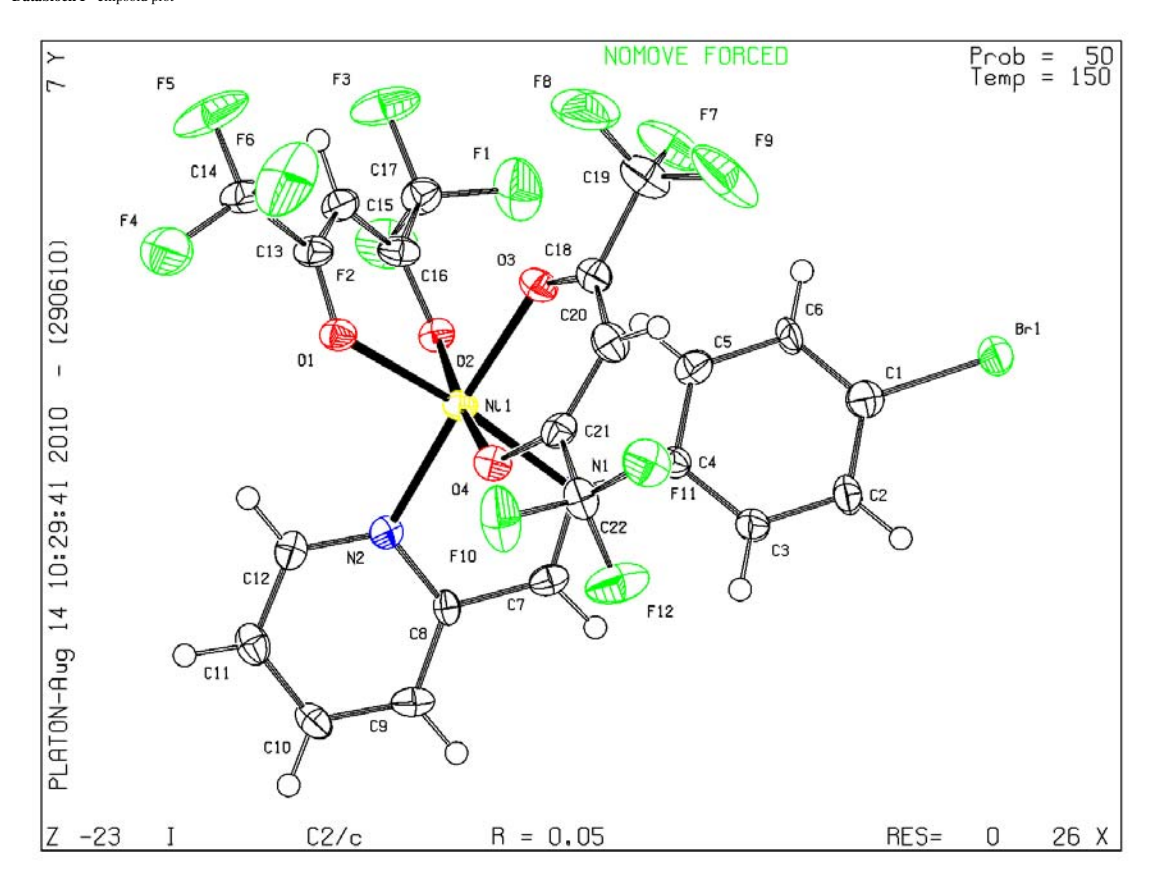
<sup>11</sup> ALERT level C = Check and explain

```
0 ALERT level G = General alerts; check
0 ALERT type 1 CIF construction/syntax error, inconsistent or missing data
7 ALERT type 2 Indicator that the structure model may be wrong or deficient
3 ALERT type 3 Indicator that the structure quality may be low
1 ALERT type 4 Improvement, methodology, query or suggestion
0 ALERT type 5 Informative message, check
```

## database duplication summary

- Chemical name =
- R factor = 0.054
- Space group = C2/c
- Formula = C22 H11 Br F12 N2 Ni O4
- a=31.251 b=10.006 c=17.653
- alpha=90 beta=103.952 gamma=90

## No duplication found.



Submitted to Acta Cryst. E

# Bis(1,1,1,5,5,5-hexafluoropentane-2,4-dionato- $\kappa^2$ -O,O')[(4-bromophenyl)pyridin-2-ylmethylene amine– $\kappa^2$ -N,N']nickel(II)

## Phimphaka Harding\*, a David J. Harding, a Nitisastr Soponrat and Harry Adams<sup>c</sup>

<sup>a</sup>Molecular Technology Research Unit, Department of Chemistry, Walailak University, Thasala, Nakhon Si Thammarat, 80161, THAIL-AND, <sup>b</sup>Department of Chemistry, Faculty of Science, Taksin University, Songkhla, 90000, THAILAND, and <sup>c</sup>Department of Chemistry, Faculty of Science, University of Sheffield, Brook Hill, Sheffield, S3 7HF, UK

Correspondence email: kphimpha@wu.ac.th

#### **Abstract**

[Ni(hfac)<sub>2</sub>(ppa<sup>Br</sup>)] **1** crystallizes in the space group C2/c and exhibits a *pseudo*-octahedral coordination geometry. The structure packs through C—H···Br interactions (H6···Br 3.015 Å, H2···Br 3.017 Å) forming a hydrogen bonding ladder and strong hydrogen bonding interactions between two of the oxygen atoms of the  $\beta$ -diketonate ligands and two hydrogen atoms on the pyridyl ring of the ppa<sup>Br</sup> (O1···H12 2.532 Å, O4···H11 2.610 Å).

## **Related literature**

For related literature see: Harding et al. (2010); Aäkeroy et al. (2004, 2005, 2007). For a general introduction to crystal engineering see: Braga et al., (2002).

## **Computing details**

Data collection: Bruker *SMART* (Bruker, 1997); cell refinement: Bruker *SMART*; data reduction: Bruker *SAINT* (Bruker, 1997); program(s) used to solve structure: *SHELXS97* (Sheldrick, 2008); program(s) used to refine structure: *SHELXL97* (Sheldrick, 2008); molecular graphics: Bruker *SHELXTL* (Bruker, 1997); software used to prepare material for publication: Bruker *SHELXTL*.

Bis(1,1,1,5,5,5-hexafluoropentane-2,4-dionato- $\kappa^2$ -O,O') [(4-bromo-phenyl)pyridin-2-ylmethylene amine- $\kappa^2$ -N,N'] nickel(II)

Crystal data

 $C_{22}H_{11}BrF_{12}N_2NiO_4$   $V = 5358 (2) \text{ Å}^3$ 

 $M_r = 733.95$  Z = 8

Monoclinic, C2/c Mo  $K\alpha$  radiation

## **Acta E preprint**

a = 31.251 (8) Å	$\mu = 2.33 \text{ mm}^{-1}$
b = 10.006 (3) Å	T = 150  K

c = 17.653 (5) Å $0.22 \times 0.12 \times 0.11 \text{ mm}$ 

 $\beta = 103.952 (5)^{\circ}$ 

Data collection

CCD area detector 5988 independent reflections diffractometer

Absorption correction: multi-scan

3422 reflections with  $I > 2\sigma(I)$ SADABS (Bruker, 1997)

 $T_{\min} = 0.628, T_{\max} = 0.784$  $R_{\rm int} = 0.145$  $\theta_{max} = 27.5^{\circ}$ 27645 measured reflections

Refinement

 $R[F^2 > 2\sigma(F^2)] = 0.054$ H-atom parameters constrained

 $\Delta \rho_{max} = 1.24~e~\text{Å}^{-3}$  $wR(F^2) = 0.132$ S = 0.91 $\Delta \rho_{min} = -1.12 \text{ e Å}^{-3}$ 5988 reflections Absolute structure: ? 379 parameters Flack parameter: ?

Table 1

0 restraints

Selected geometric parameters (Å)

Ni1—O3	2.020 (3)	Ni1—N2	2.063 (3)
Ni1—O4	2.044 (3)	Nil—O1	2.066 (3)
Ni1—O2	2.045 (3)	Ni1—N1	2.113 (4)

Rogers parameter: ?

### Acknowledgements

We thank the Thailand Research Fund (Grant No.: RSA5080007) for funding this research.

### References

Aäkeroy, C. B., Schultheiss, N., Desper, J. & Moore, C. (2007). CrystEngComm, 9, 421-426.

Aäkeroy, C. B., Desper, J. & V.-Martínez, J., (2004). CrystEngComm, 6, 413–418.

Aäkeroy, C. B., Schultheiss, N. & Desper, J. (2005). Inorg. Chem. 44, 4983–4991.

Allen, F. H. (2002). Acta Crsyt., B58, 380-388.

Braga, D., Desiraju, G. R., Miller, J. S., Orpen, A. G. & Price, S. L. (2002). CrystEngComm, 4, 500-509.

Bruker (1997). SMART, SAINT, SHELXTL and SADABS. Bruker AXS Inc., Madison, Wisconsin, USA.

Cotton, F. A., Wilkinson, G., Murillo, C. A. & Bochmann, M. (1999). Advanced Inorganic Chemistry, 6<sup>th</sup> ed.; John Wiley&Sons: New York, pp. 479-482.

Chassot, P. & Emmenegger, F. (1996). Inorg. Chem. 35, 5931–5934.

Emmenegger, F., Schlaepfer, C. W., Stoeckli-Evans, H., Piccand, M. & Piekarski, H. (2001). Inorg. Chem. 40, 3884–3888.

Harding, P., Harding, D. J., Tinpun, K., Samuadnuan, S., Sophonrat, N. & Adams, H. (2010). *Aust. J. Chem.* **63**, 75–82. Harding, P., Harding, D. J., Sophonrat, N. & Adams, H. (2010). Unpublished results. Sheldrick, G. M. (2008). *Acta Cryst.* A**64**, 112–122.

## Scheme 1

$$F_3C$$
 $CF_3$ 
 $N$ 
 $N$ 
 $O$ 
 $CF_3$ 
 $F_3C$ 



# Bis(1,1,1,5,5,5-hexafluoropentane-2,4-dionato- $\kappa^2$ -O,O')[(4-bromophenyl)pyridin-2-ylmethylene amine– $\kappa^2$ -N,N']nickel(II)

Phimphaka Harding\*, a David J. Harding, a Nitisastr Soponrat b and Harry Adams<sup>c</sup>

#### Comment

Metal  $\beta$ -diketonates represent an important class of complexes and are much studied owing to their ease of synthesis, ready modification and multiple applications (Cotton *et al.*, 1999). In the case of divalent metal ions, the [ $M(\beta$ -diketonate)<sub>2</sub>] complexes are able to coordinate additional ligands forming either *cis*- or *trans*-octahedral metal complexes (Chassot & Emmenegger, 1996; Emmenegger *et al.*, 2001). Of particular relevence to this paper is the use metal  $\beta$ -diketonates complexes in the preparation of crystal engineered networks (Braga *et al.*, 2002) and while hydrogen bonded *trans*-isomers are well represented few compounds containing *cis*-isomers are described (Aäkeroy *et al.*, 2004, 2005, 2007). In this paper we describe the synthesis and structure of [Ni(hfac)<sub>2</sub>(ppa<sup>Br</sup>)] (hfac = 1,1,1,5,5,5-hexafluoropentane-2,4-dionato; ppa<sup>Br</sup> = (4-bromo-phenyl)pyridin-2-ylmethylene amine).

[Ni(hfac)<sub>2</sub>(H<sub>2</sub>O)<sub>2</sub>] reacts readily with ppa<sup>Br</sup> to give [Ni(hfac)<sub>2</sub>(ppa<sup>Br</sup>)] **1** which recrystallizes from CH<sub>2</sub>Cl<sub>2</sub>/*n*-hexane to give yellow crystals in the space group C2/c (Figure 1). This contrasts markedly with the analogous cobalt compound which crystallizes in *P*T (Harding, Harding, Soponrat and Adams, 2010). The nickel metal centre is *pseudo*-octahedral with a *cis*-arrangement enforced by the chelating ppa<sup>Br</sup> ligand. The Ni—O and Ni—N bond lengths are typical of values reported for other nickel hfac and diimine complexes reported in the CSD (mean Ni—O distance = 2.01 Å, Ni—N distance = 2.11 Å, Allen, 2002). The β-diketonate ligands exhibit a *bent* coordination mode in which the angles between the planes defined by the Ni and oxygen atoms and the carbon and oxygen atoms of the β-diketonate ligand are 11.0° and 26.8°. In contrast, in *trans*-[M(hfac)<sub>2</sub>(py-CH=CH—C<sub>6</sub>F<sub>4</sub>Br)<sub>2</sub>] (M = Co, Cu) the β-diketonate ligands exhibit a *planar* coordination mode (Aäkeroy *et al.*, 2007). In addition, the phenyl ring is twisted with to the pyridylimine unit by 30.0° a little greater than the angle observed in [Ni(dbm)<sub>2</sub>(ppa<sup>X</sup>)] (X = Me 22.9°, Cl 24.0°, Harding *et al.*, 2010).

The packing in the structure is composed of two sets of interactions. The first set is involves a series of C—H···Br interactions (H6···Br 3.015 (3) Å, H2···Br 3.017 (3) Å) forming a hydrogen bonding ladder (Figure 2). The second interaction involves a strong hydrogen bonding interactions between two of the oxygen atoms of the  $\beta$ -diketonate ligands and two hydrogen atoms on the pyridyl ring of the ppa<sup>Br</sup> ligand (O1···H12 2.532 (4) Å, O4···H11 2.610 (3) Å) forming a dimer (Figure 3). In contrast, the cobalt analogue has extensive  $\pi$ ··· $\pi$  interactions and interactions between the Br atom on the ppa<sup>Br</sup> ligand and the  $\beta$ -diketonate ligand (Harding, Harding, Soponrat and Adams, 2010).

## **Experimental**

To a green solution of [Ni(hfac)<sub>2</sub>(H<sub>2</sub>O)<sub>2</sub>] (0.128 g, 0.25 mmol) in CH<sub>2</sub>Cl<sub>2</sub> (10 ml) was added a solution of ppa<sup>Br</sup> (0.065 g, 0.25 mmol) in CH<sub>2</sub>Cl<sub>2</sub> (3 ml). The orange solution was stirred overnight then concentrated *in vacuo*. n-Hexane (10 ml) was added to precipitate a yellow brown solid which was washed with n-hexane (2 x 5 ml) and dried *in vacuo* yielding a deep

yellow solid (0.096 g, 52%). Found: C 36.2, H 1.7, N 3.9. Calc. for  $C_{22}H_{11}BrF_{12}N_2NiO_4$ : C 36.0, H 1.5, N 3.8%. m/z (ESI) 527  $[M-hfac^-]^+$ .  $n_{max}(KBr)/cm^{-1}$  1651  $(n_{C=O})$ .  $l_{max}(CH_2Cl_2)/nm$  (log  $e/M^1cm^{-1}$ ) 319 (4.46), 342 (4.34).

#### Refinement

Hydrogen atoms were placed geometrically and refined with a riding model and with  $U_{\rm iso}$  constrained to be 1.2 (aromatic CH) times  $U_{\rm eq}$  of the carrier atom.

## **Figures**

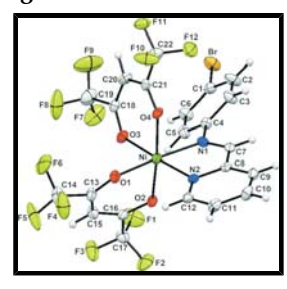
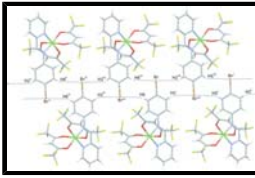


Fig. 1. The molecular structure of (1) showing the atom-labelling scheme. Displacement ellipsoids are drawn at the 50% probability level.



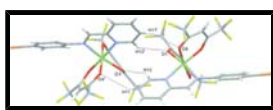


Fig. 3. The molecular packing in (1) showing the O···H interactions between the oxygen atoms of the β-diketonate ligands and the two hydrogen of the ppa<sup>Br</sup> ligand. Only selected atoms are labelled for clairty. [Symmetry codes: (i) -x, y, 1/2 - z].

# Bis(1,1,1,5,5,5-hexafluoropentane-2,4-dionato- $\kappa^2$ -O,O') [(4-bromo-phenyl)pyridin-2-ylmethylene amine- $\kappa^2$ -N,N'] nickel(II)

## Crystal data

 $C_{22}H_{11}BrF_{12}N_2NiO_4$ F(000) = 2880 $M_r = 733.95$  $D_{\rm x} = 1.820 \; {\rm Mg \; m}^{-3}$ Mo  $K\alpha$  radiation,  $\lambda = 0.71073 \text{ Å}$ Monoclinic, C2/c Hall symbol: -C2yc Cell parameters from 3767 reflections  $\theta = 2.4-24.9^{\circ}$ a = 31.251 (8) Å b = 10.006 (3) Å  $\mu = 2.33 \text{ mm}^{-1}$ c = 17.653 (5) Å T = 150 K $\beta = 103.952 (5)^{\circ}$ Block, brown  $V = 5358 (2) \text{ Å}^3$  $0.22\times0.12\times0.11~mm$ Z = 8

Data collection

CCD area detector 5988 independent reflections

diffractometer

Radiation source: fine-focus sealed tube 3422 reflections with  $I > 2\sigma(I)$ 

graphite  $R_{\rm int} = 0.145$ 

 $\theta_{\text{max}} = 27.5^{\circ}, \, \theta_{\text{min}} = 1.3^{\circ}$ Detector resolution: 100 pixels mm<sup>-1</sup>

 $h = -39 \rightarrow 40$ phi and ω scans

Absorption correction: multi-scan  $k = -12 \rightarrow 12$ 

SADABS (Bruker, 1997)  $T_{\min} = 0.628, T_{\max} = 0.784$  $l = -22 \rightarrow 22$ 

27645 measured reflections

Refinement

Primary atom site location: structure-invariant direct Refinement on  $F^2$ methods

Least-squares matrix: full Secondary atom site location: difference Fourier map Hydrogen site location: inferred from neighbouring

 $R[F^2 > 2\sigma(F^2)] = 0.054$ 

 $wR(F^2) = 0.132$ H-atom parameters constrained

 $w = 1/[\sigma^2(F_0^2) + (0.0546P)^2]$ S = 0.91

where  $P = (F_0^2 + 2F_c^2)/3$ 

 $(\Delta/\sigma)_{\text{max}} < 0.001$ 5988 reflections

379 parameters  $\Delta \rho_{\text{max}} = 1.24 \text{ e Å}^{-3}$ 

 $\Delta \rho_{min} = -1.12 \text{ e Å}^{-3}$ 0 restraints

## Special details

Geometry. All e.s.d.'s (except the e.s.d. in the dihedral angle between two l.s. planes) are estimated using the full covariance matrix. The cell e.s.d.'s are taken into account individually in the estimation of e.s.d.'s in distances, angles and torsion angles; correlations between e.s.d.'s in cell parameters are only used when they are defined by crystal symmetry. An approximate (isotropic) treatment of cell e.s.d.'s is used for estimating e.s.d.'s involving l.s. planes.

**Refinement.** Refinement of  $F^2$  against ALL reflections. The weighted R-factor wR and goodness of fit S are based on  $F^2$ , conventional R-factors R are based on F, with F set to zero for negative  $F^2$ . The threshold expression of  $F^2 > \sigma(F^2)$  is used only for calculating Rfactors(gt) etc. and is not relevant to the choice of reflections for refinement. R-factors based on  $F^2$  are statistically about twice as large as those based on F, and R- factors based on ALL data will be even larger.

Fractional atomic coordinates and isotropic or equivalent isotropic displacement parameters  $(\mathring{A}^2)$ 

	x	y	z	$U_{\rm iso}*/U_{\rm eq}$
Ni1	0.089498 (18)	0.60018 (5)	0.17271 (3)	0.01947 (16)
Br1	0.279804 (16)	0.50379 (5)	-0.01356 (3)	0.03493 (16)
N1	0.10544 (11)	0.4874 (3)	0.0821 (2)	0.0180(8)
N2	0.03045 (12)	0.5037 (3)	0.1283 (2)	0.0193 (8)
O1	0.06741 (10)	0.7013 (3)	0.25796 (16)	0.0227 (7)
O2	0.07571 (10)	0.7678 (3)	0.10485 (16)	0.0206 (7)
O3	0.14882 (9)	0.6873 (3)	0.21444 (17)	0.0253 (7)
O4	0.10989 (9)	0.4413 (3)	0.24516 (16)	0.0215 (7)
C1	0.22491 (15)	0.4979 (4)	0.0144 (3)	0.0268 (11)